Response to Co-Editor

We greatly appreciate this editor's critical comments and suggestions, which have helped us improve the paper quality substantially. We have addressed all of the comments carefully as detailed below in our point-by-point responses. Our responses start with "R:".

Comments to the Author:

Please further revise the paper considering the following comments:

Introduction section is too long. Many materials are not direly related to the topic of this study. Reorganize this section in the following way: First briefly discuss ILAPS roles in climate, especially ILAPS in snow. Then discuss what studies have been conducted on this specific topic, such as available field measurements and modeling treatments of these particles, using summarizing form, not listed by one study after another. Then point out knowledge gaps on this topic and why the present study is needed. And finally point out the goals of the present study.

R: We have simplified the introduction section, which became more related to the topic of this study based on the comments from the editor.

Avoid repetition or redundancy wherever possible. Some materials provided for reviewers' information (that have been posted as response to reviewers 'comments) do not necessarily be presented in the final version of the paper if these materials do not add much scientific value to the paper.

R: We have revised the final manuscript avoiding repetition and redundancy based on the comments from the editor.

Several paragraphs are too long to follow easily. Split into short ones for easy reading. Some very long sentences do not have the clean meaning and need to be fixed.

R: We have revised the long paragraphs into short ones.

Conclusion section needs to be polished. Avoid repeating statements that are already in the abstract.

R: We have revised the conclusion section more accurately to better reflect the topic of this study.

Polish the language and remove grammar issues.

R: We have made major revisions to polish the language and remove grammar issues of the manuscript.

Observations and model simulations of s~~S~~now albedo reduction in seasonal snow due to insoluble light-absorbing particles during 2014 Chinese survey~~anthropogenic dust and carbonaceous aerosols across northern China~~

Xin Wang[1], Wei Pu[1], Yong Ren[1], Xuelei Zhang[2], Xueying Zhang[1], Jinsen Shi[1], Hongchun Jin[1], Mingkai Dai[1], Quanliang Chen[3]

[1] Key Laboratory for Semi-Arid Climate Change of the Ministry of Education, College of Atmospheric Sciences, Lanzhou University, Lanzhou, 730000, China
[2] Key Laboratory of Wetland Ecology and Environment, Northeast Institute of Geography and Agroecology, Chinese Academy of Sciences, Changchun 130102, China
[3] College of Atmospheric Science, Chengdu University of Information Technology, and Plateau Atmospheric and Environment Laboratory of Sichuan Province, Chengdu 610225, China

Correspondence to: X. Wang (wxin@lzu.edu.cn)

Abstract.

A snow survey was carried out to collect 13 surface snow samples (109 for fresh snow, and 3 for aged snow)~~,~~ and 79 sub-surface snow samples in seasonal snow at 13 sites in January 2014 across ~~northeast~~northeastern China. A spectrophotometer combined with~~and the~~ chemical analysis ~~were~~was used to quantify s~~separate s~~now particulate absorption by insoluble light-absorbing particles (ILAPs, ~~(~~e.g. black carbon, BC; mineral dust, MD~~ organic carbon, OC~~; and organic carbon, OC~~mineral dust, MD~~) in snow.~~,~~ ~~and the s~~Snow albedo was measured by using a field spectroradiometer~~ during this periods~~. ~~In this study, a~~AA new radiative transfer model (Spectral Albedo Model for Dirty Snow, or SAMDS) ~~is~~was then developed to ~~model~~ simulate the spectral albedo ~~reduction due to ILAPs of~~in snow based on the asymptotic radiative transfer theory. ~~The~~A comparison between SAMDS and an existing model - the Snow, Ice, and Aerosol Radiation (SNICAR) ~~model~~ indicates that good agreements in the model simulated ~~the~~ spectral albedos of pure snow~~ derived from these models agree well~~, however, ~~there is a slight tendency for~~ the SNICAR model values tended to be slightly~~to become~~ lower than those of SAMDS ~~model values~~ when BC and MD ~~are~~were considered.~~The results indicate that~~ Given the measured BC, MD and OC mixing ratios of 100-5000~~ ng g^{-1}~~, 2000-6000~~ ng g^{-1}~~, and 1000-30000 ng g^{-1}, respectively, in surface snow across northeastern China, SAMDS model produced a snow albedo in the range of 0.95-0.75 for~~the snow albedo of~~ fresh snow at 550 nm with a snow grain optical effective radius (R_{eff}) of 100 μm~~ is generally in a range of 0.95-0.75 by using SAMDS model~~. ~~t~~The snow albedo reduction due to spherical snow grains assumed as~~for aged snow due to spherical~~aged snow ~~grains~~ is gradual~~ll~~~~tel~~y larger than fresh snow ~~for~~such as ~~Koch snowflake~~fractal snow grains, and hexagonal plates/columns snow grains associated with the increased BC in snow. For typical~~ly~~

BC mixing ratios of 100 ng g^{-1} in remote areas and 3000 ng g^{-1} in heavy industrial areas across northern China, ~~an effective radius of 100 μm,~~ the snow albedo ~~reduction caused by 100 ppb of~~for ~~–~~internal ~~mixed BC~~mixing of BC and snow ~~is XX, but only XX~~is lower by 0.005 and 0.036 than that ~~for~~of external ~~mixed BC~~mixing for hexagonal plates/columns snow grains with R_{eff} of 100 μm. ~~A comparison between SAMDS and the Snow, Ice, and Aerosol Radiation (SNICAR) model indicated that the spectral albedos of pure snow derived from these models agreed well, however, a slight tendency for the SNICAR model values to become lower than SAMDS model values when BC and MD mixing ratios range from 1 to 5 μg g^{-1} and 4 to 6 μg g^{-1}, respectively.~~ The result also shows that the simulated snow albedos by both SAMDS and SNICAR agree well with the observed values at low ILAPs mixing ratios, but tend to be higher ~~compared with~~than surface observations at high ILAPs mixing ratios.

~~This study offers not only an explanation for the discrepancy of the snow albedo reduction between modeled and observed snow albedo reduction due to ILAPs in snow, but also demonstrates the enhancement of the model simulations of the snow albedo reduction by using the optical effective radii (R_{eff}) of snow grains than that the measured snow grian radii due to SMDAS and SNICAR models, especially in the case of near-infrared wavelengths.~~ ~~A survey was performed to collect 92 seasonal snow samples at 13 sties across northern China in January 2014, and the mixing ratios of Insoluble Light-Absorbing Particles (ILAPs, e.g. black carbon, organic carbon, and mineral dust (MD) in seasonal snow were measured by using an integrating sphere/integrating sandwich spectrophotometer (ISSW), and the chemical analysis~~methods~~. Based on the surface measurements of ILAPs in snow, a new~~

radiative transfer model (Spectral Albedo Model for Dirty Snow, or SAMDS) is developed to simulate the spectral albedo reduction due to ILAPs in snow based on the asymptotic radiative transfer theory. We calculate that XX-XX %, and XX-XX % of snow albedo reduction in surface snow resides within the concentrations of BC and MD in the ranges of XX ng g, and XX ng g, respectively. A comparison between SAMDS and the SNICAR models indicated that the snow albedo can reduce 1-3%, 2-5%, and 2-4% due to ng g, XXX ng g, and xxx ng g of black carbon (BC), and mineral dust (MD) in snow. We note that tThe organic carbon (OC) is also another key parameter in affecting snow albedo of 1-5% due to XXX ppb in snow due to SDAMS model simulation. For a given shape (Koch snowflake, hexagonal plates/columns, and spheres), the snow albedo reduction due to spherical snow grains is graduately larger than Koch snowflake, and hexagonal plates/colums with the increased concentration of BC in snow. The internal mixing of BC in snow absorbs substantially higher than the external mixing at the wavelengths of 400 nm -1400 nm. In addition to the BC and AD parameters in the Snow, Ice, and Aerosol Radiation (SNICAR) model, the OC content in snow is considered an initial parameter for calculating snow albedo through a new radiative transfer model (Spectral Albedo Model for Dirty Snow, or SAMDS). The spectral albedo of snow reduction caused by OC (20 μg g^{-1}) is up to a factor of 3 for a snow grain size of 800 μm compared to 100 μm. We find a larger difference in snow albedo levels between the model simulations and surface measurements for higher insoluble light-absorbing impurities (ILAPs) using the measured snow grain radii. Compared with the observed snow albedo, we also note that the optical effective radii (R_{eff}) of snow grains can significantly enhance the model simulations of snow albedo reduction than that the measured snow grian radii due to SMDAS and SNICAR models, especially in the case of near-infrared

~~wavelengths.~~

~~1~~ 1 Introduction

Mineral dust (MD), black carbon (BC) and organic carbon (OC) are three main types of insoluble light-absorbing particles (ILAPs) that play key roles in regional and global climate (Bond et al., 2013; Dang and Hegg~~Dang et al.~~, 2014~~; Flanner et al., 2007, 2009~~; Hansen et al., 2005; IPCC, 2013; Li et al., 2016; McConnell et al, 2007; Pu et al., 2015~~Jaffe et al., 1999~~). ~~Anthropogenic dust (AD) is a major form of mineral dust.~~ ILAPs deposited on snow have been found to shorten the snow cover season by decreasing the snow albedo and accelerating snow melt (Brandt et al., 2011; Flanner et al., 2007, 2009; Hadley and Kirchstetter, 2012).~~The AD~~ MD particles ~~content can influence air quality and human health through emission, transport, removal, and deposit processes (Aleksandropoulou et al., 2011; Chen et al., 2013; Huang et al., 2014, 2015a, 2015b; Kim et al., 2009; Li et al., 2009; Mahowald and Luo, 2003; Zhang et al., 2005, 2015). AD~~ They~~MD~~ particles ~~also act as cloud condensation nuclei that affect cloud formation (Coz et al., 2010; Givati and Rosenfeld, 2004; Rosenfeld et al., 2001) and deliver various trace nutrients to terrestrial and marine ecosystems (Acosta et al., 2011; Mahowald et al., 2005; Qiao et al., 2013).~~ The Taklimakan and Gobi desert, and several other deserts are well known ~~to be major~~ dust sources across northern China~~, and~~. MD particles produced in these deserts can be lifted up in the atmosphere and transported to the downwelling regions ~~via wet and dry depositions~~ (Che et al., 2011, 2013; Chen et al., 2013; Huang et al., 2008; Jaffe, et al., 1999; Wang et al., 2008, 2010a; Zhang et al., 2003). C~~But recent studies indicated that the anthropogenic dust emissions from disrupted soils by human activities, such as deforestation, overgrazing, agricultural and industrial activities, are not well constrained (Aleksandropoulou et al., 2011; Tegen and Fung, 1995; Tegen et al., 2002, 2004; Thompson et al., 1988), which differs from natural MD originating from desert~~

regions (Che et al., 2011, 2013, 2015a; Goudie and Middleton, 2001; Li et al., 2012; Park and Park, 2014; Pu et al., 2015; Wallach and Fischer, 1970; Wang et al., 2008, 2010b). For instance, Kamani et al. (2015)Ginoux et al. (2010) estimated that MD due to anthropogenic dust activities accounts for 25% of dust aerosols using observational data from MODIS Deep Blue satellite products combined with a land-use fraction dataset (Ginoux et al., 2010). Anthropogenic dust originates primarily from urban and regional sources, especially during the winter,Recent studies indicated that and anthropogenicMD dust influenced by anthropogenic activities has already been enriched with heavy metals and other toxic elements (Kamani et al., 2015; Li et al., 2013; Wang et al., 2015; Zhang et al., 2013). Northeastern China and surrounding regions are generally regarded as industrial areas most affected by human activities. Because anthropogenic dust emissions from disturbed soils are not well constrained, we define mineral dust from areas disrupted by human activities, such as deforestation, overgrazing, agricultural and industrial activities, as anthropogenic dust (Aleksandropoulou et al., 2011; Tegen and Fung, 1995; Tegen et al., 2002, 2004; Thompson et al., 1988), which differs from natural mineral dust originating from desert regions (Che et al., 2011, 2013, 2015a; Goudie and Middleton, 2001; Li et al., 2012; Park and Park, 2014; Pu et al., 2015; Wallach and Fischer, 1970; Wang et al., 2008, 2010b). This assumption is consistent with the results of a recent study by Huang et al. (2015a), who found that anthropogenic dust contributions to regional emissions in eastern China are 91.8%, with and 76.1% in India at 76.1% (e.g., Figure 10 in Huang et al., 2015a). This may be due to larger population densities, which are characterized by more intense human activity in eastern China and India (Guan et al., 2016; Huang et al., 2015a; Wang et al., 2013a; Zhang et al., 2013).)

~~Compared to ADMD, c~~arbonaceous aerosols, such as BC and OC, generated from the incomplete combustion of fossil fuels and from biomass burning are also major anthropogenic pollutants. ~~ILAPs deposited on snow have been found to shorten the snow cover season by decreasing the snow albedo and accelerating snow melt (Flanner et al., 2007, 2009). Warren and Wiscombe (1980) found that a mixing ratio of 10 ng g^{-1} of soot in snow can reduce snow albedo levels by 1%. Light et al. (1998) determined that 150 ng g^{-1} of BC embedded in sea ice can reduce ice albedo levels by a maximum of 30% (Light et al., 1998). Among its main light-absorbing impurities, 1 ng g^{-1} of BC has approximately the same effect on the albedo of snow and ice at 500 nm as 50 ng g^{-1} of dust (Warren, 1982). Doherty et al. (2013) analyzed field measurements of vertical distributions of BC and other ILAPs in snow in the Arctic during the melt season and found significant melt amplification owing to an increased mixing ratio of BC by up to a factor of 5.~~

~~It is widely known that small snow albedo changes can have significant effects on global warming patterns, involving changes in snow morphology, sublimation, and melt rates (Brandt et al., 2011; Hadley and Kirchstetter, 2012; Warren and Wiscombe, 1985~~Brandt et al., 2011; Hadley and Kirchstetter, 2012; Warren and Wiscombe, 1985~~).~~ ~~Warren and Wiscombe (1980) found that~~ A~~a~~ mixing ratio of 10 ng g^{-1} of soot in snow can reduce snow albedo ~~levels~~ by 1% (Warren and Wiscombe, 1980). ~~Light et al. (1998) determined that~~ 150 ng g^{-1} of BC embedded in sea ice can reduce ice albedo ~~levels~~ by ~~a maximum of~~up to 30% (Light et al., 1998). 1 ng g^{-1} of BC has approximately the same effect ~~on the albedo of snow and ice at 500 nm~~ as 50 ng g^{-1} of dust on the albedo of snow and ice at 500 nm (Warren, 1982). ~~Doherty et al. (2013) analyzed field measurements of vertical distributions of BC and other ILAPs in snow in the Arctic during the melt season and found significant melt amplification due to an~~

~~increased mixing ratio of BC by up to a factor of 5.~~ Yasunari et al. (2015) suggest~~ed~~s that the existence of snow darkening effect in the Earth system associated with ~~dust, BC, and OC~~ILAPs contributes significantly to enhanced surface warming over continents in northern hemisphere midlatitudes during boreal spring, raising the surface skin temperature by approximately 3–6 K near the snowline. Modeling soot in snow as an "external mixture" (impurities particles separated from ice particles), if it is actually located inside the ice grains as an "internal mixture", may underestimate its true effect on albedo reduction by 50% (Warren and Wiscombe, 1985).~~Warren and Wiscombe (1985) pointed out that modeling soot in snow as an "external mixture" (impurities particles separated from ice particles), may underestimate the true effect of the impurities as a given reduction of albedo by about half as much soot, if the soot is instead located inside the ice grains as an "internal mixture".~~ Assuming internal rather than external mixing of BC in snow increases BC absorption coefficient by a factor of two and gained better agreement with empirical data (Cappa et al., 2012; Hansen and Nazarenko, 2004~~Hansen et al., 2004; Cappa et al., 2012~~).~~Hansen et al. (2004) and Cappa et al. (2012) noted that for a given BC mass on snow albedo, the internal mixing of BC in snow is a better approximation than external mixing, whereas internal mixing increases the BC absorption coefficient by a factor of two, for better agreement with empirical data. Hadley and Kirchstetter (2012) also indicated that~~ I~~i~~ncreasing the size of snow grains could decrease snow albedo and amplifi~~ed~~y the radiative perturbation of BC (Hadley and Kirchstetter, 2012). For a snow grain~~n~~ optical effective radius (R_{eff}) of 100 μm~~mm~~, the albedo reduction caused by 100 ng g^{-1} of BC is 0.019 for spherical snow grains but only 0.012 for equidimensional nonspherical snow grains (Dang et al., 2016). ~~Fierce et al. (2016) pointed out that~~ BC ~~that is~~ coated with non-absorbing particles ~~material~~ absorbs more strongly than the

same amount of BC in an uncoated particle, but the magnitude of this absorption enhancement is yet to be quantified (Fierce et al., 2016). ~~still a challenge.~~ A modeling study suggested that~~He et al. (2014) indicated that~~ BC-snow internal mixing increases the albedo forcing by 40–60% compared with external mixing, and coated BC increases the forcing by 30–50% compared with uncoated BC aggregates, whereas Koch snowflakes reduce the forcing by 20–40% relative to spherical snow grains (He et al., 2014) ~~using a global chemical transport model in conjunction with a stochastic snow model and a radiative transfer model~~.

~~Climate models have indicated that the reduction in surface albedo caused by BC leads to global warming and nearly global melting of snow and ice (Hansen and Nazarenko, 2004). Recent modeling studies have estimated regional and global radiative forcing caused by ILAPs deposited on snow by reducing the surface albedo (Flanner, 2013; Flanner et al., 2007; Hansen and Nazarenko, 2004; Jacobson, 2004; Koch et al., 2009; Qian et al., 2015; Zhao et al., 2014). Flanner et al. (2012) demonstrated that the simulated global-mean fraction of BC residing within ice grains of surface snow increases the global BC/snow radiative forcing by 34–86% relative to paired control simulations that apply external optical properties to all BC. Bond et al. (2013) estimated the industrial-era climate forcing of BC through all forcing mechanisms to be approximately +1.1 W m^{-2}, with 90% uncertainty boundsconfidence limits of +0.17 to +2.1 W m^{-2}. This value includes the net effect of BC on radiation, clouds, and snow albedo, which have been found to heavily impact the earth's climate (Bond et al, 2013; IPCC, 2013; Li et al., 2016). Recent modeling studies have estimated regional and global radiative forcing caused by ILAPs deposited on snow by reducing the surface albedo (Flanner, 2013; Flanner et al.,~~

~~2007; Hansen and Nazarenko, 2004; Jacobson, 2004; Koch et al., 2009; Qian et al., 2015; Zhao et al., 2014).~~

~~Climate models have indicated that the reduction in surface albedo caused by BC leads to global warming and nearly global melting of snow and ice (Hansen and Nazarenko, 2004).~~ ~~Regional forcing by BC contamination in snow in snow covered regions, e.g., the Arctic and Himalayas (0.6 and 3.0 W m^{-2}, respectively), is comparable to carbon dioxide levels (1.5 W m^{-2}) in the atmosphere since the pre-industrial period (Flanner et al., 2007). The efficacy of radiative forcing due to BC deposited on snow has been estimated to be as high as 236% (Hansen et al., 2005).~~

Although ~~AD~~ MD is a less efficient absorber than BC and OC, ~~in situ~~ field campaigns ~~measurements~~ on collecting~~of~~ seasonal snow samples across northern China and the Himalayas have shown high ~~AD~~ MD loadings (Guan et al., 2015; Kang et al., 2016; Wang et al., 2012; Wang et al.,~~,~~ 2013a). In some regions, especially areas with thin and patchy snow cover and mountainous regions, soil dust significantly decreases the snow albedo, exceeding the influence of BC. However, models di~~d~~o not capture these potential~~ly~~ large sources of local dust in snowpack and may overestimate BC forcing processes (Painter et al., 2007, 2010, 2012). Recently, several seasonal snow collection campaigns were performed across northern China, the Himalayas, North America, Greenland and the Arctic (Cong et al., 2015; Dang and Hegg, 2014; Doherty et al., 2010, 2014; Huang et al., 2011; Xu et al., 2009, 2012; Zhao et al., 2014). However, determining the effects of ~~light-absorbing impurities~~ILAPs on snow albedo reduction continues to ~~involve~~ be challenging~~present numerous challenges~~ (Huang et al., 2011; Wang et al., 2013a, 2015; Ye et al., 2012; Zhang et al., 2013a).

To date~~our knowledge~~, ~~there are~~ only a few studies have ~~that~~ compared modeled and observed snow albedo reduction due to ILAPs in snow (Dang et al., 2015; Flanner et al., 2007, 2012; Grenfell et al., 1994; Liou et al., 2014; Warren and Wiscombe~~Warren et al.~~, 1980~~Ref.~~). ~~We analyzed observed ILAPs in seasonal snow through a Chinese survey in 2014 following a snow campaign held in 2010 across northern China carried out by Huang et al. (2011). The area is seasonally covered with snow for approximately 3-6 months from late fall to early spring (Wang et al., 2014). Our sampling sites were located across northeastern China and were positioned far from the northern boundaries of desert regions, such as the Gobi Desert in southern Mongolia and the Badain Jaran and Tengger Deserts in northwestern China (Li et al., 2009). Zhang et al. (2013), using a positive matrix factorization (PMF) receptor model, showed that industrial pollution sources are a major factor affecting seasonal snow across northeastern China. Huang et al. (2015a) developed a new technique for distinguishing anthropogenic dust from natural dust based on Cloud-Aerosol Lidar and Infrared Pathfinder Satellite Observation (CALIPSO) dust and planetary boundary layer (PBL) height retrievals along with a land-use dataset. The authors found that the annual mean contribution of anthropogenic dust in eastern China is approximately 91.8% owing to recent urbanization and human activity (Huang et al., 2015a). In this paper~~ To gain some in-depth knowledge on this topic~~In this study~~, a 2014 snow survey was first performed across northeastern China to analyze light absorption of ILAPs in seasonal snow, and modeling studies were then conducted to~~the comparison of~~ compare snow albedo reduction due to various assumptions of internal/external mixing of~~ed~~ BC in snow and different snow grain shapes.~~This paper is organized as follows. In section 2, we present the~~, experimental procedures, ~~including a new radiative transfer model (Spectral Albedo Model for Dirty Snow, or~~

SAMDS). After describing our methods (Sect. 2)In section 3, wwe demonstrateed explore the climatic effectslight absorption by snowpack containing of ILAPs (including BC, OC, and AD) on seasonal snowacross northeastnortheastern China for less snow fallen year through a Chinese survey in 2014 following the snow surveys held in 2010 and 2012 across northern China carried out by Huang et al. (2011), and Ye et al. (2012). Then, a comparison of the snow albedo reduction under clear sky conditions measured by using a field spectroradiometer and simulated bycollected through surface measurements and the Snow, Ice, and Aerosol Radiation (SNICAR) model and SAMDS model based on two-stream radiative transfer solution is present. The SAMDS model is also used for the computation of light absorption by complex ILAPs in snow for application to analyze the effects of aggregates and snow grain shapes (fractal particlesgrains, hexagonal plates/columns, and spheres) with the snow albedo reduction due to and internal and /external mixing structuresof BC and snow on snow albedo. Finally, conclusions areConcluding and discussing remarks are given in section 4. across northeastern China, which are highly correlated with industrial pollution resulting from human activity. Therefore, ILAPs in seasonal snow are examined during a snow campaign, and the snow albedo is measured using an HR-1024 field spectroradiometer and simulated using two radiative transfer models (i.e., SNICAR and SAMDS).

2 Experimental procedures

2.1 Snow field campaign in January 2014 ~~January~~

In 2014, tThere was less snowfall in January 2014 than in previous years (e.g., 2010), and thus only 92 snow samples (13 surface snow including 10 fresh and 3 aged ones, and 79 sub-surface snow samples) at 13 sites were collected during this snow survey.

There were 10 fresh snow, and 3 aged snow for surface snow. In 2014, there was less snowfall in January than in previous years (e.g., 2010), and only 92 snow samples at 13 sites were collected. The snow sampling sites in this study were numbered starting began at 90 (see Figure 1 and Table 1), following thewhich are numbered in chronological order fromfollowed by Wang et al. (2013a), and Ye et al. (2012). Samples from at sites 90-93 were collected from grassland and cropland areas in Inner Mongolia. Sites 94-98 and sites 99-102 were located in the Heilongjiang and Jilin provinces, respectively, which are were the most heavily polluted areas in northern China during winter. The snow sampling procedures routes were similar to those used in the previous survey conducted in 2010 across northern China (Huang et al., 2011). To prevent contamination, the sampling sites were positioned 50 km from cities and at least 1 km upwind of approach roads or railways; the only exception was site 101, which was positioned downwind and close to villages. Two vertical profiles of snow samples ("left" and "right") were collected through the whole depth of the snowpack at all the sites to reduce the possible contamination by artificial effects during the sampling process, and we note that the dusty or polluted layers were separately collected during the sampling process.We gathered the "left" and "right" snow samples at vertical intervals of snow samples every 5 cm for each layer from the surface to the bottom unless a particularly dusty or polluted layer was present. All of the datasets of C_{BC}^{equiv}, C_{BC}^{equiv}, and C_{BC}^{est} in seasonal snow listed in from Ttable 1 are the average values from the two adjacent snow samples through the whole depth of the snowpack. Snow grain sizes (R_m) were measured by visual inspection on millimeter-gridded sheets viewed through a magnifying glass. The snow samples were kept frozen until the filtration process was initiated. In a temporary lab based in a hotel, we quickly melted the snow samples in a microwave, let them settle for 3-5

minutes, and then filtered the resulting water samples through a 0.4-μm nuclepore filter to extract particulates. ~~and~~

2.2 Chemical speciation

~~The m~~Major water-soluble ions and trace elements in surface snow samples during this snow survey have already been investigated by Wang et al. (2015). However, the importance of ILAPs in seasonal snow during this survey ~~have~~has not been discussed ~~shown~~ yet~~,~~ which will be addressed below. ~~For the importance of the ILAPs in snow, we will present the contribution and discuss the potential the emission sources of the ILAPs together with suites of other corresponding chemical constituents in seasonal snow. For instance, Hegg et al., (2009, 2010) shown that~~analysed the source attribution of the ILAPs in arctic snow by using a positive matrix factorization (PMF) model consisted with trajectory analysis and satellite fire maps. ~~The chemical analysis of snow samples from the 2014 Chinese survey was described by Wang et al. (2015), and it was similar to the analysis applied for snow samples described by Hegg et al. (2009, 2010).~~ Briefly, major ions (SO_4^{2-}~~SO42−~~, NO_3^-~~NO3−~~, Cl^-, Na^+, K^+, and NH_4^+~~NH4+~~) were analyzed with an ion chromatograph (Dionex, Sunnyvale, CA), and trace elements of Fe and Al were measured by inductively coupled plasma mass spectrometry (ICP-MS). These analytical procedures have been described elsewhere (Yesubabu et al., 2014). In this paper, the major ions are used to retrieve the sea salt ~~components aerosol~~ and biosmoke potassium ($K^+_{Biosmoke}$) ~~$K^+_{Biosmoke}$~~ $K^+_{Biosmoke}$~~, which datasets were not shown by Wang et al. (2015). However, only SO_4^{2-}, NO_3^-~~SO_4^{2-}~~, NO_3^-, and NH_4^+~~NH4+~~ were reprinted from Wang et al. (2015) to reveal the mass contribution of the ILAPsS and the chemical constituents in seasonal snow during this snow survey.~~ Previous studies have revealed considerable variations in iron (Fe) of

2-5% in dust (Lafon et al., 2006), although Al is more stable than Fe in the earth's crust. Hence, we retrieved the mass concentration of ~~minerals~~ MD via the Al concentration assuming a fraction of 7% ~~when estimating the~~in MD~~dust levels~~ (Arhami et al., 2006; Lorenz et al., 2006; Zhang et al., 2003). Sea salt was estimated following the method presented in Pio et al. (2007):

$$\text{Sea salt} = Na^{+}_{Ss} + Cl^{-} + 0.12Na^{+}_{Ss} + 0.038Na^{+}_{Ss} + 0.038Na^{+}_{Ss} + 0.25Na^{+}_{Ss}, \quad (1)$$

where subscript Ss means sea salt~~–~~ sources, ~~where~~ Na_{Ss} was calculated using the following formula (Hsu et al., 2009):

$$Na_{Ss} = Na_{Total} - Al \times (Na/Al)_{Crust}. \quad (2)$$

Following Hsu et al. (2009), the contribution of $K^{+}_{Biosmoke}$ ~~$K^{+}_{Biosmoke}$~~ was determined using the following equations:

$$K^{+}_{Biosmoke} = K_{Total} - K_{Dust} - K_{Ss}, \quad (3)$$

$$K_{Dust} = Al \times (K/Al)_{Crust}, \quad (4)$$

$$Na_{Ss} = Na_{Total} - Al \times (Na/Al)_{Crust}, \quad (5)$$

$$K_{Ss} = Na_{Ss} \times 0.038, \quad (6)$$

where $K^{+}_{Biosmoke}$ ~~$K^{+}_{Biosmoke}$~~, K_{Dust}, and K_{Ss} refer to biosmoke potassium, dust-derived potassium, and sea-salt-derived potassium, respectively. Equations (4), (5), and (6) were derived from Hsu et al. (2009) and Pio et al. (2007).

2.3 Spectrophotometric analysis

Recent studies indicated that the light absorption by MD should be more sensitive to the presence of strongly absorbing iron oxides such as hematite and goethite than to other minerals (Alfaro et al., 2004; Sokolik and Toon, 1999)~~As Alfaro et al., (2004) indicated that the light absorption by mineral dust~~MD ~~should be highly sensitive to~~

~~their content in iron oxides (hematite, goethite, etc.) based on Mie theory. Sokolik and Toon., (1999) also pointed out that computations performed with optical models show that the absorbing potential of mineral dustMD is more sensitive to the presence of strongly absorbing iron oxides such as hematite and goethite than to other minerals (Sokolik and Toon, 1999)~~. Thus, it is now possible to assess the absorption properties of ~~mineral dust~~MD by using iron oxide content (Bond et al., 1999). In this study, the iron (Hereinafter ~~Hereafter~~ simply "Fe"~~the same as Fe~~) in seasonal snow is assumed to be originating ~~originated~~ from ~~mineral dust~~MD during this survey, ~~which~~ following~~ed~~ the procedures performed by Wang et al., (2013a). ~~Assuming that iron originated from mineral dust in seasonal snow, w~~We measured the mixing ratios of BC and OC using an integrating sphere/integrating sandwich spectrophotometer (ISSW), which was first described by Grenfell et al. (2011) and used by Doherty et al. (2010, 2014) and Wang et al. (2013a)~~ to measure mixing ratios of BC and OC~~. The equivalent BC (C_{BC}^{equiv} C_{BC}^{equiv}), maximum BC (C_{BC}^{max} C_{BC}^{max}), estimated BC (C_{BC}^{est} C_{BC}^{est}), fraction of light absorption by non-BC ILAPs (f_{non-BC}^{est} f_{non-BC}^{est}), and absorption Ångstrom exponent of all ILAPs (Å$_{tot}$) were described by Doherty et al. (2010). Previous studies have concluded that ~~light absorbing particles~~ILAPs are primarily derived from BC, OC, and Fe~~iron (Fe)~~. The mass loadings of BC (L_{BC}) and OC (L_{OC})~~and OC~~ were calculated using the following equation:

$$\tau_{tot}(\lambda) = \beta_{BC}(\lambda)\times L_{BC} + \beta_{OC}(\lambda)\times L_{OC} + \beta_{Fe}(\lambda)\times L_{Fe}. \quad (7)$$

Here, $\tau_{tot}(\lambda)$ refers to the measured optical depth. L_{BC} and L_{OC} ~~L_{BC} and L_{OC}~~ can be determined from this equation assuming that the mass absorption coefficients~~mass absorption efficiencies~~ (MACs~~β~~) for BC, OC, and Fe are 6.3, 0.3, and 0.9 m^2 g^{-1}, respectively, at 550 nm and that the absorption Ångstrom exponents (Å or AAE) for

BC, OC and Fe are 1.1, 6, and 3, respectively (e.g., Equations (2) and (3) in Wang et al., 2013a).

2.4 Aerosol optical depth and snow albedo measurements

The Microtops Π Sun photometer has been widely used to measure aerosol optical depth (AOD) in recent years (More et al., 2013; Porter et al., 2001; Zawadzka et al., 2014), and is recognized as a very useful tool for validating aerosol retrievals from satellite sensors.~~We used a portable and reliable Microtops Π Sun photometer at wavelengths of 340, 440, 675, 870, and 936 nm instead of the CE318 sun tracking photometer (Holben et al., 2006) to measure the in situsurface aerosol optical depth (AOD).~~ Ichoku et al. (2002b) and Morys et al. (2001) provided a general description of the Microtops Π Sun photometer's design, calibration, and performance. ~~The Microtops Π Sun photometer has been widely used in recent years (de Mourgues et al., 1970; Porter et al., 2001; Zawadzka et al., 2014) and is recognized as a very useful tool for validating aerosol retrievals from satellite sensors. A Microtops Π Sun photometer was calibrated following the methods presented by Morys et al. (2001) and Ichoku et al. (2002b).~~ To better understand the background weather conditions in the local atmosphere during this snow survey, we used a portable and reliable Microtops Π Sun photometer at wavelengths of 340, 440, 675, 870, and 936 nm instead of the CE318 sun tracking photometer to measure the surface AOD in this study.~~, a Microtops Π Sun photometer was used during the 2014 Chinese surveyin this study.~~ AOD measurements were collected in cloud-free conditions between 11:00 am and 1:00 pm (Beijing local time) to prevent the effects of optical distortions due to large solar zenith angles. ~~We used~~Then, the Moderate Resolution Imaging Spectroradiometer (MODIS) on the Aqua and Terra satellites was used to retrieve the

AOD and fire spot datasets (Kaufman et al., 1997; Zhang et al., 2013b; Zhao et al., 2014). The retrieved MODIS AOD is reliable and accurate when applied to three visible channels over vegetated land and ocean surfaces (Chu et al., 2002; Ichoku et al., 2002a; Remer et al., 2002). Fire locations are based on data provided by the MODIS FIRMS system from October ~~2014~~2013 to January ~~2015~~2014. The land-cover types (Figures 6 and 7) were obtained from the Collection 5.1 MODIS global land-cover type product (MCD12C1) at a 0.05° spatial resolution and included 17 different surface vegetation types (Friedl et al., 2010; Loveland and Belward, 1997).

Snow albedo plays a key role in ~~affecting the~~ energy balance and climate in the cryosphere (e.g. Hadley and Kirchstetter, 2012; Liou et al., 2014; Warren and Wiscombe, 1985). Wright et al. (2014) indicated that the spectral albedo measured ~~by~~ using an Analytical Spectral Devices (ASD) s~~S~~pectroradiometer~~s~~ at 350-2200 nm is in agreement with albedo measurements at the baseline Surface Radiation Network (BSRN). Wuttke et al. (2006a) pointed out that the spectroradiometer instrument is considered as ~~the more~~the most capable, rapid, and mobile to conduct spectral albedo measurements during short time periods, especially in the very cold regions (e.g. in the Arctic). The major advantage is the more extensive wavelength range, and the cosine error is less than 5% for solar zenith angles below 85° at the wavelength of 320 nm~~have been used to measure the surface spectral albedo~~ (~~Kotthaus et al., 2014; Wright et al., 2014;~~ Wuttke et al., 2006a, b). In ~~the 2014 Chinese survey~~this study, snow albedo measurements were obtained using a HR-1024 field ~~–~~spectroradiometer (SVC, Spectra Vista Corporation, Poughkeepsie, NY, USA). This instrument has a spectral range of 350-2500 nm with resolutions of 3.5 nm (350~~–~~1000 nm), 9.5 nm (1000~~–~~1850 nm), and 6.5 nm (1850~~–~~2500 nm). Normally, the relative position of the

spectroradiometer is at a distance of 1m from the optical element for the active field of view ~~According to previously described procedures, we measured the snow albedo 1 m above the ground~~ (Carmagnola et al., 2013). A standard "white" reflectance panel with a VIS–SWIR broadband albedo of 0.98 (P_λ) was used to measure the reflectance spectra along with the target. The reflectance spectra of surface snow (R_s) and the standard panel (R_p) were measured at least ten times. Then, the snow albedo (α) was calculated as follows:

$$\alpha = (R_s/R_p)\times P_\lambda. \quad (8)$$

The nominal fi~~ll~~ed of view (FOV) lens is 8° to enable the instrument to look at different size targets. In order to receive more direct solar radiation, t~~T~~he direction of the instrument was oriented to the s~~S~~un~~.~~ h~~H~~orizon angles to measure snow albedo~~in order to receive more direct solar radiation~~. The small size of the fore optics greatly reduces errors associated with instrument self-shadowing. Even when the area viewed by the fore optic is outside the direct shadow of the instrument, the instrument still blocks some of the illumination (either diffuse skylight or light scattered off surrounding objects) that would normally be striking the surface under observation for measuring full-sky-irradiance throughout the entire 350~~–~~–~~–~~2500 nm wavelengths. Further information on HR-1024 field spectroradiometer use and on the calibration procedure can be found in Wright et al. (2014)~~.~~. The measured solar zenith angles and the other parameters ~~datasets~~ used to simulate snow albedo in this study have been labeled in Figure 11.

2.5 Model simulations

BC and ~~dust~~ MD sensitivity effects on the snow albedo simulated by the Snow, Ice, and Aerosol Radiation (SNICAR) model have been validated through recent

simulations and field measurements (Flanner et al., 2007, 2009; Qian et al., 2014; Zhao et al., 2014). We used the offline SNICAR model to simulate the reduction in surface snow albedo resulting from ILAPs contamination (Flanner et al., 2007), and we compared the results with our spectroradiometer surface measurements. The SNICAR model calculates the snow albedo as the ratio of the upward ~~and~~ to downward solar flux at the snow surface. The measured parameters, including the measured snow grain radius (R_m), snow density, snow thickness, solar zenith angle θ, and mixing ratios of BC and ~~AD~~MD, were used to run the SNICAR model under clear sky conditions. The visible and near-infrared albedos of the underlying ground were 0.2 and 0.4, respectively, as derived from MODIS remote sensing. The ~~mass absorption cross section (~~MAC~~)~~ of BC was assumed to be 7.5 m^2 g^{-1} at 550 nm.

The Spectral Albedo Model for Dirty Snow (SAMDS) based on asymptotic radiative transfer theory was used for calculating spectral snow albedo as a function of the snow grain radius, the mixing ratios of ILAPs (BC, ~~AD~~MD, and OC), and ~~mass absorption efficiencies~~MACs of impurities~~ was used and is based on asymptotic radiative transfer theory~~. A detailed description of asymptotic analytical radiative transfer theory for ~~snowpack~~SAMDS ~~was~~~~could~~can be found ~~presented by~~in Zhang et al. (2017~~6~~).~~This model explicitly considers (i) mixing states between impurities and snow grains, (ii) the irregular morphology of snow grains and aerosol particles, (iii) specific mineral compositions and size distributions of dust in snow, (iv) aging processes of snow grains and soot aggregates, and (v) multilayers for studying vertical distributions of snow grains and impurities.~~

Briefly, the surface albedo can be calculated using the following asymptotic approximate analytical solution derived from radiative transfer theory (Kokhanovsk and Zege, 2004; Rozenberg, 1962; Zege et al., 1991):

$$R_d(\lambda) = \exp(-4S(\lambda)\mu(\nu_0)). \quad (9)$$

Here, $R_d(\lambda)$ $R_d(\lambda)$ is the plane albedo, ν_0 ν_0 is the solar zenith angle, and $u(\nu_0)$ $\mu(\nu_0)$ refers to the escape function in radiative transfer theory, and ~~can~~ is ~~be~~ parameterized following Kokhanovsky and Zege (2004):

$$\mu(\nu_0) = \frac{3}{7}(1+2\cos\nu_0), \quad (10)$$

where λ λ is the wavelength, $S(\lambda)$ $S(\lambda)$ is the similarity parameter, and

$$S(\lambda) = \sqrt{\frac{\sigma_{abs}}{3\sigma_{ext}(1-g)}}. \quad (11)$$

Here, σ_{abs} and σ_{ext} σ_{abs} ~~and~~ σ_{ext} are the absorption and extinction coefficients, respectively, and g g is the asymmetry parameter (the average cosine of the phase function of the medium).

According to Equations (18) and (25) in Kokhanovsky and Zege (2004), the extinction coefficients of particles can be expressed as follows:

$$\sigma_{ext} = \frac{l_{tr}}{1-g} = \frac{3C_v}{2r_{eff}}, \quad (12)$$

where l_{tr} l_{tr} is the photon transport path length, C_v C_v is the volumetric snow particle concentration, and r_{ef} r_{eff} is the effective grain size, which ~~is~~ equals to the radius of the volume-to-surface equivalent sphere: $r_{ef} = \frac{3\overline{V}}{4\overline{A}}$ $r_{eff} = \frac{3\overline{V}}{4\overline{A}}$, where $\overline{V}$ and $\overline{A}$ $\overline{V}$ ~~and~~ $\overline{A}$ are the average volume and ~~average~~ cross-sectional (geometric shadow) area of snow grains, respectively.

The absorption coefficient σ_{abs} σ_{abs} in Equation (11) for arbitrarily shaped and weakly absorbing large grains is proportional to the volume concentration (Kokhanovsky and Zege, 2004):

$$\sigma_{abs}=B\cdot\frac{4\pi k(\lambda)}{\lambda}\cdot C_v, \quad (13)$$

where $k(\lambda)$ k(λ) is the imaginary component of the complex refractive index for ice, and B ~~*B*~~ is a factor that is only dependent on ~~the~~ particle shape. The theory based on the ray-optics approach shows that g in Equation (11) and B in Equation (13) are 0.89 and 1.27 for spheres, 0.84 and 1.50 for hexagonal plates/columns, and 0.75 and 1.84 for fractal grains, respectively.

The total absorption coefficient, σ_{abs} σ_{abs}, can be derived from the absorption by snow, S_{abs}^{snow} σ_{abs}^{snow}, and the absorption by ~~light-absorbing impurities~~ILAPs (~~,~~ σ_{abs}^{dust} ~~,~~ σ_{abs}^{BC}, σ_{abs}^{MD}~~dust~~, and σ_{abs}^{OC}): ~~S_{abs}^{dust}, S_{abs}^{BC}, and S_{abs}^{OC}:~~

$$\sigma_{abs}=\sigma_{abs}^{snow}+\sigma_{abs}^{BC}+\sigma_{abs}^{dust}\text{MD}+\sigma_{abs}^{BC}+\sigma_{abs}^{OC}. \quad (14)$$

The hemispherical reflectance with a zenith angle ν_0 ν_0 can be expressed as follows:

$$R_d(\lambda) = \exp\Big(- 4\cdot\sqrt{\frac{4B}{9(1-g)}\cdot\frac{2\pi\cdot r_{eff}}{\lambda}\cdot k(\lambda)+\frac{\rho_{ice}\cdot 2r_{eff}}{9(1-g)}\cdot MAC_{abs}^{BC}\cdot C_{BC}^{*}+\frac{\rho_{ice}\cdot 2r_{eff}}{9(1-g)}\cdot MAC_{abs}^{dustMD}\cdot C_{dustMD}^{*}+\frac{\rho_{ice}\cdot 2r_{eff}}{9(1-g)}\cdot MAC_{abs}^{BC}\cdot C_{BC}^{*}+\frac{\rho_{ice}\cdot 2r_{eff}}{9(1-g)}\cdot MAC_{abs}^{OC}\cdot Cs C_{OC}^{*}}\cdot\frac{3}{7}(1+2\cos\nu_0)\Big)$$

$$\exp\Big(- \sqrt{94.746\cdot\frac{r_{eff}}{\lambda}\cdot k(\lambda)+5.163\cdot r_{eff}\cdot(MAC_{abs}^{BC}\cdot C_{BC}^{*}+MAC_{abs}^{dustMD}\cdot C_{dustMD}^{*}+MAC_{abs}^{BC}\cdot C_{BC}^{*}+MAC_{abs}^{OC}\cdot C_{OC}^{*})}\cdot(1+2\cos\nu_0)\Big) \quad , \quad \text{for spherical grains;}$$

$$= \exp\Big(-4.95\cdot\sqrt{\frac{\pi\cdot r_{eff}\cdot\rho(k(\lambda)+\alpha\cdot C_{dustBC}^{*}+\beta\cdot C_{BCMD}^{*}+\chi\cdot C_{OC}^{*})}{\lambda}}\cdot(1+2\cos\nu_0)\Big) \quad , \quad \text{for hexagonal grains;}$$

(15)

$$\exp\Big(-4.38\cdot\sqrt{\frac{\pi\cdot r_{eff}\cdot\rho(k(\lambda)+\alpha\cdot C_{dustBC}^{*}+\beta\cdot C_{BCMD}^{*}+\chi\cdot C_{OC}^{*})}{\lambda}}\cdot(1+2\cos\nu_0)\Big), \quad \text{for fractal grains.}$$

~~A detailed description of asymptotic analytical radiative transfer theory for snowpack was presented by Zhang et al. (2016).~~ Previous studies have also shown that the spectral snow albedo is more sensitive to snow grain size and light conditions than BC contamination and snow depths at near-infrared wavelengths (Warren, 1982). Therefore, the snow grain optical effective radius (R_{eff}) was retrieved based on the spectral albedo measured at λ=1.3 μm ~~(Table 4)~~, where snow grain size dominates the snow albedo variations and the effects of ~~light-absorbing particles~~ILAPs at this wavelength are negligible (Warren and Wiscombe, 1980).

3 Results

3.1 The spatial distribution of AOD

~~The~~ AOD is a major optical parameter for aerosol particles and a key factor affecting global climate (Holben et al., 1991, 2001, 2006; Smith et al., 2014; Srivastava and Bhardwaj, 2014). Most of the snow samples were collected in the afternoon at the Aqua-MODIS (13:30 LT) overpass time in order to compare the local AODs at~~in~~ sampling sites by using a~~n~~ spectroradiometer with the satellite remote sensing. The AOD~~s~~ spatial distribution derived from the Aqua-MODIS satellite over northern China ~~from October to January~~ associated with sampling site numbers is shown in Figure 1 during this snow survey. ~~For most of the snow samples collected in the afternoon at the Aqua-MODIS (13:30 LT) overpass time, the averaged spatial AOD distribution was derived from the Aqua-MODIS satellite "Aerosol" product during the sampling period across northern China. The AOD spatial distribution over northern China is shown in Figure 1 for the period from October to January.~~ The average AOD in the studied area ranged from 0.1 to 1.0 and exhibited strong spatial inhomogeneity. The largest AOD~~s~~ values (up to approximately 1.0) retrieved from the MODIS

satellite were associated with anthropogenic pollution over northeastern China during the 2014 sampling period. These large values, which exceeded 0.6, were related to local air pollution from industrial areas (Che et al., 2015~~b~~; Wang et al., 2010b~~a~~). In contrast, the MODIS-Aqua results indicate that the smallest AOD~~s~~ values (as low as 0.1) at 550 nm were found over the Gobi Desert in Inner Mongolia and were related to strong winter winds. Similar patterns in the retrieved MODIS AOD were found by Zhao et al. (2014) and Zhang et al. (2013b). Although previous studies have indicated that AOD~~s~~ values ~~in~~ across northeastern~~ern~~ China are among the highest in East Asia (Ax et al., 1970; Bi et al., 2014; Che et al., 2009; Routray et al., 2013; Wang et al., 2013b; Xia et al., 2005, 2007), field experiments of aerosol optical properties across northeastern China ~~have been~~were limited. Compared with the retrieved AOD by the remote sensing, the surface measurements of AOD were also conducted during this snow survey. Generally, the measured AOD ~~were~~ gradually increased ~~higher~~ from Inner Mongolia regions ~~moved~~ to the industrial areas across ~~northeast~~northeastern China. ~~To evaluate the accuracy of the AODs, in situ AOD measurements were collected during the snow sampling period in January 2014. The in situ AOD measurements were generally consistent with the spatial AOD distribution retrieved from MODIS across northern China, although the retrieved AOD was slightly higher than that retrieved from the in situ measurements in the study area.~~ In Inner Mongolia, the average AOD was less than 0.25 for sites ~~1 XX~~90 to ~~6 XX~~93 under clear sky conditions. We found large discrepancy ~~variations~~ of 40-50% in the same area within ~~in~~ the 1-hour measurements collected from sites ~~6a~~ 95a~~XX~~ and ~~6b~~~~XX~~95b, which could be possibly~~; these variations were~~ correlated with regional biomass burning ~~processes~~. However, AOD~~s~~ exceeded 0.3 at sites ~~9 XX~~98 and ~~12XX~~101, which were significantly influenced by anthropogenic air pollution from industrial areas across

northern China. MODIS active fires ~~are~~ were often spatially distributed over northeastern China and mainly resulted from human activities during cold~~er~~ seasons.

3.2 ~~Sampling statistics~~ Contributions to light absorption by ILAPs

~~Generally, we only collected t~~The aged surface snow samples were collected at ~~in~~ three sites ~~, while~~and fresh surface snow samples ~~were~~~~was~~were collected ~~in~~at the other sites during this snow survey conducted in January 2014. C_{BC}^{est} C_{BC}^{est}, C_{BC}^{max} C_{BC}^{max}, C_{BC}^{equiv} C_{BC}^{equiv}, f_{nonBC}^{est} $f_{non\text{-}BC}^{est}$, $Å_{tot}$ and snow parameters, such as snow depth, snow density, measured snow grain radius (R_m), and snow temperature, are given in Table 1 and Figure 3 for each snow layer following Wang et al. (2013a). ~~Average~~ C_{BC}^{est}~~,~~ C_{BC}^{max}~~, and~~ C_{BC}^{equiv} ~~values were calculated using "left" and "right" samples for each layer.~~ In Inner Mongolia~~Generally~~, t~~T~~he snow cover was thin and patchy ~~in Inner Mongolia, and t~~. The average snow depth at sites 90, 91, 93, and 94 was less than 10 cm, which was significantly smaller than those (13 to 20 cm) at sites 95-97 near the northern border of China~~The average snow depth was less than 10 cm from sites 90, 91, 93, and 94, which are~~was significantly lower than ~~that near the northern border of China, ranging from 13 to 20 cm at sites 95-97~~. The snow samples were collected from drifted snow in Inner Mongolia, and the mass loadings of ILAPs in seasonal snow are mainly due to blowing soil dust. Therefore, the vertical profiles of snow samples mixed with blowing soil from these sites are insufficient to represent the seasonal evolution of wet and dry deposition to snow (Wang et al., 2013a). However, the light absorption of ILAPs is still dominated by OC in these regions, which ~~will be~~has been illustrated in the following section~~., which are slightly lower than that near the northern border of China, ranging from 13 to 20 cm at sites 95-97.~~~~The snow cover~~

~~was thin and patchy in Inner Mongolia, and the average snow depth was less than 10 cm from sites 90, 91, 93, and 94, which slightly higher values near the northern border of China, ranging from 13 to 20 cm at sites 95-97.~~ The maximum snow depth was found to be 46 cm at site 102 inside a forest near the Changbai Mountains. Snow depth varied from 13 to 46 cm at sites 98 to 102 with an average of 27 cm~~The maximum snow depth of 46 cm at site 102 was found in a forest near the Changbai Mountains, averaging 27 cm and varying from 13 to 46 cm at sites 98 to 102~~. ~~Because less snow fell during the 2014 snow survey period than that in 2010Because less snow fell during the 2014 snow survey period,~~ R_m of the ~~surface~~ snow samples ~~grain radius~~ varied considerably from 0.07 to 1.3 mm. R_m~~The snow grain size~~ increased with the snow depth from the surface to the bottom~~ and was~~, larger than ~~that previously~~ recorded in previous studies because of snow melting by solar radiation and the ILAPs (Hadley and Kirchstetter, 2012; Motoyoshi et al., 2005; Painter et al., 2013; Pedersen et al., 2015). The snow density exhibited little geographical variation across northern China at 0.13 to 0.38 g cm^{-3}. High snow densities were resulted from melting or snow aging. Similar snow densities have been found in the Xinjiang region in northern China (Ye et al., 2012). At~~In this study~~site 90, we only collected one layer of snow samples from central Inner Mongolia, and C_{BC}^{est}~~the BC mixing ratio~~ was 330~~4~~ ng g^{-1} for~~in~~ aged snow. Along the northern Chinese border at sites 91-95, C_{BC}^{est}~~BC contamination~~ in the cleanest snow ranged from 30~~27~~ to 260 ng g^{-1}~~;~~ with only a few values exceeded 200 ng g^{-1}. The f_{nonBC}^{est} $f_{non\text{-}BC}^{est}$ value varied remarkably from 29 to 78%, although BC was still a major absorber in this region. Heavily polluted sites were located in industrial regions across northeastern China (sites 99-102). The surface snow C_{BC}^{est} ~~BC~~ in this region ranged from 510~~08~~ to 3~~651~~700 ng g^{-1}, and the

highest C_{BC}^{est} ~~BC~~ in the sub-surface layer of the four sites ~~(?? Check the sites and the values)~~ was 2900~~882~~ ng g^{-1} (~~in~~ Table 1). In addition, ~~the fraction of total particulate solar absorption due to~~ f_{nonBC}^{est} $f_{non\text{-}BC}^{est}$ was typically 35-74%, indicating significant light-absorbing contributions by~~that light absorption in snow is mainly attributable to~~ OC and ~~AD~~MD from human activity in the heavily polluted areas. $Å_{tot}$ ranged from 2.1 to 4.8. A higher $Å_{tot}$ is a good indicator of soil dust, which is primarily driven by the composition of mineral or soil dust. In contrast, a lower $Å_{tot}$ of 0.8-1.2 indicates that ILAPs~~light-absorbing particulates~~ in the snow are dominated by BC (Bergstrom et al., 2002; Bond et al., 1999).

To better understand the ~~BC~~ distribution of C_{BC}^{est} C_{BC}^{est} in seasonal snow across northern China, ~~an~~ the spatial distribution of ~~interannual comparison of~~ C_{BC}^{est} C_{BC}^{est} ~~the BC content~~ in the surface and average snow measured during thise snow ~~2010 and 2014 Chinese~~ surveys ~~was performed, and the results~~ isare shown in Figure 4 ~~and Table 2~~. The spatial distributions of C_{BC}^{est} C_{BC}^{est} ~~BC~~ in the surface and average snow measured using ~~an~~ the ISSW spectrophotometer during the 2014 survey generally ranged from 5~~03~~ to ~~3651~~ 3700 ng g^{-1} and 6~~02~~ to 160~~035~~ ng g^{-1},~~–~~ with the medium values of 260 ng g^{-1}~~,~~ and 260 ng g^{-1}, respectively~~respectively~~. These variations of C_{BC}^{est} C_{BC}^{est} were very similar to those of the previous snow campaign by ~~, as shown in Figure 4 (~~Wang et al.~~,~~ (2013a), ~~although~~ however, ~~they were~~ much higher than those in the Xinjiang region of northwestern China (Ye et al., 2012), along the southern edge of the Tibetan Plateau (Cong et al., 2015), and ~~in~~ across North America (Doherty et al., 2014). ~~In the 2014 Chinese survey, we only collected one layer of snow samples from central Inner Mongolia, and the BC mixing ratio was 334 ng g^{-1} in aged snow.~~

~~Along the northern Chinese border at sites 91-95, BC contamination in the cleanest snow ranged from 27 to 260 ng g^{-1}; only a few values exceeded 200 ng g^{-1}. The f_{nonBC}^{est} value varied remarkably from 29 to 78%, although BC was still a major absorber in this region. Heavily polluted sites were located in industrial regions across northeastern China (sites 99-102). The surface snow BC in this region ranged from 508 to 3651 ng g^{-1}, and the highest BC in the sub-surface layer of the four sites was 2882 ng g^{-1}. In addition, the fraction of total particulate solar absorption due to f_{nonBC}^{est} was typically 35-74%, indicating that light absorption in snow is mainly attributable to OC and AD from human activity.~~

Figure 5 compares C_{BC}^{est}~~the BC mixing ratio~~ values measured via the ISSW method with the calculations during 2010 (Wang et al., 2013a) and 2014 snow surveys. ~~Ideally, the C_{BC}^{est}BC content calculated using Equation (7) should be equal to that measured via the ISSW method.~~ The two results agreed very well (R^2=0.99), indicating that Equation (7) ~~worked~~ worked ~~agreed~~ well for this measurement~~, in Figure 5. Thus,~~and the C_{BC}^{est} ~~BC content~~ measured via the ISSW method ~~was~~ was ~~found to be reasonable and~~ reliable. To compare with the mixing ratio of OC calculated from Equation (7), we used the calculated C_{BC}^{est}~~BC mixing ratios~~ listed in Figures 6-~~7~~8 and Table ~~2~~3 in the following sections.

~~3.3 Emission factors~~

~~Typically, chemical components in seasonal snow originate from different emission sources. For example, OC and BC are emitted from the incomplete combustion of fossil fuels and biofuels. K^+ is a good tracer of biomass burning (Cachier et al., 1995), whereas NO_3^- and SO_4^{2-} originate primarily from diesel oil and gasoline combustion and from coal burning with sulfur. NH_4^+ is an important indicator of fertilizer used in~~

agricultural processes. OC/BC ratios are used to represent possible emission sources of biomass burning (Bond et al., 2013; Cao et al., 2007; Cong et al., 2015; Novakov et al., 2005). The OC/BC ratio in the sampled surface snow ranged from 1.4 to 17.6 (Figure 6); a very high OC/BC ratio (17.6) was found at site 90, suggesting that biomass burning may have been a major contributor of OC through photochemical reactions during the 2014 Chinese survey. A relatively high correlation (R^2=0.87, n=13) was observed between OC and BC, indicating similar emission sources at all sampling sites except for those in central Inner Mongolia, as shown in Figure 6a. These results are consistent with those of previous studies (Ming et al., 2010). The strong correlations between NH_4^+/SO_4^{2-} and NH_4^+/NO_3^- shown in Figures 6b and 6c (R^2=0.91 and R^2=0.94, respectively; n=12) suggest that fine particles characterized as $(NH_4)_2SO_4$ and NH_4NO_3 were derived from more intense agricultural and human activities occurring near farmland areas (Ianniello et al., 2011). It is widely accepted that crustal Al originates from mineral or soil dust (Wedepohl, 1995). Therefore, the weak correlation between K^+ and Al could be explained by different emission sources of K^+ and Al (Figure 6d) often attributed to biomass burning and mineral or soil dust, respectively, in local or remote regions. Sampling site 101 (red dot in Figure 6d) is positioned very close to a village. As a result, we found a much higher K^+ than Al value owing due to high biomass burning via human activity in winter.

3.4 Mass contributions of chemical components

In Figure 6, the sampling areas were located in grasslands, croplands, and urban and built-up regions across northern China that arewere likely influenced by human activity (Huang et al., 2015a).The land-cover types (Figure 7) were obtained from the Collection 5.1 MODIS global land-cover type product (MCD12C1) at a 0.05° spatial resolution and included 17 different surface vegetation types (Friedl et al., 2010;

~~Loveland and Belward, 1997). The sampling areas were located in grasslands, croplands, and urban and built-up regions across northern China that are likely influenced by human activity (Huang et al., 2015a).~~ According to Table 2~~3~~ and Figure 6~~7~~, the NH_4^+ ~~NH_4^+~~ concentrations emitted from agricultural sources at all sites accounted for less than 2.8% because the sites were positioned 50 km from cities. However, large fractions of both SO_4^{2-}, and NO_3^- ~~SO_4^{2-} and NO_3^-~~ were observed, varying from 14.8 to 42.8% at all sites, with the highest fraction of 24.2-42.8% found in industrial areas. These results show that SO_4^{2-}, and NO_3^- ~~SO_4^{2-} and NO_3^-~~ made the greatest contributions to the total chemical concentration in the surface snow as a result of~~and are~~ significant anthropogenic emissions ~~sources~~ of fossil-fuel combustion in heavy industrial areas. More specifically, the largest ~~AD~~ MD contribution ranged from 35.3 to 46% at sites 91 to 95 ~~owing~~ due to strong winds during winter; while the ~~AD~~ MD fractions were only 5.7 to 31% at the other sites. Fractions of BC and OC were similar to those above, showing that biomass burning was a major source during winter in the sampling region. Zhang et al. (2013b) showed that OC and BC fractions vary more widely in the winter than other seasons ~~owing~~ due to industrial activity in China. Sulfate peaks were found in summer (15.4%), whereas nitrate peaks were observed in spring (11.1%). ~~Potassium ($K^+_{Biosmoke}$ $K^+_{biosmoke}$)~~ was found to be a good tracer of biomass burning, ranging from 1.3 to 5.1% along the northern Chinese border compared to lower values found at lower latitudes (1.5-2.3%), and it exhibited much higher contributions in Inner Mongolia and along the northern Chinese border ~~owing~~ due to increased emissions from cooking, open fires, and agricultural activities. The fraction of sea salt ~~aerosol~~ was found to range from 6.3 to 20.9%. Wang et al. (2015) showed that higher Cl^-/Na^+ ratios in seasonal snow found in the 2014 Chinese

survey were 1--2 times greater than those of seawater, implying that they constituted a significant source of anthropogenic Cl^- (Wang et al., 2015).

3.5 BC, OC and AD contributions to light absorption

As described by Wang et al. (2013a), light absorption by ILAPs can be determined from ISSW measurements combined with a chemical analysis of iron Fe concentrations by assuming that the light absorption of dust is dominated by iron (Fe) (Wang et al., 2013a). However, iron Fe can also be originated from industrial emissions, such as the metal and steel industries (Hegg et al., 2010; Ofosu et al., 2012). Doherty et al. (2014) used a similar method to distinguish between contributions of ILAPslight-absorbing impurities in snow in central North America. Although heavy ADMD loading was observed in 2014 surveythe study region, the fraction of light absorption due to ADMD (assumed to exist as goethite) was generally less than 10% across northeastern China (Figure 78), which was much smaller than that observed in the Qilian Mountains (e.g., Figure 11 of Wang et al., 2013a). Here, light absorption was mainly dominated by BC and OC in snow in January 2014. By contrast, the fraction of light absorption due to BC varied from 48.3 to 88.3% at all sites, with only one site dominated by OC (site 90 in central Inner Mongolia). Compared to the light absorption patterns in the Qilian Mountains, iron MD played a less significant role in particulate light absorption in snow across the northeastern China sampling areas.

3.6 3 Simulations of sSComparisons between the observed and modeled snow albedo reduction

Snow albedo reduction due to BC has been examined in previous studies (Brandt et al., 2011; Hadley and Kirchstetter, 2012; Yasunari et al., 2010). Here, a new radiative

transfer model (SAMDS) based on the asymptotic radiative transfer theory is developed to assess the effects of various factors on snow albedo, including ILAPs in snow, the snow grain shapes, and the internal/external mixing of BC and snow ~~on snow albedo based on the asymptotic radiative transfer theory~~. ~~However, few observations of the BC, OC, and AD~~MD ~~mixing effects on snow albedo reduction in seasonal snow at middle latitudes exist. In this study, we measured the snow albedo at six sites under clear conditions. A comparison of T~~the snow albedos derived from the SNICAR and SAMDS models are~~is~~ presented in Figure 8~~9~~. ~~Spectral snow albedos measured in our experiments and simulated through the SNICAR and SAMDS models are shown in Figure 12~~1. We ran the models at a solar zenith angle θ of 60-°~~C~~, which is ~~consistent~~ comparable with our experimental method for measuring snow albedo ~~and with ILAPslight-absorbing impurities~~ across northeastern China. The BC MAC used in the two models was 7.5 m^2 g^{-1} at 550 nm, which was assumed in the most recent climate assessment and is appropriate for freshly emitted BC (Bond and Bergstrom, 2006; Bond et al., 2013; Warren, 1982). Mixing ratios of BC, ~~OC~~MD, and OC~~dust~~ were chosen to vary in ~~exhibit~~ the following ranges: 0.1-5 μg g^{-1}, 2-6 μg g^{-1}, and 1-30 μg g^{-1} ~~0-5 μg g^{-1}, 0-30 μg g^{-1}, and 0-6 μg g^{-1}~~, respectively, encompassing the values measured in snow surfaces across northeastern China in this ~~study~~ and ~~in~~ previous studies ~~research~~ (Doherty et al., 2010, 2014; Wang et al., 2013a, 2014; Warren and Wiscombe, 1980; Ye et al., 2012~~Warren and Wiscombe, 1980~~) ~~and in this study~~. ~~The BC MAC used in this study was 7.5 m^2 g^{-1} at 550 nm, which was assumed in the most recent climate assessment and is appropriate for freshly emitted BC (Warren, 1982; Bond and Bergstrom, 2006; Bond et al., 2013).~~ Results showed that the albedo of fresh snow at 550 nm with R_{eff} of 100 μm– simulated by SAMDS is generally in the~~a~~ range of 0.95-0.75 for ILAPs-contaminated snow across northeastern

China (Figure 8). ~~The visible and near-infrared albedos of underlying ground surfaces were 0.2 and 0.4, respectively, according to the MODIS data.~~ The spectral albedos of pure snow derived from the SNICAR (dash lines) and SAMDS (solid lines) models agree~~d~~ well. However, there ~~was~~ is a slight tendency for the SNICAR model values to become lower than SAMDS model values when BC and ~~dust mixing ratios~~MD ~~range from 1 to 5 μg g^{-1} and 4 to 6 μg g^{-1}, respectively~~are considered. The 1~~.5~~-2.53% deviation between the SNICAR and SAMDS modeled snow albedos at 550 nm for ~~higher~~ BC mixing ratios of 1-5 μg g^{-1} indicates that albedo reduction by ILAPs~~light-absorbing impurities~~ in the SNICAR model was greater than that ~~of~~ in the SAMDS model. This deviation is in part due to the different parameterization of snow grain shapes, mixing states of snow and BC, and physical-chemical properties of impurities between the two models (Zhang et al., 2017~~6~~). More notably, snow albedos decrease~~d~~d significantly within the UV-visible wavelength, especially for the higher OC (dotted lines) ~~contents~~ mixing ratios in Figure ~~8~~9. This may be attributed to the fact that OC strongly absorbs UV-visible radiation and masks BC absorption for high AAE of OC, which decreases remarkably with increasing wavelengths (Warren and Wiscombe, 1980).

As is shown in Figure ~~9~~10, we also estimated the reduction in the spectrally weighted snow albedo for different R_{eff} values using the SNICAR and SAMDS models. ~~There was a~~A larger reduction in snow albedo by both BC and MD-contaminated snow was found for larger snow grains ~~Higher degrees of snow albedo reduction by both BC and dust-contaminated snow were generally found for larger snow grains~~ (Figure ~~9~~10a-b). For example, snow albedo reduction attributable to 1 μg g^{-1}~~000 ng g^{-1}~~, 1 μg g^{-1}, and 10 μg g^{-1} for BC, ~~dust~~MD, and OC, respectively, was 37%, 41%, and 38% greater in 200 μm snow grains (0.081, 0.0019, and 0.047) than that in 100 μm snow

grains (0.059, 0.0013, and 0.034). Both the SNICAR and SAMDS models indicated that the snow albedo is more sensitive to BC, especially ~~during~~ at low~~er~~ ILAP~~-~~s mixing ratios~~periods~~. For example, 200 ng g^{-1} of BC decreased 0.03~~the~~ snow albedo ~~by 3.4% for~~ at ~~an optical effective radius~~R_{eff} of 200 μm, which is much larger than the snow albedo reduction of 0.003 and 0.018 ~~of~~ by 2000 ng g^{-1}~~2 μg g^{-1} for~~ of ~~dust~~ MD and OC at R_{eff}~~an optical effective radius~~ of 200 μm. As Hadley and Kirchstetter (2012) noted, compared with pure 55 μm snow grains, 300 ng g^{-1} of BC contamination and growth of R_{eff} to 110 μm caused a net albedo reduction of 0.11 (from 0.82 to 0.71), ~~causing snow to absorb~~or 61% more solar energy absorption by snow. The difference ~~of~~in snow albedo reductions between SNICAR and SAMDS models increased with increasing~~s as~~ BC mixing ratio ~~as well as~~or R_{eff} ~~increases~~ (Figure 9a). However, the snow albedo reduction simulated by SNICAR is not always larger than that by SAMDS when the input contaminant is MD instead of BC (Figure 9b). For example, for R_{eff} of 100 μm, the snow albedo reduction from~~or~~ SAMDS is higher than that from~~or~~ SNICAR at MD mixing ratio < 2600 ng g^{-1}, but lower ~~than that for SNICAR~~ at MD mixing ratio > 2600 ng g^{-1}. The turning point of MD mixing ratio is not constant and depends on the value of R_{eff}. This phenomenon~~The complex difference~~ may be a result of the different input optical properties of MD between SAMDS and SNICAR models (Flanner et al., 2007; Zhang et al., 2017~~6~~). SAMDS model also considers the effect of OC on snow albedo while SNICAR model does not~~, which is not included in SNICAR model~~. The albedo reduction by OC is nonnegligible due to its high loading. As is shown, 5000 ng g^{-1} of OC was found to reduce the snow albedo by 0.016-0.059 depending on the snow grain size (50-800 μm).

~~As Hadley and Kirchstetter (2012) noted, compared with pure 55 μm snow, 300 ng g^{-1} of BC contamination and growth to 110 μm causes a net albedo reduction of 0.11 (from 0.82 to 0.71), causing snow to absorb 61% more solar energy (Hadley and Kirchstetter, 2012).~~

Previous studies have also indicated that the mixing ratio of BC (10-100 ng g^{-1}) in snow may decrease its albedo by 1-5% ~~depending on its aging process~~ (Hadley and Kirchstetter, 2012; Warren and Wiscombe, 1980~~; Hadley and Kirchstetter, 2012~~). Liou et al. (2011) demonstrated that a small BC particle on the order of 1 μm internally mixed with snow grains could effectively reduce visible snow albedo by as much as 5-10% ~~using a geometric-optics surface-wave approach for the computation of light absorption and scattering by complex and inhomogeneous particles for application to aggregates and snow grains with external and internal mixing structures~~. They also found that internal mixing of BC in snow reduces snow albedo substantially more than external mixing, and the snow grain shape plays a critical role in snow albedo calculations through its forward scattering strength by modeling the positions of BC internally mixed with different snow grain types (Liou et al., 2014). ~~Figure 11 shows the snow albedo reduction due to three shapes of snow grains (fractal particles, hexagonal plates/columns, and spheres) and the internal/external mixing of BC-snow for a solar zenith angle θ of 60^{O} as a function of BC mixing ratios computed by SMDAS model. The top panel of~~ Figure 10a~~1~~ illustrates the effect of snow shape (fractal grains, hexagonal plates/columns, and spheres) on ~~the~~ snow albedo ~~reduction~~ at the spectral wavelengths of 400 nm-1400 nm with R_{eff} of 100~~70~~ μm simulated by SAMDS model. As is shown, the differences of snow albedo caused by three snow shapes are~~is~~ remarkable. The snow albedo for spherical snow grains is higher than that for the other two shapes, which is because that~~,~~ the scattering by spherical snow

grains is more in forward direction and less to the sides, resulting in a larger g and a smaller B as discussed in section 2.5. In addition, the snow albedo reduction for aged snow such as spherical snow grains is gradualtely larger than fresh snow such as fractal snow grains, and hexagonal plates/columns snow grains with the increased BC in snow. It shows that snow albedo by spherical snow grains is typically ~~decrease~~lower by 0.0175-0.0763 than the fractal snow grains, and by 0.008-0.036 than the~~, and 0.0087-0.0361 as a function of BC mixing ratios (0-5000 ng g^{-1}), which is compared~~than ~~that with by the fractal snow grains and~~ hexagonal plates/columns snow grains as a function of BC mixing ratios (0-5000 ng g^{-1}). Dang et al. (2016) assessed the effects of snow grain shape on snow albedo using the asymmetry factors g of nonspherical ice crystal developed by Fu (2007). They obtained similar result that the albedo reduction caused by 100 ng g^{-1} of BC for spherical snow grains is larger by 0.007 than nonspherical snow grains with the same area-to-mass ratio for R_{eff} of 100 μm. Figure 10b shows the spectral albedo of snow for the internal/external mixing of BC and snow with R_{eff} of 100 μm for a solar zenith angle θ of 60° as a function of BC mixing ratio. For a given shape (hexagonal plates/columns), we ~~find~~ found that snow albedo as a function of BC mixing ratios calculated from this study decreases as the fraction of the internal mixing increases (Figure 10~~1~~b). In previous studies, the BC mixing ratio~~s~~ in seasonal snow were~~is~~ up to 3000 ng g^{-1} ~~ppb~~ due to heavy industrial activities across northern China, but the lowest ~~concentrations~~mixing ratios of BC were found in the remote ~~northeast~~northeastern on the border of Siberia, with a median ~~concentration~~value in surface snow of 100 ng g^{-1} ~~ppb~~ (Huang et al., 2011; Wang et al., 2013a, 2014; Ye et al., 2012). As a result, snow albedo by internal mixing of BC and ~~-~~snow is lower than external mixing by up to 0.036 for 3000 ng g^{-1} ~~ppb~~ BC in snow in the heavy industrial regions across ~~northeast~~northeastern China,

whereas by low to 0.0054 for 100 ng g^{-1}ppb BC in snow in the further north China near the border of Siberia and the northern part Xinjiang province. We indicated that the snow grain shape effect on snow albedo reduction between spherical snow grains and fractal particles for snow grains on absorption is relatively larger than the effect of the internal and /external mixing states of BC and snow as a function of the BC concentrationmixing ratios. However, He et al. (2014) also pointeds out that the snow albedo reductions computed by previous models under assorted assumptions vary by a factor of 2 to 5."

3.4 Comparisons between the observed and modeled snow albedo

Although the snow albedo reduction due to ILAPs has been investigated by model simulations in recent studies (Brandt et al., 2011; Flanner et al., 2007; Hadley and Kirchstetter, 2012; Liou et al., 2011, 2014; Warren and Wiscombe, 1980), we noted that there were still limited field campaigns on collecting snow samples and measuring ILAPs in seasonal snow associated with the snow albedo reduction at the middle latitudes in northern hemisphere (Doherty et al., 2010, 2014; Wang et al., 2013a; Ye et al., 2012). In this study, we measured the sSnow albedo under clear sky conditions was measured at six sites, which was compared tounder clear sky conditions during this snow survey, and the comparison of snow albedo reduction between surface measurements and the SNICAR and SAMDS model ls simulations based on Toon et al.'s (1989) two-stream radiative transfer solution was investigated in (Figure 11).Previous studies have also indicated that the mixing ratio of BC (10-100 ng g^{-1}) in snow may decrease its albedo by 1-5% depending on its aging process (Warren and Wiscombe, 1980; Hadley and Kirchstetter, 2012; Hansen and Nazarenko, 2004).{Warren, 1985 #2053}

~~Figure 12~~1 ~~compares snow albedo values under clear sky conditions collected through surface measurements and the SNICAR and SAMDS models based on Toon et al.'s (1989) two-stream radiative transfer solution.~~ ~~The m~~Model input parameters including θ, R_m, R_{eff}, and the mixing ratios of BC (C_{BC}^{est}), MD (C_{MD}) and OC (C_{OC}) ~~were~~are also ~~are listed~~displayed in Figure 11 ~~in Tables 1 and 4~~. The MAC of BC used in the ISSW is~~was~~ 6.3 $m^2 g^{-1}$ at 550 nm, although a value of 7.5 is~~was~~ used in the SNICAR and SAMDS models. Thus, the ~~mixing ratio~~value of ~~BC~~ C_{BC}^{est} ~~was~~ was corrected by dividing it by 1.19 (see Figure 11) when BC was used as the input parameter to the snow albedo models (Wang et al., 2013a). The snow albedos measured at 550 nm varied considerably from 0.99 to 0.61 ~~owing~~ due to different mixing ratios of ILAPs and snow parameters, such as snow grain size. The snow albedos predicted by the SNICAR and SAMDS models agreed well at ~~each~~ most sites based on the same input parameters. The snow albedos of the SNICAR and SAMDS models retrieved ~~from with measured snow grain sizes~~R_m complemented the surface measurements for lower ~~mixing ratios~~values of C_{BC}^{est} ~~BC~~, C_{MD} ~~OC~~, and ~~AD~~ C_{OC} (Figure 11a-d)~~MD~~. The highest C_{BC}^{est} ~~BC~~ values ~~mixing ratios~~ were ~~1461~~ 1500 ng g^{-1} (corrected value of 1200 ng g^{-1}) and ~~3651~~ 3700 ng g^{-1} (corrected value of 3100 ng g^{-1})~~ng g^{-1}~~ at sites 98 and 101, respectively, across industrial regions~~, with median values found in integrated layers of 264 and 1635 ng g^{-1}, respectively~~. The OC and ~~dust~~ MD mixing ratios were as high as 3200~~13.3~~ ~~μg~~ ng g^{-1} and ~~32~~ 3900 ~~μg~~ ng g^{-1}, respectively, in this region. Therefore, ~~The higher AD~~MD ~~mixing ratios are consistent with previous studies conducted by Zhang et al. (2013) and Huang et al. (2015a), who indicated that AD~~MD ~~is highly correlated with anthropogenic air pollution originating from human activity across northeastern China. Thus, w~~we found a larger difference in snow albedo of up to 0.2 at higher C_{BC}^{est}, C_{MD}, and C_{OC} ~~BC, OC, and AD~~MD

valuescontents between the surface measurements and the modeled albedos by both SAMDS and SNICAR models for with the measured snow grain sizesthe input of R_m (red and blue solid lines in Figure 11e-f) at sites 91, 98, and 101. When the snow albedo reduction in albedo caused by ILAPsslight-absorbing impurities at the inferred wavelength simulated by by using $R_m$measured snow grain size was not accounted for, we also calculated the snow albedos from byusing the SAMDS and SNICARSNICAR and SAMDS models bywith using the optical effective sizeR_{eff} as shown in Figure 1211 (light red and blueblue and red shaded bands), and. Results showed that, compared with the snow albedos simulated by using R_m, these values were more approximate to the surface measurementsconsistent with, especially at near-infrared wavelengths, although still a slightly higher than the surface measurements (gray shaded bands), especially at near-infrared wavelengths. This may be attributed to the fact that the R_{eff} optical effective size at these three two sampling sites was much larger than $R_m$the measured grain size. We assumedinnovatively suppose , indicating that, for the same snow grains, the radiative perturbation of ILAPslight-absorbing impurities was are amplified able to enhance with the R_{eff} in spite of the same $R_m$snow grain optical effective size, which should. Nevertheless, due to the limited measurements of snow albedo, this supposition is quite uncertain and needed to be verified by future numerous field measurements of measured snow albedos.

As indicated in Figure 1Results shown in Figures 9 and 11 confirmCombinations of the results of Figure 9 and Figure 1121, that that BC, OC, and ADMD are three main types of ILAPs found in snow that can reduce spectral snow albedo. The magnitudes oflevels and. rReduced snow albedo reduction due to ILAPs found in our measurements were generally comparable to the modeled effectsthose produced bythat found in the commonly used SAMDS SNICAR and commonly used SNICAR

~~SAMDS~~ models (Flanner et al., 2007; Zhang et al., 201~~7~~6). W~~w~~hen the mixing ratios of ILAPs are not quite high~~.~~, ~~Therefore~~we indicate that~~,~~ 100-500 ng g^{-1} of BC can lower the snow albedo by 0.014~~2~~-0.039~~6%~~ relative to pure snow with a snow grain size of 1~~2~~00 μm according to our snow field campaign, and ~~AD~~MD was found to be a weak absorber ~~owing~~ due to its lower ~~AD~~MD MAC, supporting previous observations made by Warren and Wiscombe (1980). The OC MAC is~~was~~ also lower and comparable to that of the ~~AD~~MD. A clear decreasing trend in the surface snow albedo ~~owing~~ due to the high ambient mixing ratios of OC from Inner Mongolia to northeastern China was found. The radiative transfer model~~ling~~ results presented by Zhang et al. (201~~7~~6) and measurement results of this study show that the spectral albedo of snow reduction due to the increased OC mixing ratios ~~concentration~~ (above 20 μg g^{-1}) is larger ~~for~~by a factor of 3 ~~by~~if assuming the snow grain size of 800 μm compared to 100 μm.

~~**4 The radiative transfer modeling results presented by Zhang et al. (2016) and measurement results of this study show that the spectral albedo of snow reduction caused OC levels (above 20 μg g^{-1}) to increase by a factor of 3 for a snow grain size of 800 μm compared to 100 μm.**~~

~~Discussion and c~~Conclusions

High AODs measured using a sun photometer and remote sensing devices showed continued heavy pollution in industrial regions across northern China.~~In this study, a snow survey was performed in January 2014, and 92 snow samples were collected at 13 sites across northern China. We found that higher AODs measured using a sun photometer and remote sensing devices showed that heavily polluted areas remain in industrial regions across northern China.~~ The measured C_{BC}^{est} ~~C_{BC}^{est}~~ ~~–~~through the 2014

survey via the ISSW spectrophotometer in surface and average snow ~~of 503 to 3651700 and 602 to 163500 ng g^{-1}, with the medium values of 260 ng g^{-1}, and 260 ng g^{-1}, respectively,~~ were much larger than those of previous snow field campaigns. Light absorption was likely dominated by BC and OC in seasonal snow during the entire campaign, as demonstrated with reasonably assumed values of MACs for BC, OC, and Fe.~~The nchemical composition analysison BC fraction showed that the mass contributionsILAPs in seasonal snow werewas dominated by OC and MD. However, assuming the MACs for BC, OC, and Fe are 6.3, 0.3, and 0.9 m^2 g^{-1}Assumption of BC and OC mass absorption efficiencies are 6.3 and 0.3 m^2 g^{-1}, respectively, at 550 nm, light absorption was still dominated by BC and OC in seasonal snow during the entire campaign. The light absorbing contribution fraction of the MD mixing ratios was larger at high latitudes than at low latitudes due to strong winds transporting snow~~

Model simulation results indicated that ~~. Then,~~

~~In this study, a Chinese survey was performed in January 2014. We collected 92 snow samples from 13 sites across northern China. Much less snow had fallen than in previous years; as a result, most of the surface snow samples were collected as aged snow, and snow grain sizes were much larger owing to solar radiation absorbed by ILAPs as a result of settlement processes. Although we selected study locations in remote regions located at least 50 km from cities, higher AODs measured using a sun photometer and remote sensing devices showed that heavily polluted areas remain in industrial regions across northern China. The estimated BC mixing ratios measured through the 2014 survey via the ISSW spectrophotometer in surface and average integrated snow of 53 to 3651 and 62 to 1635 ng g^{-1}, respectively, were much larger than those of previous snow field campaigns. The non-BC fraction showed that most of the ILAPs in seasonal snow were dominated by OC and AD. Owing to BC and OC~~

mass absorption efficiencies of 6.3 and 0.3 $m^2 g^{-1}$, respectively, at 550 nm, light absorption was still dominated by BC and OC in seasonal snow during the entire campaign. AD contributions in snow to light absorption amounted to less than 10%. The large OC/BC ratios and correlation coefficients indicated that these contributions were mainly derived from common sources (e.g., biomass burning). Similarly, NH_4^+ was attributed to intense agricultural activity compared to industrial emissions of SO_4^{2-} and NO_3^-.

The fraction of the AD mixing ratios was larger at high latitudes than at low latitudes owing to strong winds transporting snow. In this study, we indicated that thepresent a new spectral snow albedo model (SAMDS) for simulating the surface albedo of snow with deposited ILAPsaerosol impurities (e.g. Black carbon, Organic carbon, Mineral dust, volcano ash, and snow algae) by using the asymptotic analytical radiative transfer theory. Given the measured BC, MD and OC mixing ratios of 100-5000 ng g^{-1}, 2000-6000 ng g^{-1}, and 1000-30000 ng g^{-1} in surface snow across northeastern China, we ran the models at a solar zenith angle θ of 60°, and the results indicated that the albedo of fresh snow at 550 nm is generally in a range of 0.95-0.75 with R_{eff} of 100 μm. This model can also be used to investigate the snow albedo influenced by the internal/external mixing of BC and snowwith impurities, irregular morphology of snow grains and impurities , aging processes of snow grains and soot aggregates, and the vertical distribution of snow grains and impurities for multilayer snow. Additionally, the properties of different snow grain shapes (Fractal particles, Hexagonal plate/column, and spheres) and the internal/external mixing with BC in snow by using SAMDS model might be useful to researchers who are conducting studies involving ILAPs and snow interaction and feed back in snow albedo reduciton. Compare to the SNICAR model, the snow albedo reduction is in agreement with the

SAMDS model, different types of impurity could be included in the parameterization in SAMDS model, such as organic carbon and biogenic particles. For instance, thea given shape (spheres, hexagonal plates/columns, and fractal particles), it shows that snow albedo for spherical snow grains is typically lower by 0.017-0.073, and 0.008-0.036 than that for the fractal snow grains and hexagonal plates/columns snow grains as a function of BC mixing ratios (0-5000 ng g^{-1}) with R_{eff} of 100 μm.it shows that snow albedo by spherical snow grains typically decrease by 0.017-0.073, and 0.008-0.036 as a function of BC mixing ratios (0-5000 ng g^{-1}), which is compared with the fractal snow grains and hexagonal plates/columns snow grains. The internal mixing of BC and -snow absorbs substantially more light than external mixing subsequently. For fresh snow grains of hexagonal plates/columns with R_{eff} of 100 μm, the difference of snow albedo between internal and external mixing of BC and snow is up to 0.036 for 3000 ng g^{-1} BC in snow in the heavy industrial regions across northeastern China, whereas by low to 0.005 for 100 ng g^{-1} BC in snow in the further north China near the border of Siberia. The spectral albedo of snow reduction caused by OC (20 μg g^{-1}) is larger by up to a factor of 3 for a snow grain size of 800 μm compared to 100 μm by using SAMDS model.

Then, OC emitted from biomass burning and SO_4^{2-} and NO_3^- generated from fossil fuels and biofuels also played key roles in the mixing ratios of chemical components in seasonal snow. Finally, aAa comparison between measured and simulated snow albedos was conducted. Generally, tThe sSnow albedos measured from a spectroradiometer and simulated using the SNICAR and SAMDS models using R_m [LZ1]agreed well with the measured ones from the spectroradiometer with at the lower mixing ratios of BC, OCMD, and ADMDOC, but with. However, a large discrepanciesdiscrepancy in snow albedo levels between the model simulations and

surface measurements for heavy loading of ILAPs in snow was found by using the measured snow grain radiiR$_m$. We demonstrate that the simulated sSnow albedo reduction simulated by SMDAS and SNICAR models is significantly higherenhanced by using R$_{eff}$ of snow grains compared withthan using R$_m$, especially in the case of near-infrared wavelengths.Instead of the optical effective snow grains in snowBased on the snow grain optical effective size, we found good a remarkable improvement of the snow albedo reduction agreement between surface measurements and radiative transfer models. Therefore, the snow grain optical effective size is preferred to present the snow albedo reduction when measurements on snow grain size are available at the near-infrared wavelength. Although the MAC of OC iswas much lower than that of BC, we found that OC was was a major absorber in snow owing due to its high mixing ratio of OC from human activities occurring across northeastern China. Moreover, 5000 ng g^{-1} of OC was found to reduce the snow albedo by 1.5%-5%0.016-0.059 depending on the snow grain size and aging period. Therefore, we suggest that tThe mixing ratio of OC should be added as an input parameter to the SNICAR model for determining snow albedos.

Future snow surveys studies across northern China should be performed to address the large variations of ILAPs in seasonal snow across the region. Additional model simulations and comparisons with measurements are needed to verify R$_{eff}$ effect under the scenario of high mixing ratios of ILAPs in snow..

Although the SAMDS model might be useful to researchers who are conducting studies involving ILAPs and snow interaction and feedback in snow albedo change,Although the SAMDS model can be used to study the snow albedo reduction for dirty snow due to ILAPs, and multiple internal/external mixing stats of BC associated with irregular snow grains, we indicate that further snow surveys across

~~northern China should be performed for the following reasons:. First(1), large variations of ILAPs in seasonal snow across northern China can lead higher uncertainties of snow albedo reduction, especially in the industrial regions,. and (2)Second, we only measured the snow albedo at 6 sampling sites by using the spectroradiometer in the clear sky condition due to much less snow fallen in January 2014 than that in previous years. Comparinge model simulations with the observations, we found that $R_{eff}$the optical effective snow grains could seemingly be enhanced by the high concentrationsmixing ratios of ILAPs in snow, however, we note that further snow surveys on measuring snow albedo should be conducted to reveal this phenomenon. Finally, there are large uncertainties in affectingsimulating snow albedo reduction and radiative forcing due to the ILAPs mixed with snow/ice and the irregular morphology of snow grains, the potential snow albedo reductionchange for aged snow should be investigated in the following snow surveys accordingly to test the capability of SAMDS model, which will provide more valuable and useful information for the climate models.~~

Acknowledgements. This research was supported by the Foundation for Innovative Research Groups of the National Science Foundation of China (41521004), the National Science Foundation of China under Grants 41522505, and the Fundamental Research Funds for the Central Universities (lzujbky-2015-k01, lzujbky-2016-k06 and lzujbky-2015-3). The MODIS data ~~were~~ was obtained from the NASA Earth Observing System Data and Information System, Land Processes Distributed Active Archive Center (LP DAAC) at the USGS Earth Resources Observation and Science (EROS) Center.

Table 1. Statistics in~~on~~ seasonal snow variables measured using an ISSW in the study sites. All of the datasets are the average values from the left and right snow samples. The site numbers begin ~~ning~~ at 90 in this study, which are numbered in chronological order followed by Wang et al. (2013a), and Ye et al. (2012).

Site –	Layer	Latitude N	Longitude E	Snow type	Site average snow depth (cm)	Sample depth (cm)		Temperature	Snow density	R_m	C_{BC}^{equiv} –	C_{BC}^{max}	C_{BC}^{est}	$f_{non\text{-}BC}^{est}$	$Å_{tot}$
						Top	Bottom	(°C)	(g cm^{-3})	(mm)	(ng g^{-1})	(ng g^{-1})	(ng g^{-1})	(%)	450:600 nm
90	1	45°02’44”	116°22’45”	Aged	3	0	5	-14	0.38	0.15	860	530	330 (–, 470)	61 (45, 110)	3.8
91	1	50°02’48”	124°22’41”	Fresh	8	0	5	-25	0.23	0.08	250	200	160 (110, 200)	35 (18, 55)	2.1
	2			Aged		5	10	-25	0.18	0.15	–	–	–	–	–
92	1	50°39’07”	122°23’53”	Fresh	14	0	5	-16	0.17	0.08	80	70	50 (30, 70)	34 (15, 60)	2.3
	2			Aged		5	10	-16	0.18	1.25	110	100	80 (50, 100)	29 (11, 55)	2.2
93	1	50°24’50”	124°54’20”	Fresh	8	0	1	–	–	0.07	170	100	70 (40, 90)	53 (39, 73)	2.5
	2			Aged		2	6	-21	0.21	0.175	310	140	100 (50, 130)	68 (59, 85)	2.7
94	1	50°09’05”	125°46’06”	Fresh	8	0	1	-24	–	0.1	1200	400	260 (110, 360)	78 (69, 91)	2.8
95	1	50°54’43”	127°04’50”	Aged	18	0	3	-22	0.23	0.175	280	110	80 (40, 100)	73 (64, 86)	2.6
	2			Aged		3	8	-23	0.18	0.9	230	80	50 (30, 70)	77 (68, 89)	2.7
	3			Aged		8	13	-25	0.27	1	90	50	30 (10, 40)	71 (55, 92)	3.2
	4			Aged		13	18	-25	0.14	1.3	520	310	130 (–, 240)	75 (54, 148)	4.8
96	1	49°14’21”	129°43’13”	Fresh	13	0	5	-22	0.37	0.08	1300	390	240 (20, 330)	83 (76, 99)	3.4
	2			Aged		5	10	-23	0.25	0.6	230	90	50 (10, 70)	81 (69, 98)	3.3
	3			Aged		10	15	-22	0.22	1	370	130	80 (30, 110)	80 (71, 93)	3.0
97	1	47°39’18”	131°13’10”	Aged	20	0	5	-22	0.36	0.2	1000	360	240 (90, 310)	76 (69, 91)	2.8
	2			Aged		5	10	-18	0.27	1.1	160	80	50 (20, 70)	71 (57, 91)	3.0

Site	Layer	Latitude N	Longitude E	Snow type	Site average snow depth (cm)	Sample depth (cm)		Temperature	Snow density	R_m	C_{BC}^{equiv}	C_{BC}^{max}	C_{BC}^{est}	$f_{non\text{-}BC}^{est}$	$Å_{tot}$
						Top	Bottom	(°C)	(g cm^{-3})	(mm)	(ng g^{-1})	(ng g^{-1})	(ng g^{-1})	(%)	450:600 nm
	3			Aged		10	15	-14	0.32	0.9	30	20	10 (5, 20)	74 (44, 90)	3.1
98	1	45°25’38”	130°58’55”	Fresh	35	0	5	-20	0.22	0.09	2200	2100	1500 (750, 1800)	32 (16, 65)	2.5
	2			Aged		5	10	-23	0.24	0.5	640	350	240 (120, 310)	58 (46, 79)	2.6
	3			Aged		10	15	-15	0.24	0.75		60	20 (10, 50)	74 (52, 90)	3.1
	4			Aged		15	20	-14	0.26	0.75	60	40	20 (10, 30)	75 (48, 89)	3.1
	5			Aged		20	25	-13	0.28	1.1	430	260	170 (60, 220)	62 (49, 86)	2.8
	6			Aged		25	30	-11	0.29	1.3	350	170	110 (70, 150)	68 (58, 81)	2.5
	7			Aged		30	35	–	0.33	1.3	290	120	70 (40, 100)	75 (65, 87)	2.6
99	1	43°36’10”	125°42’04”	Fresh	13	0	5	-2	0.18	0.085	1500	920	640 (240, 820)	54 (40, 84)	2.8
	2			Aged		5	12	-3	0.23	1.1	5800	3800	2900 (1500, 3600)	51 (39, 74)	2.5
	3			Aged		12	18	-4	0.28	1.1	2800	1400	1100 (630, 1300)	62 (53, 77)	2.3
	4			Aged		18	24	-4	0.28	0.7	2000	1500	1100 (540, 1400)	46 (32, 73)	2.6
100	1	43°30’45”	127°15’34”	Fresh	18	0	2.5	–	0.14	0.075	1700	700	510 (250, 650)	71 (63, 86)	2.6
	2			Aged		2.5	4	-2	0.18	0.25	4100	2900	1700 (–, 2400)	58 (43, 103)	3.6
	3			Aged		4	9	-2	0.23	0.9	1100	560	410 (210, 530)	60 (49, 80)	2.6
	4			Aged		9	15	-3	0.24	0.8	1600	730	540 (270, 690)	66 (57, 83)	2.6
101	1	43°47’25”	125°46’08”	Fresh	22	0	5	-19	0.24	0.07	5600	5100	3700 (1300, 4600)	35 (18, 76)	2.9
	2			Aged		5	10	-17	0.24	0.9	4300	3800	2600 (880, 3300)	40 (24, 79)	2.9
	3			Aged		10	15	-15	0.23	1.1	660	390	310 (210, 390)	46 (33, 63)	2.1
	4			Aged		15	20	-14	0.28	1.3	300	250	190 (110, 240)	39 (21, 67)	2.5
102	1	42°12’34”	126°37’50”	Fresh	46	0	3	-8	0.13	0.07	2100	1700	1400 (810, 1800)	37 (19, 61)	2.3
	2			Aged		3	8	-8	0.26	0.1	590	380	280 (150, 370)	53 (37, 75)	2.6
	3			Aged		8	13	-8	0.24	0.3	2500	2100	1600 (430, 2100)	35 (15, 81)	3.1

Site	Layer	Latitude N	Longitude E	Snow type	Site average snow depth (cm)	Sample depth (cm)		Temperature	Snow density	Snow grain radius	R_m	C_{BC}^{equiv}	C_{BC}^{max}	C_{BC}^{est}	f_{nonBC}^{est}	$\mathring{A}_{tot}$ 450:600 nm
						Top	Bottom									
–	4			Aged		13	18	-8	0.28	0.6	1900	1100	770 (230, 1000)	60 (48, 88)		3.0
	5			Aged		18	23	-7	0.32	1	1100	630	450 (200, 520)	60 (47, 82)		2.7
	6			Aged		23	28	-6	0.27	1.2	1500	1300	900 (300, 1200)	38 (21, 80)		2.9
90	1	45°02’44”	116°22’45”	3	0	5	-14	0.38	0.15	862	530	334 (, 473)	61 (45, 110)		3.8	
	7			Aged		28	33	-5	0.26	1.2	860	490	340 (130, 460)	66 (53, 87)		2.9
91	1	50°02’48”	124°22’41”	8	0	5	-25	0.23	0.08	250	200	161 (110, 200)	35 (18, 55)		2.1	
	8			Aged		33	38	-5	0.3	1	430	200	110 (30, 160)	74 (61, 95)		3.2
	2				5	10	-25	0.18	0.15	–	–	–	–	–		–
	9			Aged		38	43	-4	0.29	0.8	520	250	160 (70, 220)	71 (58, 87)		2.8
92	1	50°39’07”	122°23’53”	14	0	5	-16	0.17	0.08	80	72	53 (32, 68)	34 (15, 60)		2.3	

	2				5	10	-16	0.18	1.25	108	97	77 (49, 97)	29 (11, 55)	2.2
93	1	50°24’50”	124°54’20”	8	0	1	–	–	0.07	172	97	70 (39, 90)	53 (39, 73)	2.5
	2				2	6	-21	0.21	0.175	313	136	100 (46, 128)	68 (59, 85)	2.7
94	1	50°09’05”	125°46’06”	8	0	1	-24	–	0.1	1173	404	260 (108, 363)	78 (69, 91)	2.8
95	1	50°54’43”	127°04’50”	18	0	3	-22	0.23	0.175	278	110	75 (37, 100)	73 (64, 86)	2.6
	2				3	8	-23	0.18	0.9	230	83	54 (25, 73)	77 (68, 89)	2.7
	3				8	13	-25	0.27	1	91	50	27 (7, 40)	71 (55, 92)	3.2
	4				13	18	-25	0.14	1.3	521	308	131 (, 237)	75 (54, 148)	4.8
96	1	49°14’21”	129°43’13”	13	0	5	-22	0.37	0.08	1340	385	241 (21, 332)	83 (76, 99)	3.4
	2				5	10	-23	0.25	0.6	234	85	45 (6, 71)	81 (69, 98)	3.3
	3				10	15	-22	0.22	1	371	126	78 (26, 111)	80 (71, 93)	3.0
97	1	47°39’18”	131°13’10”	20	0	5	-22	0.36	0.2	1005	362	236 (93, 306)	76 (69, 91)	2.8
	2				5	10	-18	0.27	1.1	160	79	45 (15, 65)	71 (57, 91)	3.0
	3				10	15	-14	0.32	0.9	32	23	9 (3, 18)	74 (44, 90)	3.1
98	1	45°25’38”	130°58’55”	35	0	5	-20	0.22	0.09	2154	2080	1461 (754, 1818)	32 (16, 65)	2.5
	2				5	10	-23	0.24	0.5	641	349	241 (123, 307)	58 (46, 79)	2.6
	3				10	15	-15	0.24	0.75	97	55	25 (10, 45)	74 (52, 90)	3.1
	4				15	20	-14	0.26	0.75	61	39	16 (7, 31)	75 (48, 89)	3.1
	5				20	25	-13	0.28	1.1	432	261	166 (62, 221)	62 (49, 86)	2.8
	6				25	30	-11	0.29	1.3	348	165	112 (66, 148)	68 (58, 81)	2.5
	7				30	35	–	0.33	1.3	288	118	72 (37, 101)	75 (65, 87)	2.6
99	1	43°36’10”	125°42’04”	13	0	5	-2	0.18	0.085	1459	922	636 (235, 823)	54 (40, 84)	2.8
	2				5	12	-3	0.23	1.1	5847	3778	2882 (1549, 3559)	51 (39, 74)	2.5
	3				12	18	-4	0.28	1.1	2795	1360	1059 (630, 1306)	62 (53, 77)	2.3
	4				18	24	-4	0.28	0.7	2027	1518	1105 (537, 1381)	46 (32, 73)	2.6

100	1	43°30’45”	127°15’34”	18	0	2.5	–	0.14	0.075	1739	703	508 (250, 651)	71 (63, 86)	2.6
	2				2.5	4	-2	0.18	0.25	4126	2891	1729 (, 2371)	58 (43, 103)	3.6
	3				4	9	-2	0.23	0.9	1062	564	414 (208, 529)	60 (49, 80)	2.6
	4				9	15	-3	0.24	0.8	1601	728	541 (266, 691)	66 (57, 83)	2.6
101	1	43°47’25”	125°46’08”	22	0	5	-19	0.24	0.07	5634	5070	3651 (1333, 4644)	35 (18, 76)	2.9
	2				5	10	-17	0.24	0.9	4318	3826	2575 (882, 3284)	40 (24, 79)	2.9
	3				10	15	-15	0.23	1.1	657	389	313 (206, 386)	46 (33, 63)	2.1
	4				15	20	-14	0.28	1.3	297	254	188 (108, 239)	39 (21, 67)	2.5
102	1	42°12’34”	126°37’50”	46	0	3	-8	0.13	0.07	2109	1734	1357 (808, 1755)	37 (19, 61)	2.3
	2				3	8	-8	0.26	0.1	594	377	279 (149, 371)	53 (37, 75)	2.6
	3				8	13	-8	0.24	0.3	2513	2088	1623 (425, 2120)	35 (15, 81)	3.1
	4				13	18	-8	0.28	0.6	1922	1073	773 (229, 1013)	60 (48, 88)	3.0
	5				18	23	-7	0.32	1	1112	629	450 (197, 590)	60 (47, 82)	2.7
	6				23	28	-6	0.27	1.2	1466	1281	903 (300, 1167)	38 (21, 80)	2.9
	7				28	33	-5	0.26	1.2	858	493	344 (133, 457)	66 (53, 87)	2.9
	8				33	38	-5	0.3	1	426	197	109 (27, 163)	74 (61, 95)	3.2
	9				38	43	-4	0.29	0.8	524	245	157 (67, 220)	71 (58, 87)	2.8

Table 2. Estimates of integrated snowpack BC content in seasonal snow in the study sites for 2010 and 2014. (change as surface and average BC)

Site	Date sampled (2014)		Snowpack average Integrated BC (ng g^{-1})
90	10-Jan		334
91	13-Jan		161
92	14-Jan		65
93	15-Jan		94
94	15-Jan		260
95	16-Jan		62
96	17-Jan		140
97	18-Jan		105
98	19-Jan		264
99	23-Jan		1507
100	24-Jan		592
101	26-Jan		1635
102	27-Jan		583

Table 23. Chemical species (ng g^{-1}) in surface snow for sites across northeastern China in January 2014. The datasets of SO_4^{2-}, NO_3^-, and NH_4^+ were reprinted fromoriginated from Wang et al. (2015).

Site	ADMD	BC	OC	$K^+_{biosmoke}$	SO_4^{2-}	NO_3^-	NH_4^+	Sea salt
90	1900	380	6700	327	1685	213	22	868
91	1700	180	590	179	853	465	36	827
92	1300	60	280	150	511	105	19	456
93	1700	80	450	213	718	387	90	960
94	3300	300	2700	118	1335	550	28	554
95	2000	90	600	164	587	523	39	669
96	2300	280	3900	309	1285	493	91	1227
97	2400	280	2400	173	1163	407	38	753
98	3900	1600	13300	633	3096	747	195	2516
99	3000	770	4700	372	3379	1492	155	2310
100	3800	570	4000	260	4237	2258	487	2195
101	3500	4200	32000	1337	12382	2364	–	5131
102	5800	1700	2400	488	8034	3631	769	4420

Table 4. Measured and calculated snow grain sizes for sites in northeastern China in January 2014.

Site	Measured Snow grain radius (μm)	Calculated R_{eff} using SAMDS (μm)	Calculated R_{eff} using SNICAR (μm)
90	150	203-236	168-197
91	80	178-220	148-183
93	70	73-80	60-65
95	175	148-188	123-156
98	90	248-302	209-259
101	70	362-446	312-390

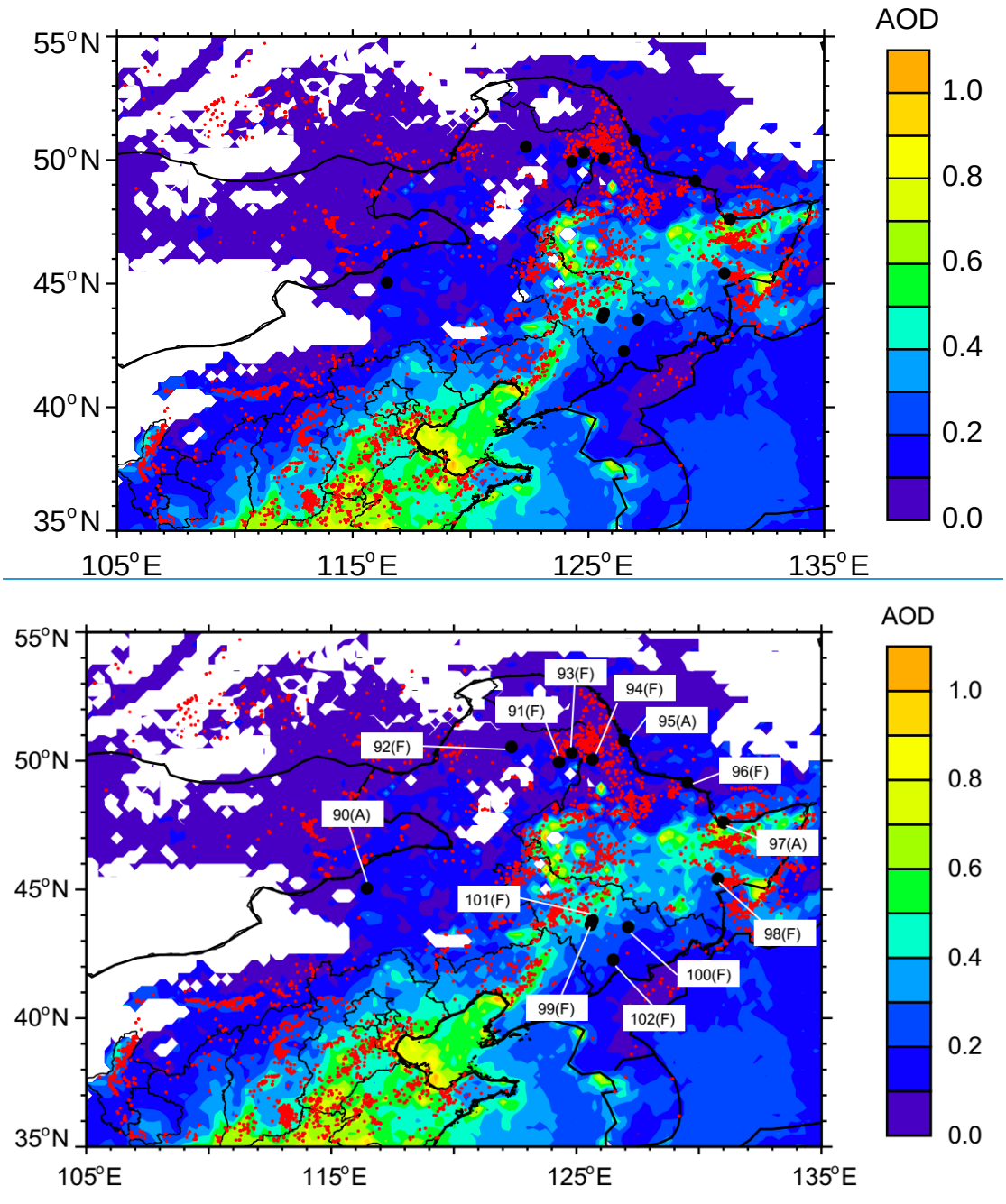

Fig. 1. Spatial distribution of the averaged AOD retrieved from Aqua-MODIS over northern China from October 2013 to January 2014.; The red ~~regions~~ dots are MODIS active fire locations.; the black dots are the sampling locations. The site

numbers begin~~ning~~ at 90 in this study, which are numbered in chronological order followed by Wang et al. (2013a), and Ye et al. (2012). The “A” and “F” refer to aged snow and fresh snow, respectively.

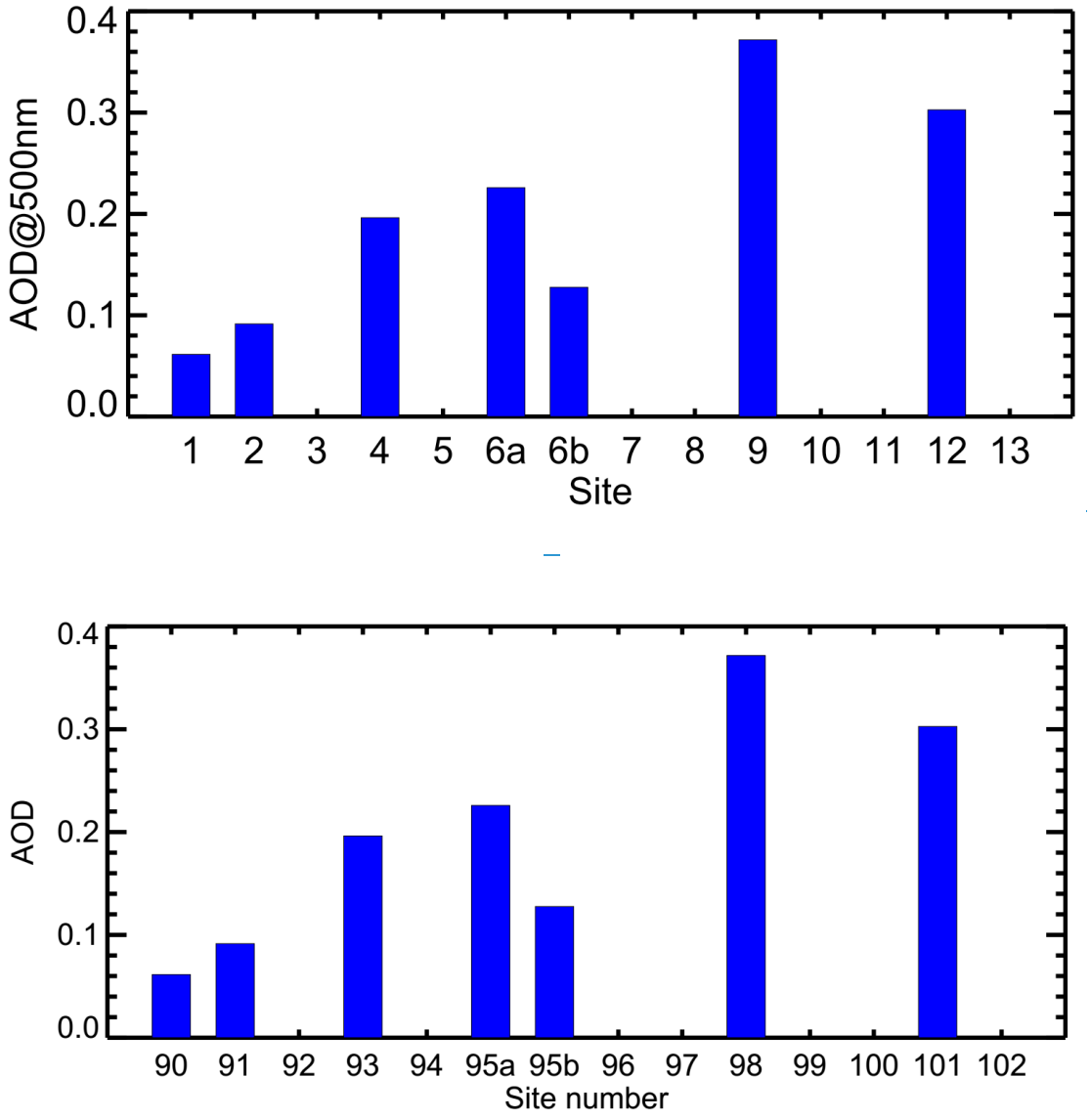

Fig. 2. The variation in AOD at 500 nm at different sites measured using a Microtops II Sun photometer over northeastern China in January 2014.

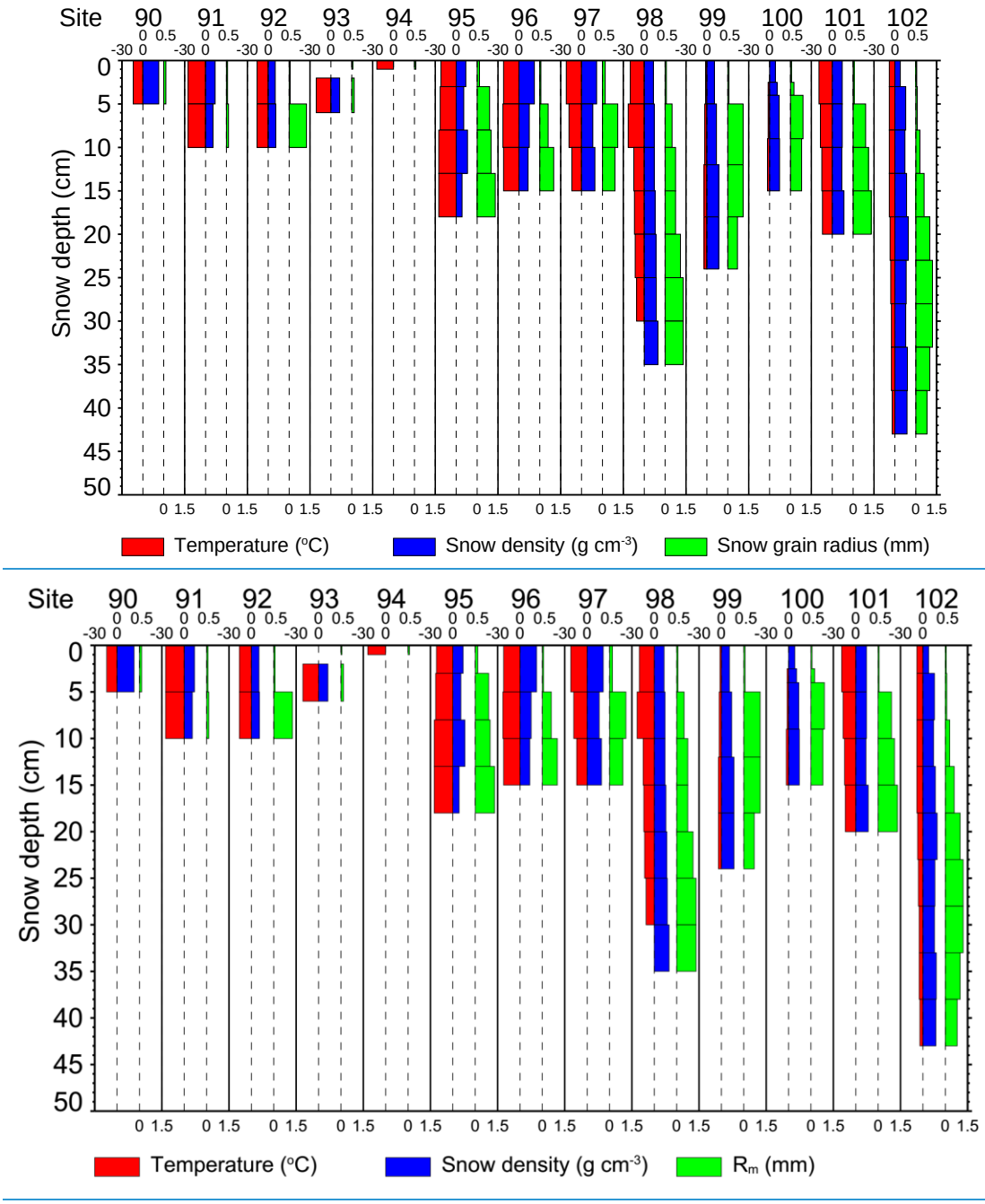
Site 90 91 92 93 94 95 96 97 98 99 100 101 102
Snow depth (cm)
0 5 10 15 20 25 30 35 40 45 50
Temperature (°C)
Snow density (g cm-3)
Snow grain radius (mm)
Rm (mm)

Fig. 3. Vertical temperature, snow density, and measured snow grain radius (R_m) profiles at each site during the 2014 Chinese snow survey.

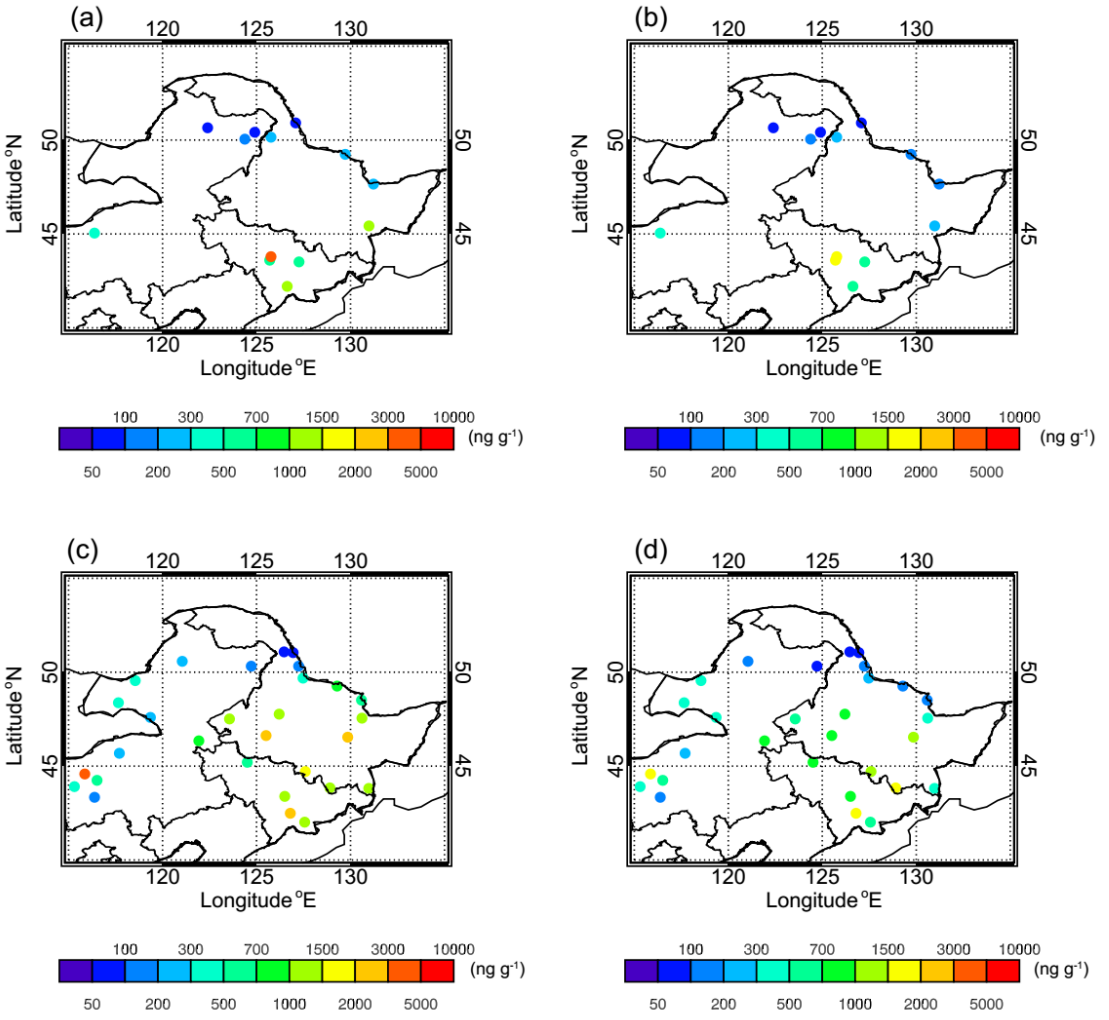
(a)
(b)
(c)
(d)
120
125
130
50
45
Latitude °N
Longitude °E
100
300
700
1500
3000
10000
50
200
500
1000
2000
5000
(ng g-1)

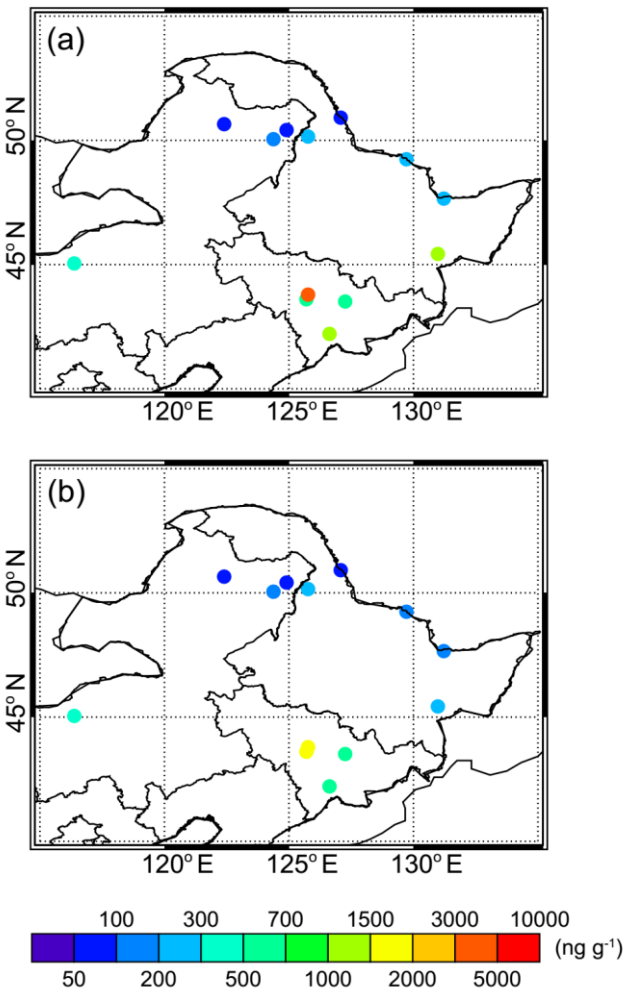

Fig. 4. The spatial distribution of C_{BC}^{est} in the (a) surface and (b) average snow~~Surface (a, c) and averaged and integrated (b, d) BC content in seasonal snow~~ in 2014 ~~and 2010~~ across northeastern China.

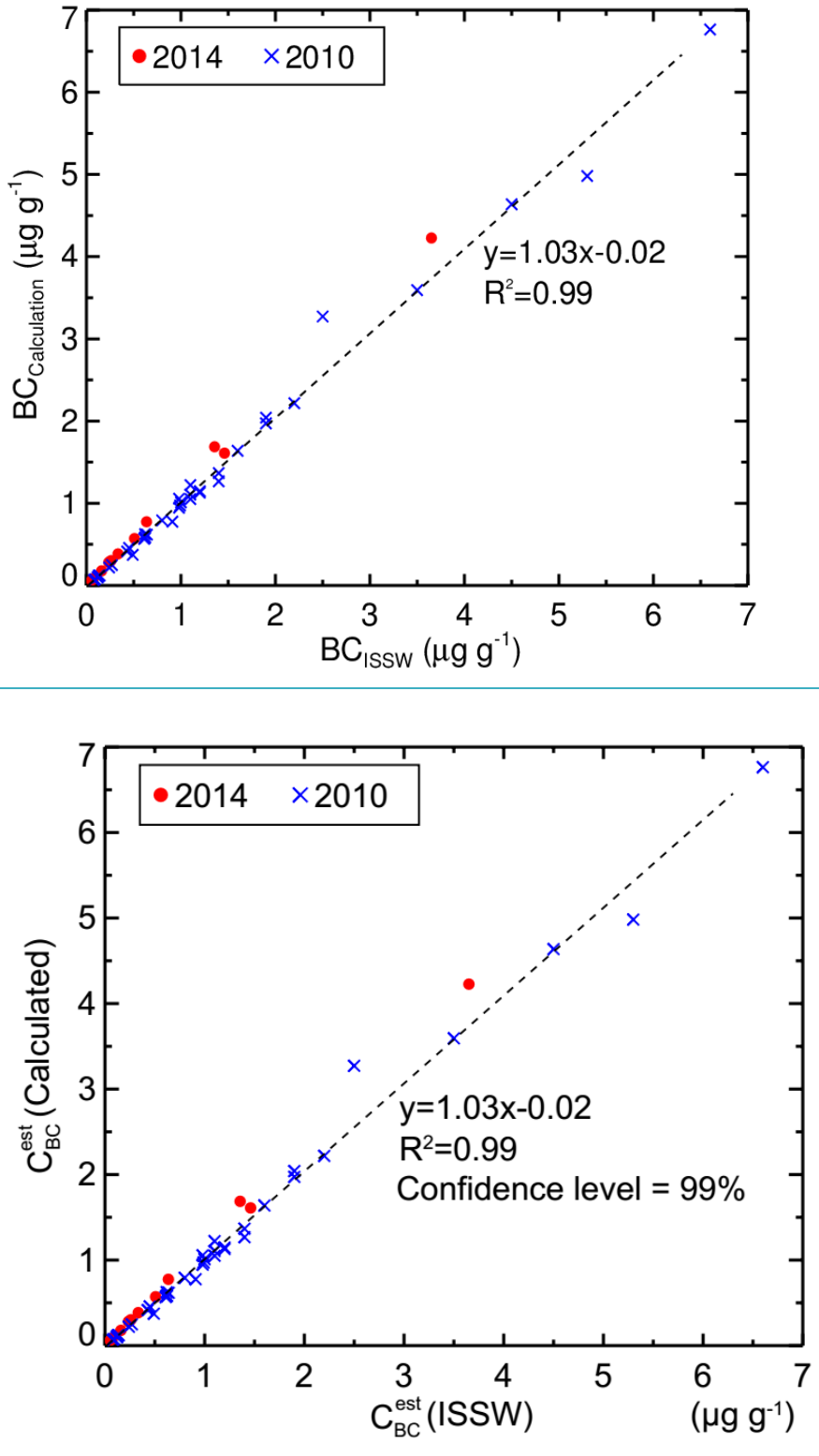

Fig. 5. Comparisons between the calculated and optically measured C_{BC}^{est} ~~BC contents~~ in surface snow during 2010 and 2014 snow surveys ~~in January 2014~~. The datasets of

measured C_{BC}^{est} in 2010 from sites 3-40 were reprinted from Wang et al. (2013a). ~~The datasets in 2010 were originated from sites 3-40 in Wang et al. (2013).~~

~~**Fig. 6.** Ratios of OC and BC, NH_4^+ and SO_4^{2-}, NH_4^+ and NO_3^-, and K^+ and Al in surface snow in January 2014.~~

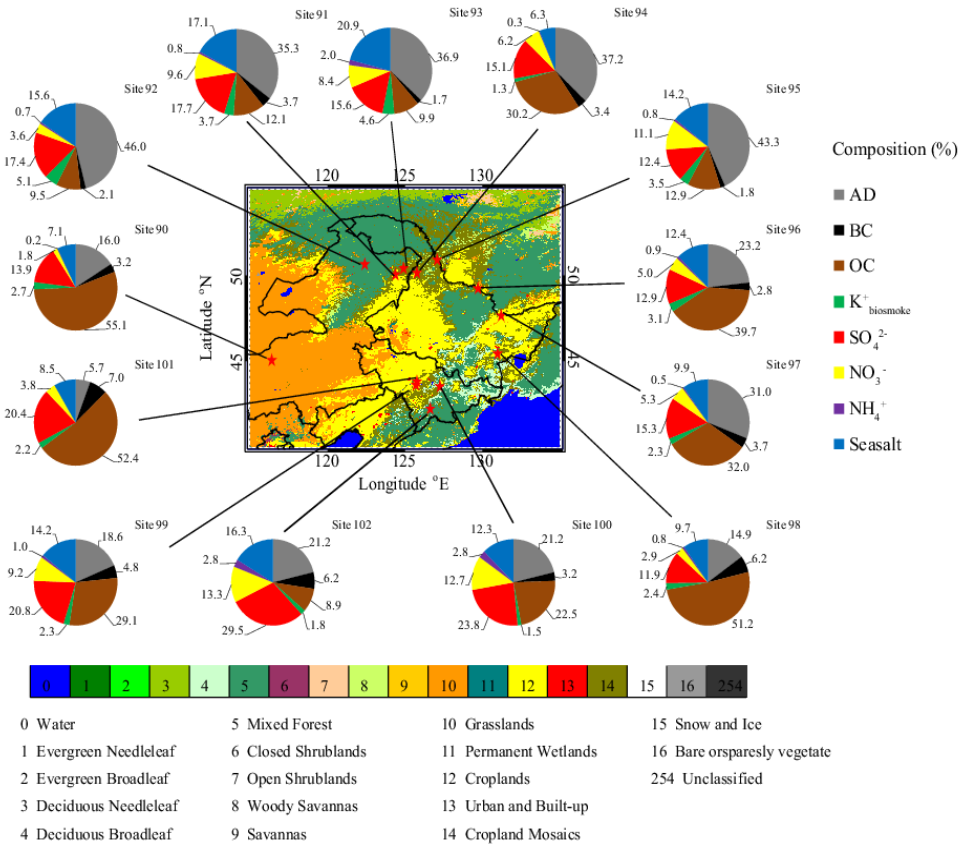
Site 91
17.1
0.8
35.3
9.6
3.7
17.7
3.7
12.1
Site 93
20.9
2.0
36.9
8.4
1.7
15.6
4.6
9.9
Site 94
0.3
6.3
6.2
37.2
15.1
1.3
30.2
3.4
Site 92
15.6
0.7
3.6
46.0
17.4
5.1
9.5
2.1
Site 95
14.2
0.8
11.1
43.3
12.4
3.5
12.9
1.8
Site 90
7.1
0.2
16.0
1.8
3.2
13.9
2.7
55.1
Site 96
12.4
0.9
23.2
5.0
2.8
12.9
3.1
39.7
Site 101
8.5
5.7
3.8
7.0
20.4
2.2
52.4
Site 97
9.9
0.5
31.0
5.3
15.3
2.3
3.7
32.0
Site 99
14.2
1.0
18.6
9.2
4.8
20.8
2.3
29.1
Site 102
16.3
21.2
2.8
6.2
13.3
8.9
29.5
1.8
Site 100
12.3
21.2
2.8
3.2
12.7
22.5
23.8
1.5
Site 98
9.7
14.9
0.8
2.9
6.2
11.9
2.4
51.2
120
125
130
50
45
Latitude °N
Longitude °E
Composition (%)
AD
BC
OC
K+ biosmoke
SO4 2-
NO3 -
NH4 +
Seasalt
0
1
2
3
4
5
6
7
8
9
10
11
12
13
14
15
16
254
0 Water
1 Evergreen Needleleaf
2 Evergreen Broadleaf
3 Deciduous Needleleaf
4 Deciduous Broadleaf
5 Mixed Forest
6 Closed Shrublands
7 Open Shrublands
8 Woody Savannas
9 Savannas
10 Grasslands
11 Permanent Wetlands
12 Croplands
13 Urban and Built-up
14 Cropland Mosaics
15 Snow and Ice
16 Bare orsparesly vegetate
254 Unclassified

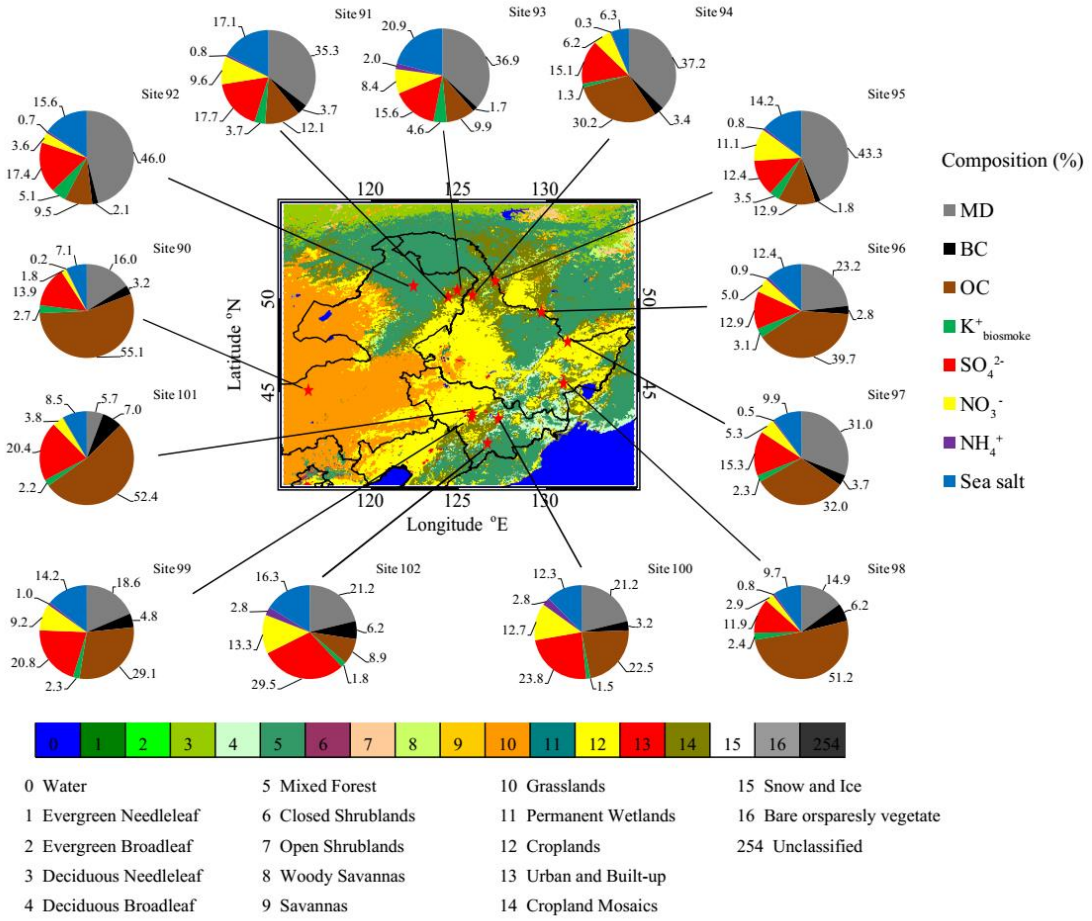

Fig. 67. The major components include ~~AD~~MD, BC, OC, $K^+_{Biosmoke}$ ~~biomass smoke potassium~~, secondary ~~aerosol~~ ions (SO_4^{2-}, NO_3^-, and NH_4^+ ~~sulfate, nitrate, and ammonium~~), and sea salt in the surface snow samples collected in January 2014. The distribution of 17 different surface vegetation types retrieved from MODIS global land cover type product (MCD12C1) with 0.05 spatial resolution ~~were~~was used in this study. The datasets of SO_4^{2-}, NO_3^-, and NH_4^+ were reprinted from~~originated from~~ Wang et al. (2015).

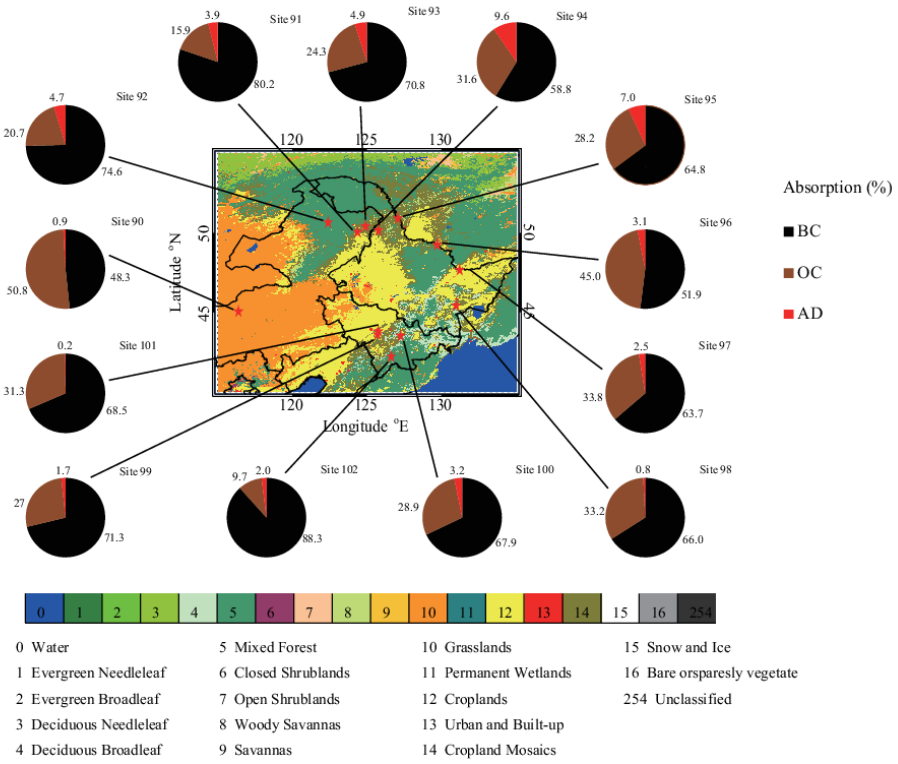
Site 91
3.9
15.9
80.2
Site 93
4.9
24.3
70.8
Site 94
9.6
31.6
58.8
Site 92
4.7
20.7
74.6
Site 95
7.0
28.2
64.8
Site 90
0.9
50.8
48.3
Site 96
3.1
45.0
51.9
Site 101
0.2
31.3
68.5
Site 97
2.5
33.8
63.7
Site 99
1.7
27
71.3
Site 102
2.0
9.7
88.3
Site 100
3.2
28.9
67.9
Site 98
0.8
33.2
66.0
120
125
130
50
45
Latitude °N
Longitude °E
Absorption (%)
BC
OC
AD
0 1 2 3 4 5 6 7 8 9 10 11 12 13 14 15 16 254
0 Water
1 Evergreen Needleleaf
2 Evergreen Broadleaf
3 Deciduous Needleleaf
4 Deciduous Broadleaf
5 Mixed Forest
6 Closed Shrublands
7 Open Shrublands
8 Woody Savannas
9 Savannas
10 Grasslands
11 Permanent Wetlands
12 Croplands
13 Urban and Built-up
14 Cropland Mosaics
15 Snow and Ice
16 Bare orsparesly vegetate
254 Unclassified

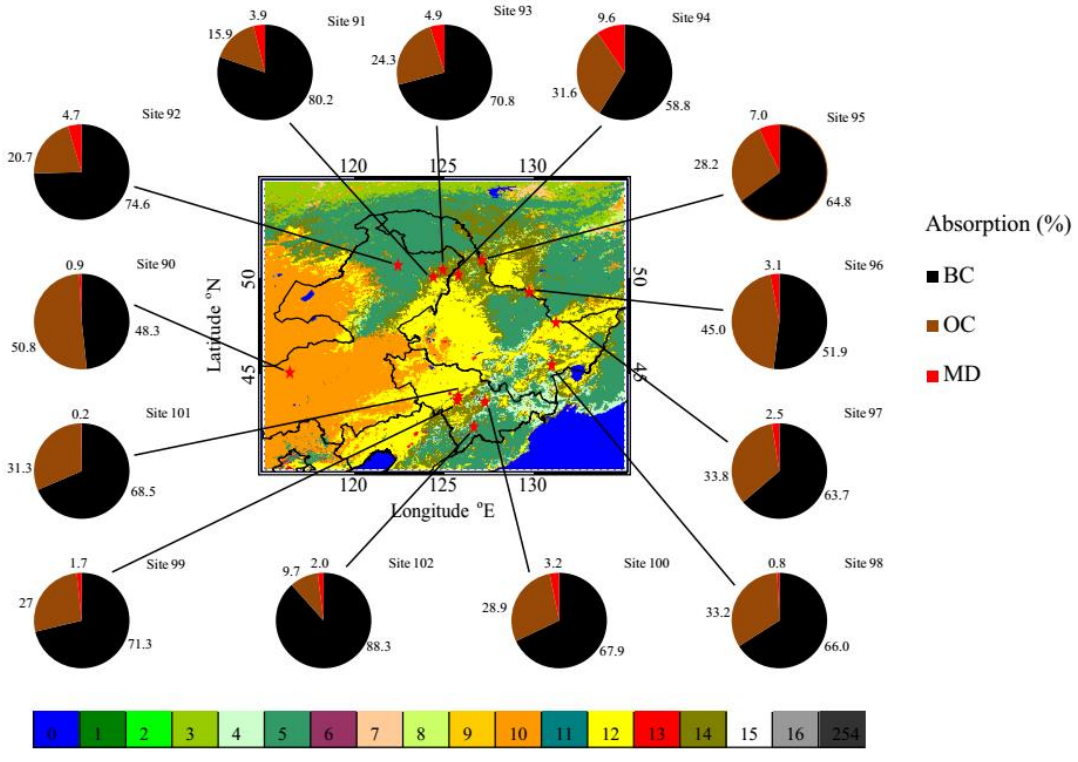
Site 91
3.9
15.9
80.2
Site 93
4.9
24.3
70.8
Site 94
9.6
31.6
58.8
Site 92
4.7
20.7
74.6
Site 95
7.0
28.2
64.8
Site 90
0.9
50.8
48.3
Site 96
3.1
45.0
51.9
Site 101
0.2
31.3
68.5
Site 97
2.5
33.8
63.7
Site 99
1.7
27
71.3
Site 102
2.0
9.7
88.3
Site 100
3.2
28.9
67.9
Site 98
0.8
33.2
66.0
120
125
130
50
45
Latitude °N
Longitude °E
Absorption (%)
BC
OC
MD
0 1 2 3 4 5 6 7 8 9 10 11 12 13 14 15 16 254
0 Water
1 Evergreen Needleleaf
2 Evergreen Broadleaf
3 Deciduous Needleleaf
4 Deciduous Broadleaf
5 Mixed Forest
6 Closed Shrublands
7 Open Shrublands
8 Woody Savannas
9 Savannas
10 Grasslands
11 Permanent Wetlands
12 Croplands
13 Urban and Built-up
14 Cropland Mosaics
15 Snow and Ice
16 Bare orsparesly vegetate
254 Unclassified

Fig. 7~~8~~. The light absorption of ILAPs in surface snow in January 2014. The distribution of 17 different surface vegetation types retrieved from MODIS global land cover type product (MCD12C1) with 0.05 spatial resolution ~~were~~was used in this study.

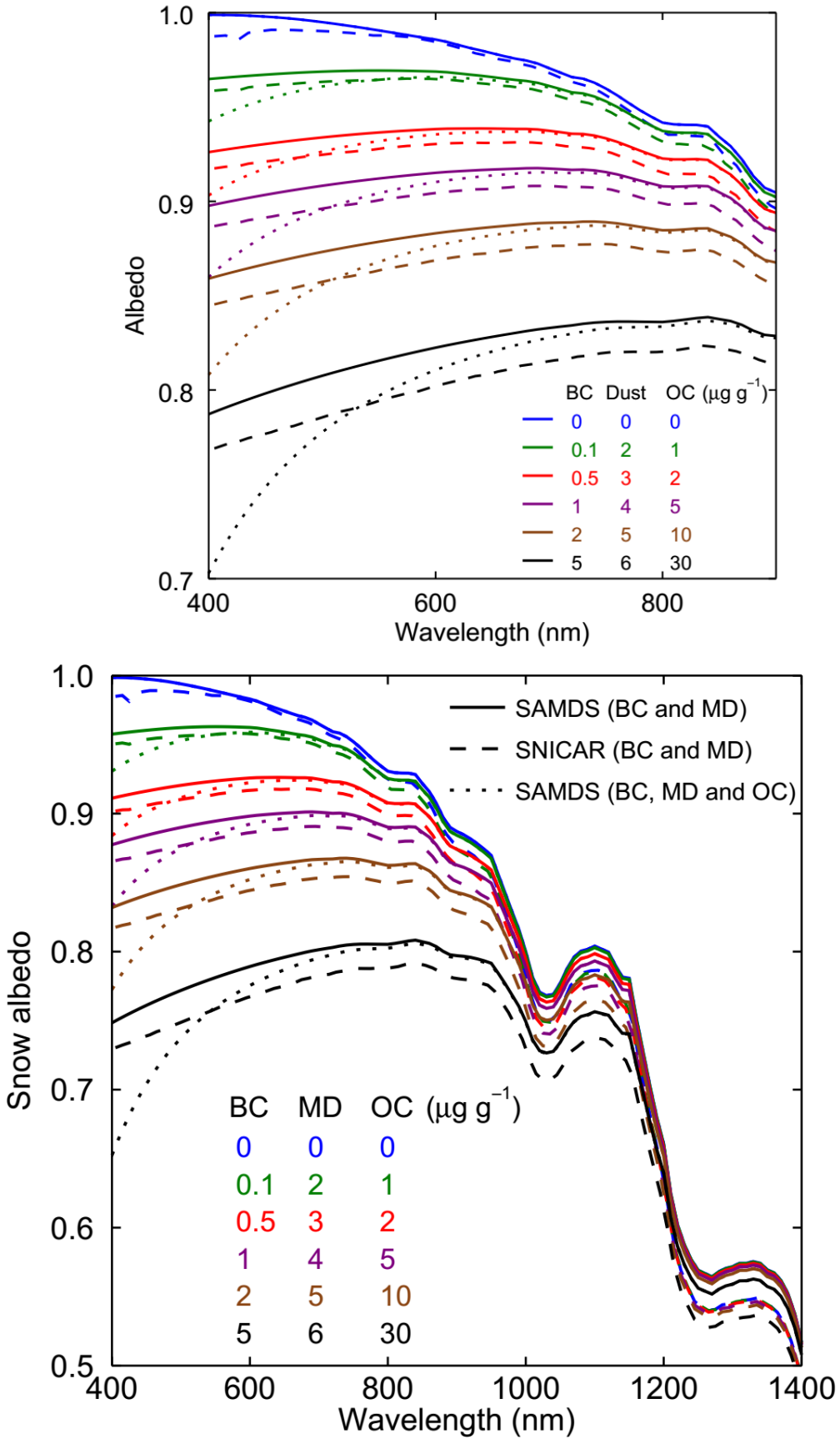

Fig. 89. Spectral albedo of snow with different contaminants for a 60° solar zenith angle and a 1070 μm ~~snow grain radius~~R_{eff}. ~~(~~Solid and dashed lines show the

SAMDS and SNICAR model predictions for~~of~~ BC and ~~mineral dust~~MD. Dotted lines show the SAMDS model predictions for all ILAPs, including BC, ~~mineral dust~~MD, and OC~~)~~.

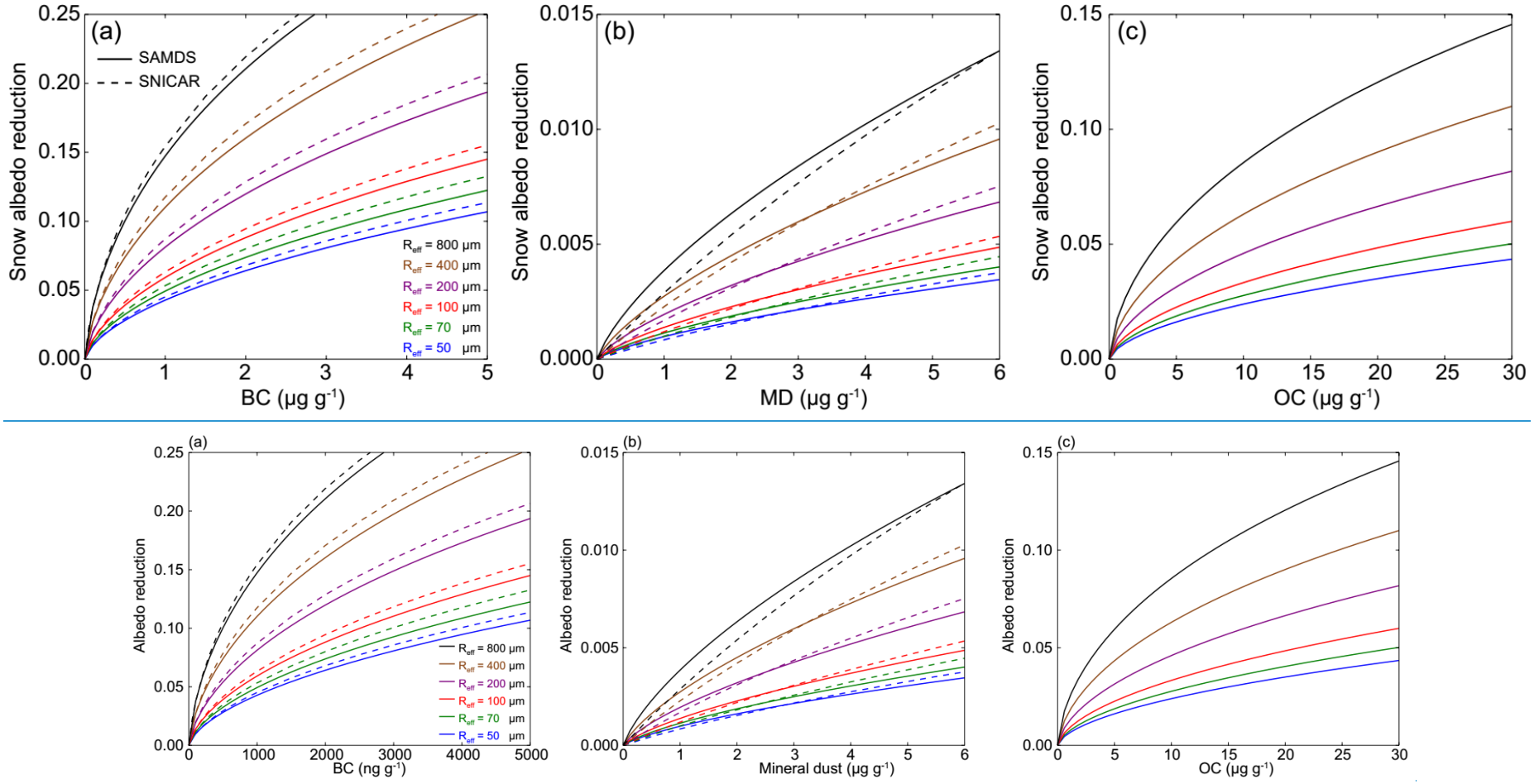
(a)
SAMDS
SNICAR
Snow albedo reduction
BC (μg g-1)
Reff = 800 μm
Reff = 400 μm
Reff = 200 μm
Reff = 100 μm
Reff = 70 μm
Reff = 50 μm
(b)
MD (μg g-1)
(c)
OC (μg g-1)
(a)
Albedo reduction
BC (ng g-1)
(b)
Mineral dust (μg g-1)
(c)
OC (μg g-1)

Fig. 910. Spectrally weighted snow albedo reduction over the 400–1400 nm solar spectrum attributed to (a) BC, (b) mineral dustMD, and (c) OC computed as the albedo of pure snow minus the albedo of contaminated snow for a 60° solar zenith angle. (Solid and dashed lines show the SAMDS and SNICAR models predictions. The MAC values of BC, FeOC, and FeOC were assumed to be 7.5 m^2 g^{-1}, 0.9 3 m^2 g^{-1}, and 0.3 9 m^2 g^{-1} at 550 nm, respectively, in SAMDS model).

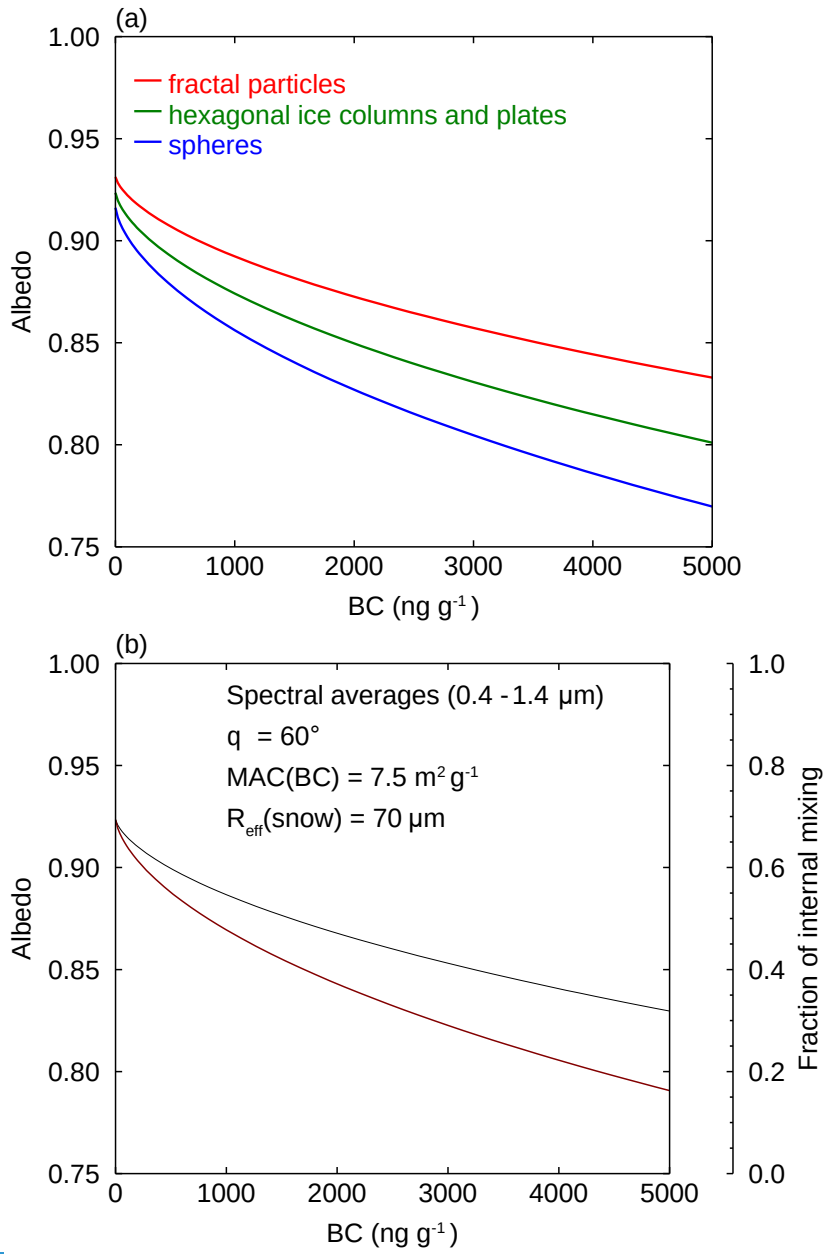
(a)
fractal particles
hexagonal ice columns and plates
spheres
Albedo
BC (ng g-1)
(b)
Spectral averages (0.4 - 1.4 μm)
q = 60°
MAC(BC) = 7.5 m2 g-1
Reff(snow) = 70 μm
Albedo
Fraction of internal mixing
BC (ng g-1)

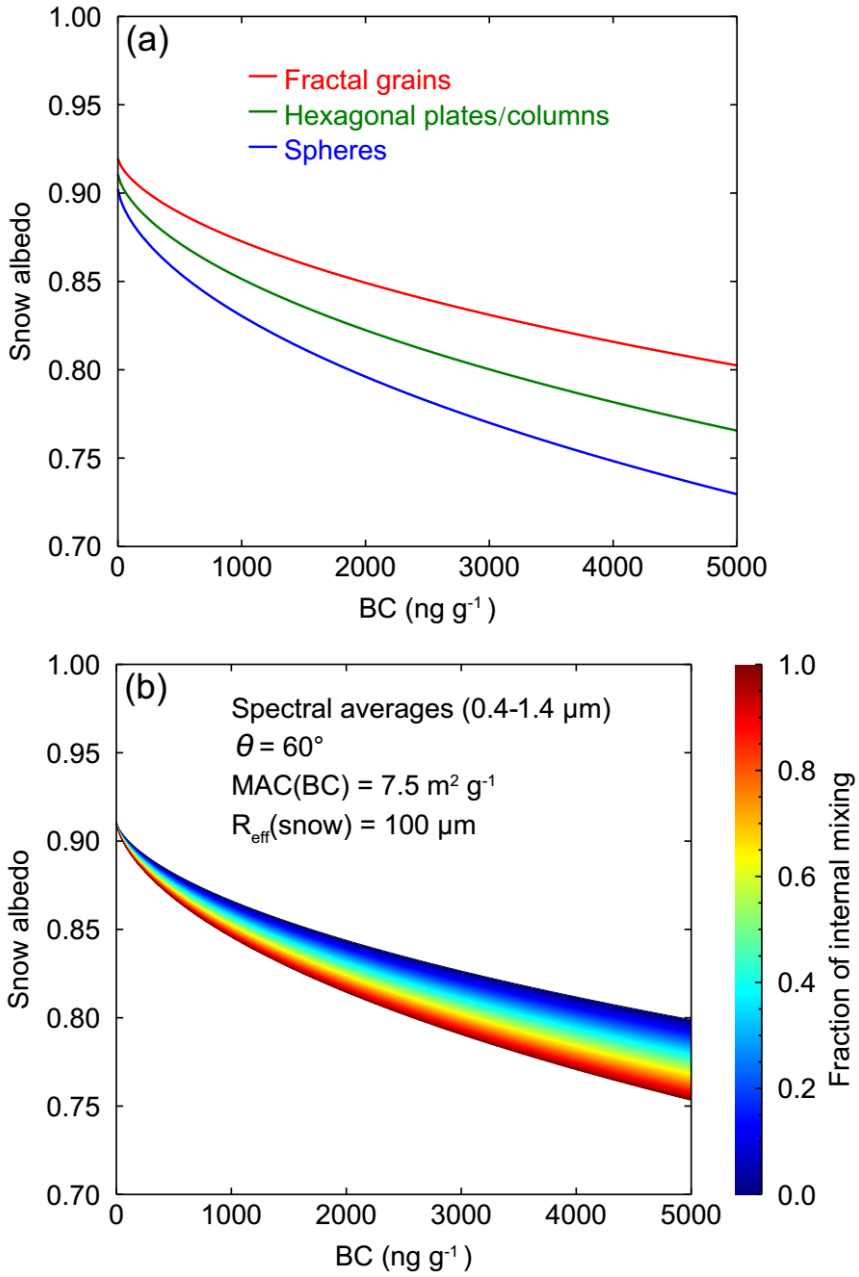

Fig. 1011 . Spectral albedo~~Snow albedo~~ of snow ~~reduction~~ as a function of BC ~~concentration~~mixing ratios in snow by using SMDAS model for: (a) the irregular morphology of snow grains (fractal ~~particles~~grains, hexagonal plates/columns, and spheres), (b) internal/ ~~and~~ external mixing of BC ~~with~~and hexagonal plates/columns ~~mixed with BC~~snow grains. Also shown are model parameters includinge integrate spectral wavelengths (400-1400 nm), solar zenith angle (θ), mass absorption coefficient (MAC) of BC, and snow grain optical effective radius (R_{eff}).

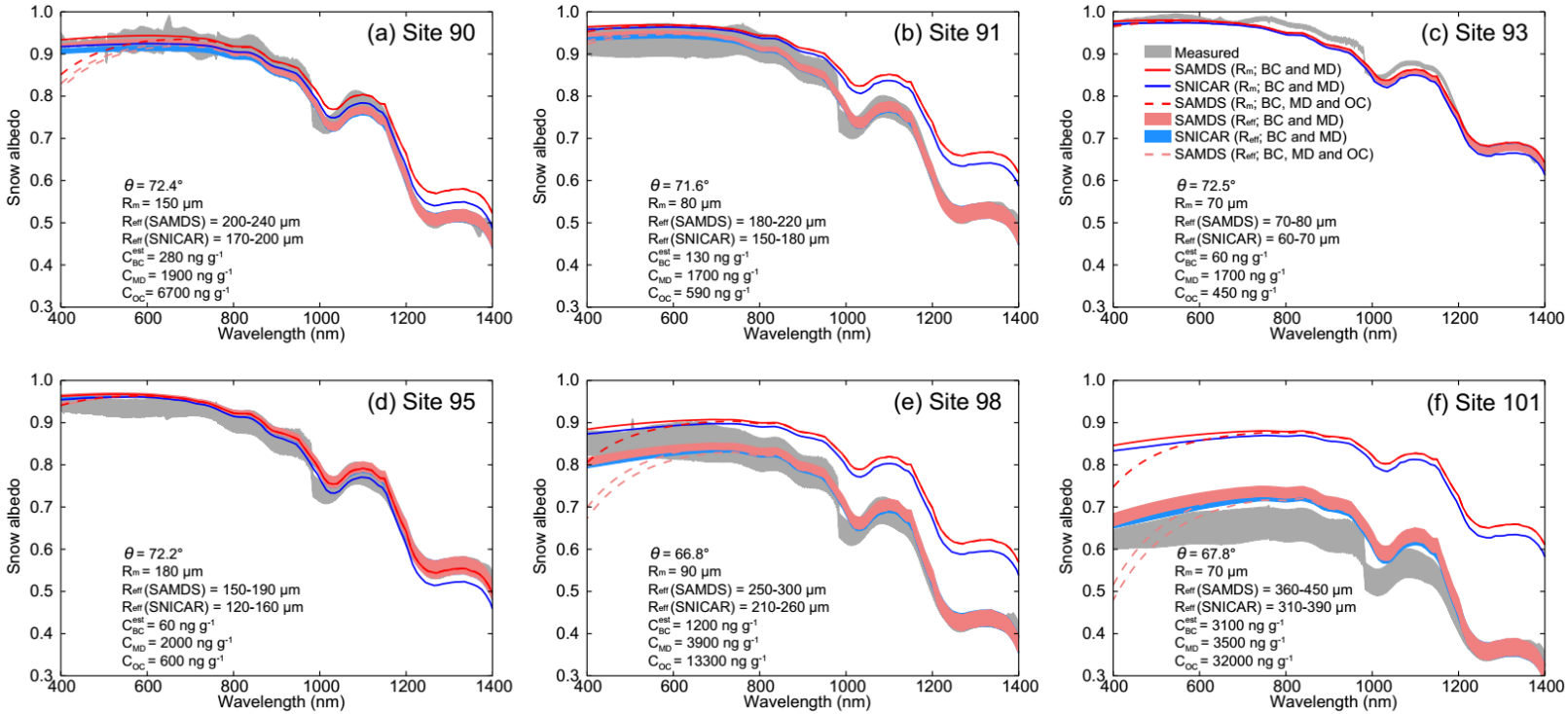
(a) Site 90
θ = 72.4°
Rm = 150 μm
Reff (SAMDS) = 200-240 μm
Reff (SNICAR) = 170-200 μm
C_BC^est = 280 ng g-1
C_MD = 1900 ng g-1
C_OC = 6700 ng g-1
(b) Site 91
θ = 71.6°
Rm = 80 μm
Reff (SAMDS) = 180-220 μm
Reff (SNICAR) = 150-180 μm
C_BC^est = 130 ng g-1
C_MD = 1700 ng g-1
C_OC = 590 ng g-1
(c) Site 93
Measured
SAMDS (Rm; BC and MD)
SNICAR (Rm; BC and MD)
SAMDS (Rm; BC, MD and OC)
SAMDS (Reff; BC and MD)
SNICAR (Reff; BC and MD)
SAMDS (Reff; BC, MD and OC)
θ = 72.5°
Rm = 70 μm
Reff (SAMDS) = 70-80 μm
Reff (SNICAR) = 60-70 μm
C_BC^est = 60 ng g-1
C_MD = 1700 ng g-1
C_OC = 450 ng g-1
(d) Site 95
θ = 72.2°
Rm = 180 μm
Reff (SAMDS) = 150-190 μm
Reff (SNICAR) = 120-160 μm
C_BC^est = 60 ng g-1
C_MD = 2000 ng g-1
C_OC = 600 ng g-1
(e) Site 98
θ = 66.8°
Rm = 90 μm
Reff (SAMDS) = 250-300 μm
Reff (SNICAR) = 210-260 μm
C_BC^est = 1200 ng g-1
C_MD = 3900 ng g-1
C_OC = 13300 ng g-1
(f) Site 101
θ = 67.8°
Rm = 70 μm
Reff (SAMDS) = 360-450 μm
Reff (SNICAR) = 310-390 μm
C_BC^est = 3100 ng g-1
C_MD = 3500 ng g-1
C_OC = 32000 ng g-1
Snow albedo
Wavelength (nm)

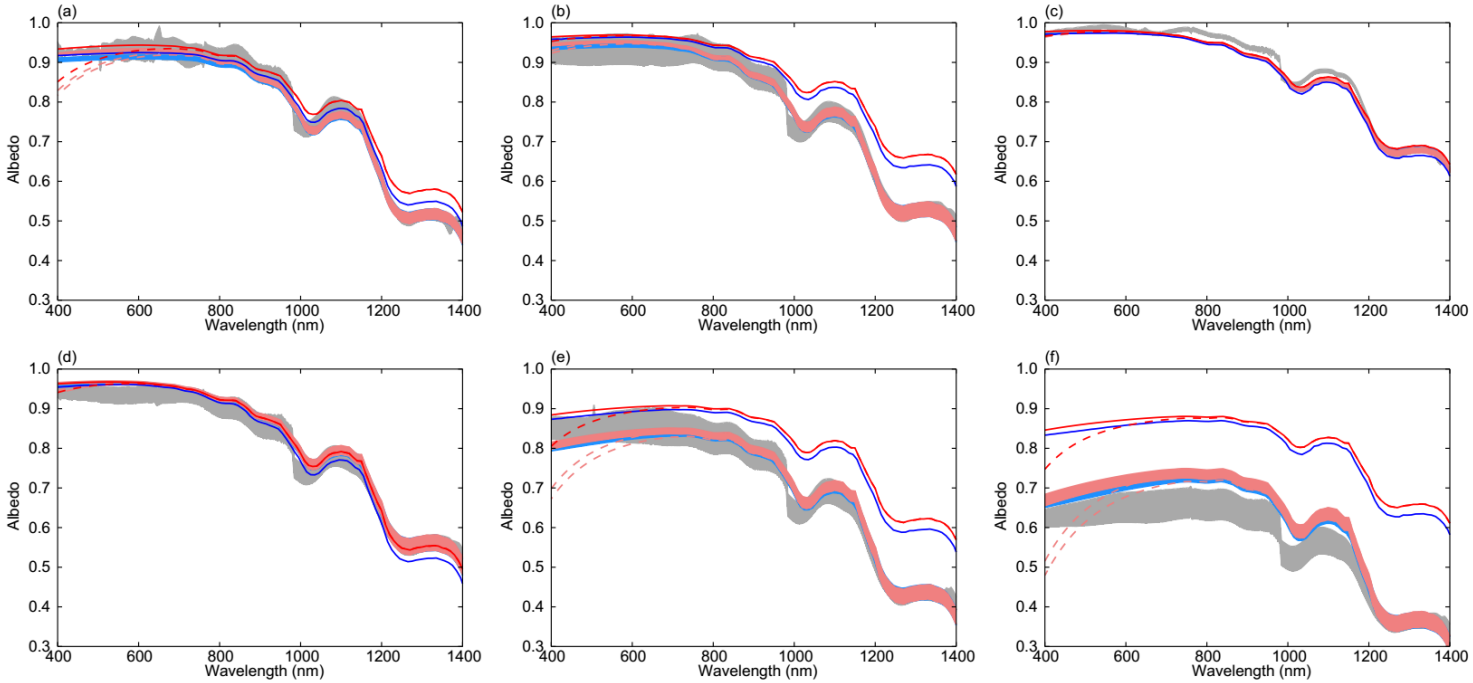

Fig. 1121. Measured and modeled spectral albedos of snow at sites (a) 90, (b) 91, (c) 93, (d) 95, (e) 98, and (f) 101. ~~(~~Gray shaded bands correspond to measured spectral albedos using an spectroradiometer ~~from the SAMDS and SNICAR models.,~~ R~~r~~ed and blue solid lines correspond to spectral albedos ~~from~~ simulated by the SAMDS and SNICAR models with measured snow grain radii (R_m), and light red and blue shaded bands correspond to the albedos ~~from the SAMDS and SNICAR models~~ with calculated snow grain optical effective radii (R_{eff}). Contaminants only include BC and ~~mineral dust~~MD in the SAMDS and SNICAR models. In the SNICAR model, the ratio of Fe in dust was ~~found~~ assumed to be 2.8%. Dashed red lines are similar to solid red lines, although OC should be added to the list of contaminants in the SAMDS model.

References

Alfaro, S. C., Lafon, S., Rajot, J. L., Formenti, P., Gaudichet, A., and Maille, M.: Iron oxides and light absorption by pure desert dust: An experimental study, J. Geophys. Res.-Atmos., 109, D08208, 2004.

Arhami, M., Kuhn, T., Fine, P. M., Delfino, R. J., and Sioutas, C.: Effects of sampling artifacts and operating parameters on the performance of a semicontinuous particulate elemental carbon/organic carbon monitor, Environ. Sci. Technol., 40, 945-954, 2006.

Ax, W., Malchow, H., Koren, H., and Fischer, H.: Studies on immunological reactions in vitro, Sbornik vedeckych praci Lekarske fakulty Karlovy university v Hradci Kralove, 13, 287-292, 1970.

Bergstrom, R. W., Russell, P. B., and Hignett, P.: Wavelength dependence of the absorption of black carbon particles: Predictions and results from the TARFOX experiment and implications for the aerosol single scattering albedo, J. Atmos. Sci., 59, 567-577, 2002.

Bi, J. R., Huang, J. P., Hu, Z. Y., Holben, B. N., and Guo, Z. Q.: Investigating the aerosol optical and radiative characteristics of heavy haze episodes in Beijing during January of 2013, J. Geophys. Res.-Atmos., 119, 9884-9900, 2014.

Bond, T. C., and Bergstrom, R. W.: Light absorption by carbonaceous particles: An investigative review, Aerosol Sci. Tech., 40, 27-67, 2006.

Bond, T. C., Bussemer, M., Wehner, B., Keller, S., Charlson, R. J., and Heintzenberg, J.: Light absorption by primary particle emissions from a lignite burning plant, Environ. Sci. Technol., 33, 3887-3891, 1999.

Bond, T. C., Doherty, S. J., Fahey, D. W., Forster, P. M., Berntsen, T., DeAngelo, B. J., Flanner, M. G., Ghan, S., Karcher, B., Koch, D., Kinne, S., Kondo, Y., Quinn, P. K., Sarofim, M. C., Schultz, M. G., Schulz, M., Venkataraman, C., Zhang, H., Zhang, S., Bellouin, N., Guttikunda, S. K., Hopke, P. K., Jacobson, M. Z., Kaiser, J. W., Klimont, Z., Lohmann, U., Schwarz, J. P., Shindell, D., Storelvmo, T., Warren, S. G., and Zender, C. S.: Bounding the role of black carbon in the climate system: A scientific assessment, J. Geophys. Res.-Atmos., 118, 5380-5552, 2013.

Brandt, R. E., Warren, S. G., and Clarke, A. D.: A controlled snowmaking experiment testing the relation between black carbon content and reduction of snow albedo, J. Geophys. Res.-Atmos., 116, D08109, 2011.

Cappa, C. D., Onasch, T. B., Massoli, P., Worsnop, D. R., Bates, T. S., Cross, E. S., Davidovits, P., Hakala, J., Hayden, K. L., Jobson, B. T., Kolesar, K. R., Lack, D. A., Lerner, B. M., Li, S. M., Mellon, D., Nuaaman, I., Olfert, J. S., Petaja, T., Quinn, P. K., Song, C., Subramanian, R., Williams, E. J., and Zaveri, R. A.: Radiative Absorption Enhancements Due to the Mixing State of Atmospheric Black Carbon, Science, 337, 1078-1081, 2012.

Carmagnola, C. M., Domine, F., Dumont, M., Wright, P., Strellis, B., Bergin, M., Dibb, J., Picard, G., Libois, Q., Arnaud, L., and Morin, S.: Snow spectral albedo at Summit, Greenland: measurements and numerical simulations based on physical and chemical properties of the snowpack, Cryosphere, 7, 1139-1160, 2013.

Che, H. Z., Wang, Y. Q., and Sun, J. Y.: Aerosol optical properties at Mt. Waliguan Observatory, China, Atmos. Environ., 45, 6004-6009, 2011.

Che, H. Z., Wang, Y. Q., Sun, J. Y., Zhang, X. C., Zhang, X. Y., and Guo, J. P.: Variation of Aerosol Optical Properties over the Taklimakan Desert in China, Aerosol Air Qual. Res., 13, 777-785, 2013.
Che, H. Z., Yang, Z. F., Zhang, X. Y., Zhu, C. Z., Ma, Q. L., Zhou, H. G., and Wang, P.: Study on the aerosol optical properties and their relationship with aerosol chemical compositions over three regional background stations in China, Atmos. Environ., 43, 1093-1099, 2009.
Che, H. Z., Zhao, H. J., Wu, Y. F., Xia, X. G., Zhu, J., Wang, H., Wang, Y. Q., Sun, J. Y., Yu, J., Zhang, X. Y., and Shi, G. Y.: Analyses of aerosol optical properties and direct radiative forcing over urban and industrial regions in Northeast China, Meteorol. Atmos. Phys., 127, 345-354, 2015.
Chen, S. Y., Huang, J. P., Zhao, C., Qian, Y., Leung, L. R., and Yang, B.: Modeling the transport and radiative forcing of Taklimakan dust over the Tibetan Plateau: A case study in the summer of 2006, J. Geophys. Res.-Atmos., 118, 797-812, 2013.
Chu, D. A., Kaufman, Y. J., Ichoku, C., Remer, L. A., Tanre, D., and Holben, B. N.: Validation of MODIS aerosol optical depth retrieval over land, Geophys. Res. Lett., 29, 1617, 2002.
Cong, Z., Kang, S., Kawamura, K., Liu, B., Wan, X., Wang, Z., Gao, S., and Fu, P.: Carbonaceous aerosols on the south edge of the Tibetan Plateau: concentrations, seasonality and sources, Atmos. Chem. Phys., 15, 1573-1584, 2015.
Dang, C., and Hegg, D. A.: Quantifying light absorption by organic carbon in Western North American snow by serial chemical extractions, J. Geophys. Res.-Atmos., 119, 10247-10261, 2014.
Dang, C., Brandt, R. E., and Warren, S. G.: Parameterizations for narrowband and broadband albedo of pure snow and snow containing mineral dust and black carbon, J. Geophys. Res.-Atmos., 120, 5446-5468, 2015.
Dang, C., Fu, Q., and Warren, S. G.: Effect of Snow Grain Shape on Snow Albedo, J. Atmos. Sci., 73, 3573-3583, 2016.
Doherty, S. J., Dang, C., Hegg, D. A., Zhang, R. D., and Warren, S. G.: Black carbon and other light-absorbing particles in snow of central North America, J. Geophys. Res.-Atmos., 119, 12807-12831, 2014.
Doherty, S. J., Warren, S. G., Grenfell, T. C., Clarke, A. D., and Brandt, R. E.: Light-absorbing impurities in Arctic snow, Atmos. Chem. Phys., 10, 11647-11680, 2010.
Fierce, L., Bond, T. C., Bauer, S. E., Mena, F., and Riemer, N.: Black carbon absorption at the global scale is affected by particle-scale diversity in composition, Nat. Commun., 7, 2016.
Flanner, M. G., Liu, X., Zhou, C., Penner, J. E., and Jiao, C.: Enhanced solar energy absorption by internally-mixed black carbon in snow grains, Atmos. Chem. Phys., 12, 4699-4721, 2012.
Flanner, M. G., Zender, C. S., Hess, P. G., Mahowald, N. M., Painter, T. H., Ramanathan, V., and Rasch, P. J.: Springtime warming and reduced snow cover from carbonaceous particles, Atmos. Chem. Phys., 9, 2481-2497, 2009.
Flanner, M. G., Zender, C. S., Randerson, J. T., and Rasch, P. J.: Present-day climate forcing and response from black carbon in snow, J. Geophys. Res.-Atmos., 112, D11202, 2007.
Friedl, M. A., Sulla-Menashe, D., Tan, B., Schneider, A., Ramankutty, N., Sibley, A., and Huang, X. M.: MODIS Collection 5 global land cover: Algorithm

refinements and characterization of new datasets, Remote Sens. Environ., 114, 168-182, 2010.
Fu, Q.: A New Parameterization of an Asymmetry Factor of Cirrus Clouds for Climate Models, J. Atmos. Sci., 64, 4140-4150, 2007.
Grenfell, T. C., Doherty, S. J., Clarke, A. D., and Warren, S. G.: Light absorption from particulate impurities in snow and ice determined by spectrophotometric analysis of filters, Appl. Opt., 50, 2037-2048, 2011.
Grenfell, T. C., Warren, S. G., and Mullen, P. C.: Reflection of Solar-Radiation by the Antarctic Snow Surface at Ultraviolet, Visible, and near-Infrared Wavelengths, J. Geophys. Res.-Atmos., 99, 18669-18684, 1994.
Guan, X., Huang, J., Guo, R., Yu, H., Lin, P., and Zhang, Y.: Role of radiatively forced temperature changes in enhanced semi-arid warming in the cold season over east Asia, Atmos. Chem. Phys., 15, 13777-13786, 2015.
Hadley, O. L., and Kirchstetter, T. W.: Black-carbon reduction of snow albedo, Nat. Clim. Change, 2, 437-440, 2012.
Hansen, J., and Nazarenko, L.: Soot climate forcing via snow and ice albedos, Proc. Nat. Acad. Sci. U.S.A., 101, 423-428, 2004.
Hansen, J., Sato, M., Ruedy, R., Nazarenko, L., Lacis, A., Schmidt, G. A., Russell, G., Aleinov, I., Bauer, M., Bauer, S., Bell, N., Cairns, B., Canuto, V., Chandler, M., Cheng, Y., Del Genio, A., Faluvegi, G., Fleming, E., Friend, A., Hall, T., Jackman, C., Kelley, M., Kiang, N., Koch, D., Lean, J., Lerner, J., Lo, K., Menon, S., Miller, R., Minnis, P., Novakov, T., Oinas, V., Perlwitz, J., Perlwitz, J., Rind, D., Romanou, A., Shindell, D., Stone, P., Sun, S., Tausnev, N., Thresher, D., Wielicki, B., Wong, T., Yao, M., and Zhang, S.: Efficacy of climate forcings, J. Geophys. Res.-Atmos., 110, D18104, 2005.
He, C. L., Li, Q. B., Liou, K. N., Takano, Y., Gu, Y., Qi, L., Mao, Y. H., and Leung, L. R.: Black carbon radiative forcing over the Tibetan Plateau, Geophys. Res. Lett., 41, 7806-7813, 2014.
Hegg, D. A., Warren, S. G., Grenfell, T. C., Doherty, S. J., and Clarke, A. D.: Sources of light-absorbing aerosol in arctic snow and their seasonal variation, Atmos. Chem. Phys., 10, 10923-10938, 2010.
Holben, B. N., Eck, T. F., and Fraser, R. S.: Temporal and Spatial Variability of Aerosol Optical Depth in the Sahel Region in Relation to Vegetation Remote-Sensing, Int. J. Remote Sens., 12, 1147-1163, 1991.
Holben, B. N., Eck, T. F., Slutsker, I., Smirnov, A., Sinyuk, A., Schafer, J., Giles, D., and Dubovik, O.: AERONET's Version 2.0 quality assurance criteria - art. no. 64080Q, Remote Sensing of the Atmosphere and Clouds, 6408, 64080q, 2006.
Holben, B. N., Tanre, D., Smirnov, A., Eck, T. F., Slutsker, I., Abuhassan, N., Newcomb, W. W., Schafer, J. S., Chatenet, B., Lavenu, F., Kaufman, Y. J., Castle, J. V., Setzer, A., Markham, B., Clark, D., Frouin, R., Halthore, R., Karneli, A., O'Neill, N. T., Pietras, C., Pinker, R. T., Voss, K., and Zibordi, G.: An emerging ground-based aerosol climatology: Aerosol optical depth from AERONET, J. Geophys. Res.-Atmos., 106, 12067-12097, 2001.
Hsu, S. C., Liu, S. C., Huang, Y. T., Chou, C. C. K., Lung, S. C. C., Liu, T. H., Tu, J. Y., and Tsai, F. J.: Long-range southeastward transport of Asian biosmoke pollution: Signature detected by aerosol potassium in Northern Taiwan, J. Geophys. Res.-Atmos., 114, D14301, 2009.
Huang, J. P., Fu, Q. A., Zhang, W., Wang, X., Zhang, R. D., Ye, H., and Warren, S. G.: Dust and Black Carbon in Seasonal Snow across Northern China, Bull. Amer. Meteor. Soc., 92, 175-181, 2011.

Huang, J. P., Liu, J. J., Chen, B., and Nasiri, S. L.: Detection of anthropogenic dust using CALIPSO lidar measurements, Atmos. Chem. Phys., 15, 11653-11665, 2015.
Huang, J. P., Minnis, P., Chen, B., Huang, Z. W., Liu, Z. Y., Zhao, Q. Y., Yi, Y. H., and Ayers, J. K.: Long-range transport and vertical structure of Asian dust from CALIPSO and surface measurements during PACDEX, J. Geophys. Res.-Atmos., 113, 2008.
Ichoku, C., Chu, D. A., Mattoo, S., Kaufman, Y. J., Remer, L. A., Tanre, D., Slutsker, I., and Holben, B. N.: A spatio-temporal approach for global validation and analysis of MODIS aerosol products, Geophys. Res. Lett., 29, 1616, 2002a.
Ichoku, C., Levy, R., Kaufman, Y. J., Remer, L. A., Li, R. R., Martins, V. J., Holben, B. N., Abuhassan, N., Slutsker, I., Eck, T. F., and Pietras, C.: Analysis of the performance characteristics of the five-channel Microtops II Sun photometer for measuring aerosol optical thickness and precipitable water vapor, J. Geophys. Res.-Atmos., 107, 4179, 2002b.
IPCC: Climate Change 2013: The Physical Science Basis. Contribution of Working Group I to the Fifth Assessment Report of the Intergovernmental Panel on Climate Change, Stocker, T. F., Qin, D., Plattner, G.-K., Tignor, M., Allen, S. K., Boschung, J., Nauels, A., Xia, Y., Bex, V., and Midgley, P. M., Cambridge Univ. Press, Cambridge, United Kingdom and New York, NY, USA, 2013.
Jaffe, D., Anderson, T., Covert, D., Kotchenruther, R., Trost, B., Danielson, J., Simpson, W., Berntsen, T., Karlsdottir, S., Blake, D., Harris, J., Carmichael, G., and Uno, I.: Transport of Asian air pollution to North America, Geophys. Res. Lett., 26, 711-714, 1999.
Kang, L. T., Huang, J. P., Chen, S. Y., and Wang, X.: Long-term trends of dust events over Tibetan Plateau during 1961-2010, Atmos. Environ., 125, 188-198, 2016.
Kaufman, Y. J., Tanre, D., Gordon, H. R., Nakajima, T., Lenoble, J., Frouin, R., Grassl, H., Herman, B. M., King, M. D., and Teillet, P. M.: Passive remote sensing of tropospheric aerosol and atmospheric correction for the aerosol effect, J. Geophys. Res.-Atmos., 102, 16815-16830, 1997.
Kokhanovsky, A. A., and Zege, E. P.: Scattering optics of snow, Appl. Opt., 43, 1589-1602, 2004.
Lafon, S., Sokolik, I. N., Rajot, J. L., Caquineau, S., and Gaudichet, A.: Characterization of iron oxides in mineral dust aerosols: Implications for light absorption, J. Geophys. Res.-Atmos., 111, D21207. 2006.
Light, B., Eicken, H., Maykut, G. A., and Grenfell, T. C.: The effect of included particulates on the spectral albedo of sea ice, J. Geophys. Res.-Oceans, 103, 27739-27752, 1998.
Liou, K. N., Takano, Y., and Yang, P.: Light absorption and scattering by aggregates: Application to black carbon and snow grains, J. Quant. Spectrosc. Ra., 112, 1581-1594, 2011.
Liou, K. N., Takano, Y., He, C., Yang, P., Leung, L. R., Gu, Y., and Lee, W. L.: Stochastic parameterization for light absorption by internally mixed BC/dust in snow grains for application to climate models, J. Geophys. Res.-Atmos., 119, 7616-7632, 2014.
Li, Z., et al.: Aerosol and monsoon climate interactions over Asia, Rev. Geophys., 54, 2016.
Lorenz, K., Preston, C. M., and Kandeler, E.: Soil organic matter in urban soils: Estimation of elemental carbon by thermal oxidation and characterization of

organic matter by solid-state C-13 nuclear magnetic resonance (NMR) spectroscopy, Geoderma, 130, 312-323, 2006.
Loveland, T. R., and Belward, A. S.: The IGBP-DIS global 1 km land cover data set, DISCover: first results, Int. J. Remote Sens., 18, 3291-3295, 1997.
McConnell, J. R., Edwards, R., Kok, G. L., Flanner, M. G., Zender, C. S., Saltzman, E. S., Banta, J. R., Pasteris, D. R., Carter, M. M., and Kahl, J. D. W.: 20th-century industrial black carbon emissions altered arctic climate forcing, Science, 317, 1381-1384, 2007.
More, S., Kumar, P. P., Gupta, P., Devara, P. C. S., and Aher, G. R.: Comparison of Aerosol Products Retrieved from AERONET, MICROTOPS and MODIS over a Tropical Urban City, Pune, India, Aerosol. Air. Qual. Res., 13, 107-121, 2013.
Morys, M., Mims, F. M., Hagerup, S., Anderson, S. E., Baker, A., Kia, J., and Walkup, T.: Design, calibration, and performance of MICROTOPS II handheld ozone monitor and Sun photometer, J. Geophys. Res.-Atmos., 106, 14573-14582, 2001.
Motoyoshi, H., Aoki, T., Hori, M., Abe, O., and Mochizuki, S.: Possible effect of anthropogenic aerosol deposition on snow albedo reduction at Shinjo, Japan, J. Meteorol. Soc. Jpn., 83A, 137-148, 2005.
Ofosu, F. G., Hopke, P. K., Aboh, I. J. K., and Bamford, S. A.: Characterization of fine particulate sources at Ashaiman in Greater Accra, Ghana, Atmos. Pollut. Res., 3, 301-310, 2012.
Painter, T. H., Barrett, A. P., Landry, C. C., Neff, J. C., Cassidy, M. P., Lawrence, C. R., McBride, K. E., and Farmer, G. L.: Impact of disturbed desert soils on duration of mountain snow cover, Geophys. Res. Lett., 34, L12502, 2007.
Painter, T. H., Bryant, A. C., and Skiles, S. M.: Radiative forcing by light absorbing impurities in snow from MODIS surface reflectance data, Geophys. Res. Lett., 39, L17502, 2012.
Painter, T. H., Deems, J. S., Belnap, J., Hamlet, A. F., Landry, C. C., and Udall, B.: Response of Colorado River runoff to dust radiative forcing in snow, Proc. Nat. Acad. Sci. U.S.A., 107, 17125-17130, 2010.
Painter, T. H., Seidel, F. C., Bryant, A. C., Skiles, S. M., and Rittger, K.: Imaging spectroscopy of albedo and radiative forcing by light-absorbing impurities in mountain snow, J. Geophys. Res.-Atmos., 118, 9511-9523, 2013.
Pedersen, C. A., Gallet, J. C., Strom, J., Gerland, S., Hudson, S. R., Forsstrom, S., Isaksson, E., and Berntsen, T. K.: In situ observations of black carbon in snow and the corresponding spectral surface albedo reduction, J. Geophys. Res.-Atmos., 120, 1476-1489, 2015.
Pio, C. A., Legrand, M., Oliveira, T., Afonso, J., Santos, C., Caseiro, A., Fialho, P., Barata, F., Puxbaum, H., Sanchez-Ochoa, A., Kasper-Giebl, A., Gelencser, A., Preunkert, S., and Schock, M.: Climatology of aerosol composition (organic versus inorganic) at nonurban sites on a west-east transect across Europe, J. Geophys. Res.-Atmos., 112, D23s02, 2007.
Porter, J. N., Miller, M., Pietras, C., and Motell, C.: Ship-based sun photometer measurements using Microtops sun photometers, J. Atmos. Oceanic Technol., 18, 765-774, 2001.
Pu, W., Wang, X., Zhang, X. Y., Ren, Y., Shi, J. S., Bi, J. R., and Zhang, B. D.: Size Distribution and Optical Properties of Particulate Matter (PM10) and Black Carbon (BC) during Dust Storms and Local Air Pollution Events across a Loess Plateau Site, Aerosol Air Qual. Res., 15, 2212-2224, 2015.

Qian, Y., Wang, H. L., Zhang, R. D., Flanner, M. G., and Rasch, P. J.: A sensitivity study on modeling black carbon in snow and its radiative forcing over the Arctic and Northern China, Environ. Res. Lett., 9, 064001, 2014.
Remer, L. A., Tanre, D., Kaufman, Y. J., Ichoku, C., Mattoo, S., Levy, R., Chu, D. A., Holben, B., Dubovik, O., Smirnov, A., Martins, J. V., Li, R. R., and Ahmad, Z.: Validation of MODIS aerosol retrieval over ocean, Geophys. Res. Lett., 29, 1618, 2002.
Routray, A., Mohanty, U. C., Osuri, K. K., and Prasad, S. K.: Improvement of Monsoon Depressions Forecast with Assimilation of Indian DWR Data Using WRF-3DVAR Analysis System, Pure Appl. Geophys., 170, 2329-2350, 2013.
Rozenberg, G.: Optical characteristics of thick weakly absorbing scattering layers, Dokl. Akad. Nauk SSSR, 145, 775-777, 1962.
Smith, T. M., Gao, J. D., Calhoun, K. M., Stensrud, D. J., Manross, K. L., Ortega, K. L., Fu, C. H., Kingfield, D. M., Elmore, K. L., Lakshmanan, V., and Riedel, C.: Examination of a Real-Time 3DVAR Analysis System in the Hazardous Weather Testbed, Weather Forecast., 29, 63-77, 2014.
Sokolik, I. N., and Toon, O. B.: Incorporation of mineralogical composition into models of the radiative properties of mineral aerosol from UV to IR wavelengths, J. Geophys. Res.-Atmos., 104, 9423-9444, 1999.
Srivastava, K., and Bhardwaj, R.: Analysis and very short range forecast of cyclone "AILA" with radar data assimilation with rapid intermittent cycle using ARPS 3DVAR and cloud analysis techniques, Meteorol. Atmos. Phys., 124, 97-111, 2014.
Toon, O. B., Mckay, C. P., Ackerman, T. P., and Santhanam, K.: Rapid Calculation of Radiative Heating Rates and Photodissociation Rates in Inhomoge'neous Multiple-Scattering Atmospheres, J. Geophys. Res.-Atmos., 94, 16287-16301, 1989.
Wang, M., Xu, B. Q., Zhao, H. B., Cao, J. J., Joswiak, D., Wu, G. J., and Lin, S. B.: The Influence of Dust on Quantitative Measurements of Black Carbon in Ice and Snow when Using a Thermal Optical Method, Aerosol Sci. Tech., 46, 60-69, 2012.
Wang, P., Che, H. Z., Zhang, X. C., Song, Q. L., Wang, Y. Q., Zhang, Z. H., Dai, X., and Yu, D. J.: Aerosol optical properties of regional background atmosphere in Northeast China, Atmos. Environ., 44, 4404-4412, 2010b.
Wang, X., Doherty, S. J., and Huang, J. P.: Black carbon and other light-absorbing impurities in snow across Northern China, J. Geophys. Res.-Atmos., 118, 1471-1492, 2013a.
Wang, X. G., Parrish, D., Kleist, D., and Whitaker, J.: GSI 3DVar-Based Ensemble-Variational Hybrid Data Assimilation for NCEP Global Forecast System: Single-Resolution Experiments, Mon. Weather. Rev., 141, 4098-4117, 2013b.
Wang, X., Huang, J. P., Ji, M. X., and Higuchi, K.: Variability of East Asia dust events and their long-term trend, Atmos. Environ., 42, 3156-3165, 2008.
Wang, X., Huang, J. P., Zhang, R. D., Chen, B., and Bi, J. R.: Surface measurements of aerosol properties over northwest China during ARM China 2008 deployment, J. Geophys. Res.-Atmos., 115, D00k27, 2010a.
Wang, X., Pu, W., Zhang, X. Y., Ren, Y., and Huang, J. P.: Water-soluble ions and trace elements in surface snow and their potential source regions across northeastern China, Atmos. Environ., 114, 57-65, 2015.

Wang, X., Xu, B. Q., and Ming, J.: An Overview of the Studies on Black Carbon and Mineral Dust Deposition in Snow and Ice Cores in East Asia, J. Meteorol. Res.-Prc., 28, 354-370, 2014.
Warren, S. G., and Wiscombe, W. J.: A Model for the Spectral Albedo of Snow .2. Snow Containing Atmospheric Aerosols, J. Atmos. Sci., 37, 2734-2745, 1980.
Warren, S. G. and Wiscombe, W. J.: Dirty Snow after Nuclear-War, Nature, 313, 467-470, 1985.
Warren, S. G.: Optical-Properties of Snow, Rev. Geophys., 20, 67-89, 1982.
Wright, P., Bergin, M., Dibb, J., Lefer, B., Domine, F., Carman, T., Carmagnola, C., Dumont, M., Courville, Z., Schaaf, C., and Wang, Z. S.: Comparing MODIS daily snow albedo to spectral albedo field measurements in Central Greenland, Remote Sens. Environ., 140, 118-129, 2014.
Wuttke, S., Seckmeyer, G., and Konig-Lang, G.: Measurements of spectral snow albedo at Neumayer, Antarctica, Ann. Geophys., 24, 7-21, 2006b.
Wuttke, S., Seckmeyer, G., Bernhard, G., Ehramjian, J., McKenzie, R., Johnston, P., and O'Neill, M.: New spectroradiometers complying with the NDSC standards, J. Atmos. Oceanic Technol., 23, 241-251, 2006a.
Xia, X. A., Chen, H. B., Wang, P. C., Zong, X. M., Qiu, J. H., and Gouloub, P.: Aerosol properties and their spatial and temporal variations over North China in spring 2001, Tellus B., 57, 28-39, 2005.
Xia, X. G., Li, Z. Q., Holben, B., Wang, P., Eck, T., Chen, H. B., Cribb, M., and Zhao, Y. X.: Aerosol optical properties and radiative effects in the Yangtze Delta region of China, J. Geophys. Res.-Atmos., 112, D22s12, 2007.
Xu, B. Q., Cao, J. J., Hansen, J., Yao, T. D., Joswia, D. R., Wang, N. L., Wu, G. J., Wang, M., Zhao, H. B., Yang, W., Liu, X. Q., and He, J. Q.: Black soot and the survival of Tibetan glaciers, Proc. Nat. Acad. Sci. U.S.A., 106, 22114-22118, 2009.
Xu, B. Q., Cao, J. J., Joswiak, D. R., Liu, X. Q., Zhao, H. B., and He, J. Q.: Post-depositional enrichment of black soot in snow-pack and accelerated melting of Tibetan glaciers, Environ. Res. Lett., 7, 2012.
Yasunari, T. J., Bonasoni, P., Laj, P., Fujita, K., Vuillermoz, E., Marinoni, A., Cristofanelli, P., Duchi, R., Tartari, G., and Lau, K. M.: Estimated impact of black carbon deposition during pre-monsoon season from Nepal Climate Observatory - Pyramid data and snow albedo changes over Himalayan glaciers, Atmos. Chem. Phys., 10, 6603-6615, 2010.
Yasunari, T. J., Koster, R. D., Lau, W. K. M., and Kim, K. M.: Impact of snow darkening via dust, black carbon, and organic carbon on boreal spring climate in the Earth system, J. Geophys. Res.-Atmos., 120, 5485-5503, 2015.
Ye, H., Zhang, R. D., Shi, J. S., Huang, J. P., Warren, S. G., and Fu, Q.: Black carbon in seasonal snow across northern Xinjiang in northwestern China, Environ. Res. Lett., 7, 044002, 2012.
Yesubabu, V., Srinivas, C. V., Hariprasad, K. B. R. R., and Baskaran, R.: A Study on the Impact of Observation Assimilation on the Numerical Simulation of Tropical Cyclones JAL and THANE Using 3DVAR, Pure Appl. Geophys., 171, 2023-2042, 2014.
Zawadzka, O., Makuch, P., Markowicz, K. M., Zielinski, T., Petelski, T., Ulevicius, V., Strzalkowska, A., Rozwadowska, A., and Gutowska, D.: Studies of aerosol optical depth with the use of Microtops II sun photometers and MODIS detectors in coastal areas of the Baltic Sea, Acta Geophysica, 62, 400-422, 2014.

Zege, Ė. P., Ivanov, A. P., and Katsev, I. L.: Image transfer through a scattering medium, Springer Verlag, 1991.

Zhang, R., Hegg, D. A., Huang, J., and Fu, Q.: Source attribution of insoluble light-absorbing particles in seasonal snow across northern China, Atmos. Chem. Phys., 13, 6091-6099, 2013a.

Zhang, R., Jing, J., Tao, J., Hsu, S. C., Wang, G., Cao, J., Lee, C. S. L., Zhu, L., Chen, Z., Zhao, Y., and Shen, Z.: Chemical characterization and source apportionment of PM2.5 in Beijing: seasonal perspective, Atmos. Chem. Phys., 13, 7053-7074, 2013b.

Zhang, X. L., Wu, G. J., Kokhanovsky, A., Yao, T. D., and Tong D.: Spectral albedo parameterization for dirty snow with considering mirco-physicochemical properties of impurities - Part I: Theory and preliminary evaluation, 2017~~6~~ (preparation).

Zhang, X. Y., Gong, S. L., Shen, Z. X., Mei, F. M., Xi, X. X., Liu, L. C., Zhou, Z. J., Wang, D., Wang, Y. Q., and Cheng, Y.: Characterization of soil dust aerosol in China and its transport and distribution during 2001 ACE-Asia: 1. Network observations, J. Geophys. Res.-Atmos., 108, 4261, 2003.

Zhao, C., Hu, Z., Qian, Y., Leung, L. R., Huang, J., Huang, M., Jin, J., Flanner, M. G., Zhang, R., Wang, H., Yan, H., Lu, Z., and Streets, D. G.: Simulating black carbon and dust and their radiative forcing in seasonal snow: a case study over North China with field campaign measurements, Atmos. Chem. Phys., 14, 11475-11491, 2014.

~~References~~

~~Acosta, J. A., Faz, A., Kalbitz, K., Jansen, B., and Martinez-Martinez, S.: Heavy metal concentrations in particle size fractions from street dust of Murcia (Spain) as the basis for risk assessment, J. Environ. Monitor., 13, 3087-3096, 2011.~~

~~Aleksandropoulou, V., Torseth, K., and Lazaridis, M.: Atmospheric Emission Inventory for Natural and Anthropogenic Sources and Spatial Emission Mapping for the Greater Athens Area, Water Air Soil Pollut., 219, 507-526, 2011.~~

~~Alfaro, S. C., Lafon, S., Rajot, J. L., Formenti, P., Gaudichet, A., and Maille, M.: Iron oxides and light absorption by pure desert dust: An experimental study, J. Geophys. Res.-Atmos., 109, D08208, 2004.~~

~~Arhami, M., Kuhn, T., Fine, P. M., Delfino, R. J., and Sioutas, C.: Effects of sampling artifacts and operating parameters on the performance of a semicontinuous particulate elemental carbon/organic carbon monitor, Environ. Sci. Technol., 40, 945-954, 2006.~~

~~Ax, W., Malchow, H., Koren, H., and Fischer, H.: Studies on immunological reactions in vitro, Sbornik vedeckych praci Lekarske fakulty Karlovy university v Hradci Kralove, 13, 287-292, 1970.~~

~~Bergstrom, R. W., Russell, P. B., and Hignett, P.: Wavelength dependence of the absorption of black carbon particles: Predictions and results from the TARFOX experiment and implications for the aerosol single scattering albedo, J. Atmos. Sci., 59, 567-577, 2002.~~

~~Bi, J. R., Huang, J. P., Hu, Z. Y., Holben, B. N., and Guo, Z. Q.: Investigating the aerosol optical and radiative characteristics of heavy haze episodes in Beijing during January of 2013, J. Geophys. Res. Atmos., 119, 9884-9900, 2014.~~

~~Bond, T. C., and Bergstrom, R. W.: Light absorption by carbonaceous particles: An investigative review, Aerosol Sci. Tech., 40, 27-67, 2006.~~

Bond, T. C., Bussemer, M., Wehner, B., Keller, S., Charlson, R. J., and Heintzenberg, J.: Light absorption by primary particle emissions from a lignite burning plant, Environ. Sci. Technol., 33, 3887-3891, 1999.

Bond, T. C., Doherty, S. J., Fahey, D. W., Forster, P. M., Berntsen, T., DeAngelo, B. J., Flanner, M. G., Ghan, S., Karcher, B., Koch, D., Kinne, S., Kondo, Y., Quinn, P. K., Sarofim, M. C., Schultz, M. G., Schulz, M., Venkataraman, C., Zhang, H., Zhang, S., Bellouin, N., Guttikunda, S. K., Hopke, P. K., Jacobson, M. Z., Kaiser, J. W., Klimont, Z., Lohmann, U., Schwarz, J. P., Shindell, D., Storelvmo, T., Warren, S. G., and Zender, C. S.: Bounding the role of black carbon in the climate system: A scientific assessment, J. Geophys. Res. Atmos., 118, 5380-5552, 2013.

Brandt, R. E., Warren, S. G., and Clarke, A. D.: A controlled snowmaking experiment testing the relation between black carbon content and reduction of snow albedo, J. Geophys. Res. Atmos., 116, D08109, 2011.

Cappa, C. D., Onasch, T. B., Massoli, P., Worsnop, D. R., Bates, T. S., Cross, E. S., Davidovits, P., Hakala, J., Hayden, K. L., Jobson, B. T., Kolesar, K. R., Lack, D. A., Lerner, B. M., Li, S. M., Mellon, D., Nuaaman, I., Olfert, J. S., Petaja, T., Quinn, P. K., Song, C., Subramanian, R., Williams, E. J., and Zaveri, R. A.: Radiative Absorption Enhancements Due to the Mixing State of Atmospheric Black Carbon, Science, 337, 1078-1081, 2012.

Carmagnola, C. M., Domine, F., Dumont, M., Wright, P., Strellis, B., Bergin, M., Dibb, J., Picard, G., Libois, Q., Arnaud, L., and Morin, S.: Snow spectral albedo at Summit, Greenland: measurements and numerical simulations based on physical and chemical properties of the snowpack, Cryosphere, 7, 1139-1160, 2013.

Che, H. Z., Wang, Y. Q., and Sun, J. Y.: Aerosol optical properties at Mt. Waliguan Observatory, China, Atmos. Environ., 45, 6004-6009, 2011.

Che, H. Z., Wang, Y. Q., Sun, J. Y., Zhang, X. C., Zhang, X. Y., and Guo, J. P.: Variation of Aerosol Optical Properties over the Taklimakan Desert in China, Aerosol Air Qual. Res., 13, 777-785, 2013.

Che, H. Z., Yang, Z. F., Zhang, X. Y., Zhu, C. Z., Ma, Q. L., Zhou, H. G., and Wang, P.: Study on the aerosol optical properties and their relationship with aerosol chemical compositions over three regional background stations in China, Atmos. Environ., 43, 1093-1099, 2009.

Che, H., Zhang, X. Y., Xia, X., Goloub, P., Holben, B., Zhao, H., Wang, Y., Zhang, X. C., Wang, H., Blarel, L., Damiri, B., Zhang, R., Deng, X., Ma, Y., Wang, T., Geng, F., Qi, B., Zhu, J., Yu, J., Chen, Q., and Shi, G.: Ground-based aerosol climatology of China: aerosol optical depths from the China Aerosol Remote Sensing Network (CARSNET) 2002-2013, Atmos. Chem. Phys., 15, 7619-7652, 2015a.

Che, H. Z., Zhao, H. J., Wu, Y. F., Xia, X. G., Zhu, J., Wang, H., Wang, Y. Q., Sun, J. Y., Yu, J., Zhang, X. Y., and Shi, G. Y.: Analyses of aerosol optical properties and direct radiative forcing over urban and industrial regions in Northeast China, Meteorol. Atmos. Phys., 127, 345-354, 2015b.

Chen, S. Y., Huang, J. P., Zhao, C., Qian, Y., Leung, L. R., and Yang, B.: Modeling the transport and radiative forcing of Taklimakan dust over the Tibetan Plateau: A case study in the summer of 2006, J. Geophys. Res. Atmos., 118, 797-812, 2013.

Chu, D. A., Kaufman, Y. J., Ichoku, C., Remer, L. A., Tanre, D., and Holben, B. N.: Validation of MODIS aerosol optical depth retrieval over land, Geophys. Res. Lett., 29, 1617, 2002.

Cong, Z., Kang, S., Kawamura, K., Liu, B., Wan, X., Wang, Z., Gao, S., and Fu, P.: Carbonaceous aerosols on the south edge of the Tibetan Plateau: concentrations, seasonality and sources, Atmos. Chem. Phys., 15, 1573-1584, 2015.

Coz, E., Casuccio, G., Lersch, T. L., Moreno, T., and Artinano, B.: Anthropogenic Influenced Mineral Dust Ambient Fine Particles At An Urban Site In Barcelona (Spain), Chem. Eng. Trans., 22, 101-106, 2010.

Dang, C., and Hegg, D. A.: Quantifying light absorption by organic carbon in Western North American snow by serial chemical extractions, J. Geophys. Res.-Atmos., 119, 10247-10261, 2014.

Dang, C., Brandt, R. E., and Warren, S. G.: Parameterizations for narrowband and broadband albedo of pure snow and snow containing mineral dust and black carbon, J. Geophys. Res.-Atmos., 120, 5446-5468, 2015.

Dang, C., Fu, Q., and Warren, S. G.: Effect of Snow Grain Shape on Snow Albedo, J. Atmos. Sci., 73, 3573-3583, 2016.

Doherty, S. J., Dang, C., Hegg, D. A., Zhang, R. D., and Warren, S. G.: Black carbon and other light-absorbing particles in snow of central North America, J. Geophys. Res.-Atmos., 119, 12807-12831, 2014.

Doherty, S. J., Grenfell, T. C., Forsstrom, S., Hegg, D. L., Brandt, R. E., and Warren, S. G.: Observed vertical redistribution of black carbon and other insoluble light-absorbing particles in melting snow, J. Geophys. Res.-Atmos., 118, 5553-5569, 2013.

Doherty, S. J., Warren, S. G., Grenfell, T. C., Clarke, A. D., and Brandt, R. E.: Light-absorbing impurities in Arctic snow, Atmos. Chem. Phys., 10, 11647-11680, 2010.

Fierce, L., Bond, T. C., Bauer, S. E., Mena, F., and Riemer, N.: Black carbon absorption at the global scale is affected by particle-scale diversity in composition, Nat. Commun., 7, 2016.

Flanner, M. G.: Arctic climate sensitivity to local black carbon, J. Geophys. Res.-Atmos., 118, 1840-1851, 2013.

Flanner, M. G., Liu, X., Zhou, C., Penner, J. E., and Jiao, C.: Enhanced solar energy absorption by internally-mixed black carbon in snow grains, Atmos. Chem. Phys., 12, 4699-4721, 2012.

Flanner, M. G., Zender, C. S., Hess, P. G., Mahowald, N. M., Painter, T. H., Ramanathan, V., and Rasch, P. J.: Springtime warming and reduced snow cover from carbonaceous particles, Atmos. Chem. Phys., 9, 2481-2497, 2009.

Flanner, M. G., Zender, C. S., Randerson, J. T., and Rasch, P. J.: Present-day climate forcing and response from black carbon in snow, J. Geophys. Res.-Atmos., 112, D11202, 2007.

Friedl, M. A., Sulla-Menashe, D., Tan, B., Schneider, A., Ramankutty, N., Sibley, A., and Huang, X. M.: MODIS Collection 5 global land cover: Algorithm refinements and characterization of new datasets, Remote Sens. Environ., 114, 168-182, 2010.

Fu, Q.: A New Parameterization of an Asymmetry Factor of Cirrus Clouds for Climate Models, J. Atmos. Sci., 64, 4140-4150, 2007.

Givati, A., and Rosenfeld, D.: Quantifying precipitation suppression due to air pollution, J. Appl. Meteorol., 43, 1038-1056, 2004.

Goudie, A. S., and Middleton, N. J.: Saharan dust storms: nature and consequences, Earth Sci. Rev., 56, 179-204, 2001.
Grenfell, T. C., Doherty, S. J., Clarke, A. D., and Warren, S. G.: Light absorption from particulate impurities in snow and ice determined by spectrophotometric analysis of filters, Appl. Opt., 50, 2037-2048, 2011.
Grenfell, T. C., Warren, S. G., and Mullen, P. C.: Reflection of Solar-Radiation by the Antarctic Snow Surface at Ultraviolet, Visible, and near-Infrared Wavelengths, J. Geophys. Res.-Atmos., 99, 18669-18684, 1994.
Guan, X. D., Huang, J. P., Zhang, Y. T., Xie, Y. K., and Liu, J. J.: The relationship between anthropogenic dust and population over global semi-arid regions, Atmos. Chem. Phys., 16, 5159-5169, 2016.
Guan, X., Huang, J., Guo, R., Yu, H., Lin, P., and Zhang, Y.: Role of radiatively forced temperature changes in enhanced semi-arid warming in the cold season over east Asia, Atmos. Chem. Phys., 15, 13777-13786, 2015.
Hadley, O. L., and Kirchstetter, T. W.: Black-carbon reduction of snow albedo, Nat. Clim. Change, 2, 437-440, 2012.
Hansen, J., and Nazarenko, L.: Soot climate forcing via snow and ice albedos, Proc. Nat. Acad. Sci. U.S.A., 101, 423-428, 2004.
Hansen, J., Sato, M., Ruedy, R., Nazarenko, L., Lacis, A., Schmidt, G. A., Russell, G., Aleinov, I., Bauer, M., Bauer, S., Bell, N., Cairns, B., Canuto, V., Chandler, M., Cheng, Y., Del Genio, A., Faluvegi, G., Fleming, E., Friend, A., Hall, T., Jackman, C., Kelley, M., Kiang, N., Koch, D., Lean, J., Lerner, J., Lo, K., Menon, S., Miller, R., Minnis, P., Novakov, T., Oinas, V., Perlwitz, J., Perlwitz, J., Rind, D., Romanou, A., Shindell, D., Stone, P., Sun, S., Tausnev, N., Thresher, D., Wielicki, B., Wong, T., Yao, M., and Zhang, S.: Efficacy of climate forcings, J. Geophys. Res.-Atmos., 110, D18104, 2005.
He, C. L., Li, Q. B., Liou, K. N., Takano, Y., Gu, Y., Qi, L., Mao, Y. H., and Leung, L. R.: Black carbon radiative forcing over the Tibetan Plateau, Geophys. Res. Lett., 41, 7806-7813, 2014.
Hegg, D. A., Warren, S. G., Grenfell, T. C., Doherty, S. J., and Clarke, A. D.: Sources of light-absorbing aerosol in arctic snow and their seasonal variation, Atmos. Chem. Phys., 10, 10923-10938, 2010.
Hegg, D. A., Warren, S. G., Grenfell, T. C., Doherty, S. J., Larson, T. V., and Clarke, A. D.: Source Attribution of Black Carbon in Arctic Snow, Environ. Sci. Technol., 43, 4016-4021, 2009.
Holben, B. N., Eck, T. F., and Fraser, R. S.: Temporal and Spatial Variability of Aerosol Optical Depth in the Sahel Region in Relation to Vegetation Remote-Sensing, Int. J. Remote Sens., 12, 1147-1163, 1991.
Holben, B. N., Eck, T. F., Slutsker, I., Smirnov, A., Sinyuk, A., Schafer, J., Giles, D., and Dubovik, O.: AERONET's Version 2.0 quality assurance criteria - art. no. 64080Q, Remote Sensing of the Atmosphere and Clouds, 6408, 64080q, 2006.
Holben, B. N., Tanre, D., Smirnov, A., Eck, T. F., Slutsker, I., Abuhassan, N., Newcomb, W. W., Schafer, J. S., Chatenet, B., Lavenu, F., Kaufman, Y. J., Castle, J. V., Setzer, A., Markham, B., Clark, D., Frouin, R., Halthore, R., Karneli, A., O'Neill, N. T., Pietras, C., Pinker, R. T., Voss, K., and Zibordi, G.: An emerging ground-based aerosol climatology: Aerosol optical depth from AERONET, J. Geophys. Res.-Atmos., 106, 12067-12097, 2001.
Hsu, S. C., Liu, S. C., Huang, Y. T., Chou, C. C. K., Lung, S. C. C., Liu, T. H., Tu, J. Y., and Tsai, F. J.: Long-range southeastward transport of Asian biosmoke

pollution: Signature detected by aerosol potassium in Northern Taiwan, J. Geophys. Res.-Atmos., 114, D14301, 2009.

Huang, J. P., Fu, Q. A., Zhang, W., Wang, X., Zhang, R. D., Ye, H., and Warren, S. G.: Dust and Black Carbon in Seasonal Snow across Northern China, Bull. Amer. Meteor. Soc., 92, 175-181, 2011.

Huang, J. P., Liu, J. J., Chen, B., and Nasiri, S. L.: Detection of anthropogenic dust using CALIPSO lidar measurements, Atmos. Chem. Phys., 15, 11653-11665, 2015a.

Huang, J. P., Minnis, P., Chen, B., Huang, Z. W., Liu, Z. Y., Zhao, Q. Y., Yi, Y. H., and Ayers, J. K.: Long-range transport and vertical structure of Asian dust from CALIPSO and surface measurements during PACDEX, J. Geophys. Res.-Atmos., 113, 2008.

Huang, J. P., Wang, T. H., Wang, W. C., Li, Z. Q., and Yan, H. R.: Climate effects of dust aerosols over East Asian arid and semiarid regions, J. Geophys. Res.-Atmos., 119, 11398-11416, 2014.

Huang, Z. W., Huang, J. P., Hayasaka, T., Wang, S. S., Zhou, T., and Jin, H. C.: Short-cut transport path for Asian dust directly to the Arctic: a case study, Environ. Res. Lett., 10, 114018, 2015b.

Ichoku, C., Chu, D. A., Mattoo, S., Kaufman, Y. J., Remer, L. A., Tanre, D., Slutsker, I., and Holben, B. N.: A spatio-temporal approach for global validation and analysis of MODIS aerosol products, Geophys. Res. Lett., 29, 1616, 2002a.

Ichoku, C., Levy, R., Kaufman, Y. J., Remer, L. A., Li, R. R., Martins, V. J., Holben, B. N., Abuhassan, N., Slutsker, I., Eck, T. F., and Pietras, C.: Analysis of the performance characteristics of the five-channel Microtops II Sun photometer for measuring aerosol optical thickness and precipitable water vapor, J. Geophys. Res.-Atmos., 107, 4179, 2002b.

IPCC: Climate Change 2013: The Physical Science Basis. Contribution of Working Group I to the Fifth Assessment Report of the Intergovernmental Panel on Climate Change, Stocker, T. F., Qin, D., Plattner, G.-K., Tignor, M., Allen, S. K., Boschung, J., Nauels, A., Xia, Y., Bex, V., and Midgley, P. M., Cambridge Univ. Press, Cambridge, United Kingdom and New York, NY, USA, 2013.

Jacobson, M. Z.: Climate response of fossil fuel and biofuel soot, accounting for soot's feedback to snow and sea ice albedo and emissivity, J. Geophys. Res.-Atmos., 109, D21201, 2004.

Jaffe, D., Anderson, T., Covert, D., Kotchenruther, R., Trost, B., Danielson, J., Simpson, W., Berntsen, T., Karlsdottir, S., Blake, D., Harris, J., Carmichael, G., and Uno, I.: Transport of Asian air pollution to North America, Geophys. Res. Lett., 26, 711-714, 1999.

Kamani, H., Ashrafi, S. D., Isazadeh, S., Jaafari, J., Hoseini, M., Mostafapour, F. K., Bazrafshan, E., Nazmara, S., and Mahvi, A. H.: Heavy Metal Contamination in Street Dusts with Various Land Uses in Zahedan, Iran, B. Environ. Contam. Tox., 94, 382-386, 2015.

Kang, L. T., Huang, J. P., Chen, S. Y., and Wang, X.: Long-term trends of dust events over Tibetan Plateau during 1961-2010, Atmos. Environ., 125, 188-198, 2016.

Kaufman, Y. J., Tanre, D., Gordon, H. R., Nakajima, T., Lenoble, J., Frouin, R., Grassl, H., Herman, B. M., King, M. D., and Teillet, P. M.: Passive remote sensing of tropospheric aerosol and atmospheric correction for the aerosol effect, J. Geophys. Res.-Atmos., 102, 16815-16830, 1997.

Kim, W., Doh, S. J., and Yu, Y.: Anthropogenic contribution of magnetic particulates in urban roadside dust, Atmos. Environ., 43, 3137-3144, 2009.

Koch, D., Menon, S., Del Genio, A., Ruedy, R., Alienov, I., and Schmidt, G. A.: Distinguishing Aerosol Impacts on Climate over the Past Century, J. Climate, 22, 2659-2677, 2009.
Kokhanovsky, A. A., and Zege, E. P.: Scattering optics of snow, Appl. Opt., 43, 1589-1602, 2004.
Lafon, S., Sokolik, I. N., Rajot, J. L., Caquineau, S., and Gaudichet, A.: Characterization of iron oxides in mineral dust aerosols: Implications for light absorption, J. Geophys. Res.-Atmos., 111, D21207, 2006.
Light, B., Eicken, H., Maykut, G. A., and Grenfell, T. C.: The effect of included particulates on the spectral albedo of sea ice, J. Geophys. Res.-Oceans, 103, 27739-27752, 1998.
Li, G. J., Chen, J., Ji, J. F., Yang, J. D., and Conway, T. M.: Natural and anthropogenic sources of East Asian dust, Geology, 37, 727-730, 2009.
Liou, K. N., Takano, Y., and Yang, P.: Light absorption and scattering by aggregates: Application to black carbon and snow grains, J. Quant. Spectrosc. Ra., 112, 1581-1594, 2011.
Liou, K. N., Takano, Y., He, C., Yang, P., Leung, L. R., Gu, Y., and Lee, W. L.: Stochastic parameterization for light absorption by internally mixed BC/dust in snow grains for application to climate models, J. Geophys. Res.-Atmos., 119, 7616-7632, 2014.
Li, S. Y., Lei, J. Q., Xu, X. W., Wang, H. F., and Gu, F.: Dust Source of Sandstorm in the Tarim Basin, Northwest China, Adv. Environ. Sci. Eng., 518-523, 4592-4598, 2012.
Li, Z., et al.: Aerosol and monsoon climate interactions over Asia, Rev. Geophys., 54, 2016.
Lorenz, K., Preston, C. M., and Kandeler, E.: Soil organic matter in urban soils: Estimation of elemental carbon by thermal oxidation and characterization of organic matter by solid-state C-13 nuclear magnetic resonance (NMR) spectroscopy, Geoderma, 130, 312-323, 2006.
Loveland, T. R., and Belward, A. S.: The IGBP-DIS global 1 km land cover data set, DISCover: first results, Int. J. Remote Sens., 18, 3291-3295, 1997.
Mahowald, N. M., and Luo, C.: A less dusty future?, Geophys. Res. Lett., 30, 1903, 2003.
Mahowald, N. M., Baker, A. R., Bergametti, G., Brooks, N., Duce, R. A., Jickells, T. D., Kubilay, N., Prospero, J. M., and Tegen, I.: Atmospheric global dust cycle and iron inputs to the ocean, Global Biogeochem. CY., 19, Gb4025, 2005.
McConnell, J. R., Edwards, R., Kok, G. L., Flanner, M. G., Zender, C. S., Saltzman, E. S., Banta, J. R., Pasteris, D. R., Carter, M. M., and Kahl, J. D. W.: 20th-century industrial black carbon emissions altered arctic climate forcing, Science, 317, 1381-1384, 2007.
More, S., Kumar, P. P., Gupta, P., Devara, P. C. S., and Aher, G. R.: Comparison of Aerosol Products Retrieved from AERONET, MICROTOPS and MODIS over a Tropical Urban City, Pune, India, Aerosol. Air. Qual. Res., 13, 107-121, 2013.
Morys, M., Mims, F. M., Hagerup, S., Anderson, S. E., Baker, A., Kia, J., and Walkup, T.: Design, calibration, and performance of MICROTOPS II handheld ozone monitor and Sun photometer, J. Geophys. Res.-Atmos., 106, 14573-14582, 2001.
Motoyoshi, H., Aoki, T., Hori, M., Abe, O., and Mochizuki, S.: Possible effect of anthropogenic aerosol deposition on snow albedo reduction at Shinjo, Japan, J. Meteorol. Soc. Jpn., 83A, 137-148, 2005.

Ofosu, F. G., Hopke, P. K., Aboh, I. J. K., and Bamford, S. A.: Characterization of fine particulate sources at Ashaiman in Greater Accra, Ghana, Atmos. Pollut. Res., 3, 301-310, 2012.

Painter, T. H., Bryant, A. C., and Skiles, S. M.: Radiative forcing by light absorbing impurities in snow from MODIS surface reflectance data, Geophys. Res. Lett., 39, L17502, 2012.

Painter, T. H., Barrett, A. P., Landry, C. C., Neff, J. C., Cassidy, M. P., Lawrence, C. R., McBride, K. E., and Farmer, G. L.: Impact of disturbed desert soils on duration of mountain snow cover, Geophys. Res. Lett., 34, L12502, 2007.

Painter, T. H., Deems, J. S., Belnap, J., Hamlet, A. F., Landry, C. C., and Udall, B.: Response of Colorado River runoff to dust radiative forcing in snow, Proc. Nat. Acad. Sci. U.S.A., 107, 17125-17130, 2010.

Painter, T. H., Seidel, F. C., Bryant, A. C., Skiles, S. M., and Rittger, K.: Imaging spectroscopy of albedo and radiative forcing by light-absorbing impurities in mountain snow, J. Geophys. Res.-Atmos., 118, 9511-9523, 2013.

Park, S. U., and Park, M. S.: Aerosol size distributions observed at Naiman in the Asian dust source region of Inner Mongolia, Atmos. Environ., 82, 17-23, 2014.

Pedersen, C. A., Gallet, J. C., Strom, J., Gerland, S., Hudson, S. R., Forsstrom, S., Isaksson, E., and Berntsen, T. K.: In situ observations of black carbon in snow and the corresponding spectral surface albedo reduction, J. Geophys. Res.-Atmos., 120, 1476-1489, 2015.

Pio, C. A., Legrand, M., Oliveira, T., Afonso, J., Santos, C., Caseiro, A., Fialho, P., Barata, F., Puxbaum, H., Sanchez-Ochoa, A., Kasper-Giebl, A., Gelencser, A., Preunkert, S., and Schock, M.: Climatology of aerosol composition (organic versus inorganic) at nonurban sites on a west-east transect across Europe, J. Geophys. Res.-Atmos., 112, D23s02, 2007.

Porter, J. N., Miller, M., Pietras, C., and Motell, C.: Ship-based sun photometer measurements using Microtops sun photometers, J. Atmos. Oceanic Technol., 18, 765-774, 2001.

Pu, W., Wang, X., Zhang, X. Y., Ren, Y., Shi, J. S., Bi, J. R., and Zhang, B. D.: Size Distribution and Optical Properties of Particulate Matter (PM10) and Black Carbon (BC) during Dust Storms and Local Air Pollution Events across a Loess Plateau Site, Aerosol Air Qual. Res., 15, 2212-2224, 2015.

Qian, Y., Wang, H. L., Zhang, R. D., Flanner, M. G., and Rasch, P. J.: A sensitivity study on modeling black carbon in snow and its radiative forcing over the Arctic and Northern China, Environ. Res. Lett., 9, 064001, 2014.

Qian, Y., Yasunari, T. J., Doherty, S. J., Flanner, M. G., Lau, W. K. M., Ming, J., Wang, H. L., Wang, M., Warren, S. G., and Zhang, R. D.: Light-absorbing Particles in Snow and Ice: Measurement and Modeling of Climatic and Hydrological impact, Adv. Atmos. Sci., 32, 64-91, 2015.

Qiao, Q. Q., Huang, B. C., Zhang, C. X., Piper, J. D. A., Pan, Y. P., and Sun, Y.: Assessment of heavy metal contamination of dustfall in northern China from integrated chemical and magnetic investigation, Atmos. Environ., 74, 182-193, 2013.

Remer, L. A., Tanre, D., Kaufman, Y. J., Ichoku, C., Mattoo, S., Levy, R., Chu, D. A., Holben, B., Dubovik, O., Smirnov, A., Martins, J. V., Li, R. R., and Ahmad, Z.: Validation of MODIS aerosol retrieval over ocean, Geophys. Res. Lett., 29, 1618, 2002.

Rosenfeld, D., Rudich, Y., and Lahav, R.: Desert dust suppressing precipitation: A possible desertification feedback loop, Proc. Nat. Acad. Sci. U.S.A., 98, 5975-5980, 2001.

Routray, A., Mohanty, U. C., Osuri, K. K., and Prasad, S. K.: Improvement of Monsoon Depressions Forecast with Assimilation of Indian DWR Data Using WRF-3DVAR Analysis System, Pure Appl. Geophys., 170, 2329-2350, 2013.

Rozenberg, G.: Optical characteristics of thick weakly absorbing scattering layers, Dokl. Akad. Nauk SSSR, 145, 775-777, 1962.

Smith, T. M., Gao, J. D., Calhoun, K. M., Stensrud, D. J., Manross, K. L., Ortega, K. L., Fu, C. H., Kingfield, D. M., Elmore, K. L., Lakshmanan, V., and Riedel, C.: Examination of a Real-Time 3DVAR Analysis System in the Hazardous Weather Testbed, Weather Forecast., 29, 63-77, 2014.

Sokolik, I. N., and Toon, O. B.: Incorporation of mineralogical composition into models of the radiative properties of mineral aerosol from UV to IR wavelengths, J. Geophys. Res.-Atmos., 104, 9423-9444, 1999.

Srivastava, K., and Bhardwaj, R.: Analysis and very short range forecast of cyclone "AILA" with radar data assimilation with rapid intermittent cycle using ARPS 3DVAR and cloud analysis techniques, Meteorol. Atmos. Phys., 124, 97-111, 2014.

Tegen, I., and Fung, I.: Contribution to the Atmospheric Mineral Aerosol Load from Land Surface Modification, J. Geophys. Res.-Atmos., 100, 18707-18726, 1995.

Tegen, I., Harrison, S. P., Kohfeld, K. E., Engelstaedter, S., and Werner, M.: Emission of soil dust aerosol: Anthropogenic contribution and future changes, Geochimica Et Cosmochimica Acta, 66, A766-A766, 2002.

Tegen, I., Werner, M., Harrison, S. P., and Kohfeld, K. E.: Relative importance of climate and land use in determining present and future global soil dust emission, Geophys. Res. Lett., 31, L05105, 2004.

Thompson, L. G., Davis, M. E., Mosleythompson, E., and Liu, K. B.: Pre-Incan Agricultural Activity Recorded in Dust Layers in 2 Tropical Ice Cores, Nature, 336, 763-765, 1988.

Toon, O. B., Mckay, C. P., Ackerman, T. P., and Santhanam, K.: Rapid Calculation of Radiative Heating Rates and Photodissociation Rates in Inhomoge'neous Multiple-Scattering Atmospheres, J. Geophys. Res.-Atmos., 94, 16287-16301, 1989.

Wallach, D. F. H., and Fischer, H.: Membrane aspects of the immune response. Report of a workshop held in Titisee, Schwarzwald, Germany, October 13-15, 1969, FEBS Lett., 9, 129-135, 1970.

Wang, M., Xu, B. Q., Zhao, H. B., Cao, J. J., Joswiak, D., Wu, G. J., and Lin, S. B.: The Influence of Dust on Quantitative Measurements of Black Carbon in Ice and Snow when Using a Thermal Optical Method, Aerosol Sci. Tech., 46, 60-69, 2012.

Wang, P., Che, H. Z., Zhang, X. C., Song, Q. L., Wang, Y. Q., Zhang, Z. H., Dai, X., and Yu, D. J.: Aerosol optical properties of regional background atmosphere in Northeast China, Atmos. Environ., 44, 4404-4412, 2010a.

Wang, X., Doherty, S. J., and Huang, J. P.: Black carbon and other light-absorbing impurities in snow across Northern China, J. Geophys. Res.-Atmos., 118, 1471-1492, 2013a.

Wang, X. G., Parrish, D., Kleist, D., and Whitaker, J.: GSI 3DVar-Based Ensemble-Variational Hybrid Data Assimilation for NCEP Global Forecast

System: Single-Resolution Experiments, Mon. Weather. Rev., 141, 4098-4117, 2013b.
Wang, X., Huang, J. P., Ji, M. X., and Higuchi, K.: Variability of East Asia dust events and their long-term trend, Atmos. Environ., 42, 3156-3165, 2008.
Wang, X., Huang, J. P., Zhang, R. D., Chen, B., and Bi, J. R.: Surface measurements of aerosol properties over northwest China during ARM China 2008 deployment, J. Geophys. Res.-Atmos., 115, D00k27, 2010b.
Wang, X., Pu, W., Zhang, X. Y., Ren, Y., and Huang, J. P.: Water-soluble ions and trace elements in surface snow and their potential source regions across northeastern China, Atmos. Environ., 114, 57-65, 2015.
Wang, X., Xu, B. Q., and Ming, J.: An Overview of the Studies on Black Carbon and Mineral Dust Deposition in Snow and Ice Cores in East Asia, J. Meteorol. Res.-Prc., 28, 354-370, 2014.
Warren, S. G., and Wiscombe, W. J.: A Model for the Spectral Albedo of Snow .2. Snow Containing Atmospheric Aerosols, J. Atmos. Sci., 37, 2734-2745, 1980.
Warren, S. G. and Wiscombe, W. J.: Dirty Snow after Nuclear War, Nature, 313, 467-470, 1985.
Warren, S. G.: Optical Properties of Snow, Rev. Geophys., 20, 67-89, 1982.
Wright, P., Bergin, M., Dibb, J., Lefer, B., Domine, F., Carman, T., Carmagnola, C., Dumont, M., Courville, Z., Schaaf, C., and Wang, Z. S.: Comparing MODIS daily snow albedo to spectral albedo field measurements in Central Greenland, Remote Sens. Environ., 140, 118-129, 2014.
Wuttke, S., Seckmeyer, G., and Konig-Lang, G.: Measurements of spectral snow albedo at Neumayer, Antarctica, Ann. Geophys., 24, 7-21, 2006b.
Wuttke, S., Seckmeyer, G., Bernhard, G., Ehramjian, J., McKenzie, R., Johnston, P., and O'Neill, M.: New spectroradiometers complying with the NDSC standards, J. Atmos. Oceanic Technol., 23, 241-251, 2006a.
Xia, X. A., Chen, H. B., Wang, P. C., Zong, X. M., Qiu, J. H., and Gouloub, P.: Aerosol properties and their spatial and temporal variations over North China in spring 2001, Tellus B., 57, 28-39, 2005.
Xia, X. G., Li, Z. Q., Holben, B., Wang, P., Eck, T., Chen, H. B., Cribb, M., and Zhao, Y. X.: Aerosol optical properties and radiative effects in the Yangtze Delta region of China, J. Geophys. Res.-Atmos., 112, D22s12, 2007.
Xu, B. Q., Cao, J. J., Hansen, J., Yao, T. D., Joswia, D. R., Wang, N. L., Wu, G. J., Wang, M., Zhao, H. B., Yang, W., Liu, X. Q., and He, J. Q.: Black soot and the survival of Tibetan glaciers, Proc. Nat. Acad. Sci. U.S.A., 106, 22114-22118, 2009.
Xu, B. Q., Cao, J. J., Joswiak, D. R., Liu, X. Q., Zhao, H. B., and He, J. Q.: Post-depositional enrichment of black soot in snow-pack and accelerated melting of Tibetan glaciers, Environ. Res. Lett., 7, 2012.
Yasunari, T. J., Bonasoni, P., Laj, P., Fujita, K., Vuillermoz, E., Marinoni, A., Cristofanelli, P., Duchi, R., Tartari, G., and Lau, K. M.: Estimated impact of black carbon deposition during pre-monsoon season from Nepal Climate Observatory – Pyramid data and snow albedo changes over Himalayan glaciers, Atmos. Chem. Phys., 10, 6603-6615, 2010.
Yasunari, T. J., Koster, R. D., Lau, W. K. M., and Kim, K. M.: Impact of snow darkening via dust, black carbon, and organic carbon on boreal spring climate in the Earth system, J. Geophys. Res.-Atmos., 120, 5485-5503, 2015.

Ye, H., Zhang, R. D., Shi, J. S., Huang, J. P., Warren, S. G., and Fu, Q.: Black carbon in seasonal snow across northern Xinjiang in northwestern China, Environ. Res. Lett., 7, 044002, 2012.

Yesubabu, V., Srinivas, C. V., Hariprasad, K. B. R. R., and Baskaran, R.: A Study on the Impact of Observation Assimilation on the Numerical Simulation of Tropical Cyclones JAL and THANE Using 3DVAR, Pure Appl. Geophys., 171, 2023-2042, 2014.

Zawadzka, O., Makuch, P., Markowicz, K. M., Zielinski, T., Petelski, T., Ulevicius, V., Strzalkowska, A., Rozwadowska, A., and Gutowska, D.: Studies of aerosol optical depth with the use of Microtops II sun photometers and MODIS detectors in coastal areas of the Baltic Sea, Acta Geophysica, 62, 400-422, 2014.

Zege, Ė. P., Ivanov, A. P., and Katsev, I. L.: Image transfer through a scattering medium, Springer Verlag, 1991.

Zhang, R., Hegg, D. A., Huang, J., and Fu, Q.: Source attribution of insoluble light-absorbing particles in seasonal snow across northern China, Atmos. Chem. Phys., 13, 6091-6099, 2013a.

Zhang, R. J., Arimoto, R., An, J. L., Yabuki, S., and Sun, J. H.: Ground observations of a strong dust storm in Beijing in March 2002, J. Geophys. Res.-Atmos., 110, D18, 2005.

Zhang, R., Jing, J., Tao, J., Hsu, S. C., Wang, G., Cao, J., Lee, C. S. L., Zhu, L., Chen, Z., Zhao, Y., and Shen, Z.: Chemical characterization and source apportionment of PM2.5 in Beijing: seasonal perspective, Atmos. Chem. Phys., 13, 7053-7074, 2013b.

Zhang, X. L., Wu, G. J., Kokhanovsky, A., Yao, T. D., and Tong D.: Spectral albedo parameterization for dirty snow with considering mirco-physicochemical properties of impurities – Part I: Theory and preliminary evaluation, 2016 (preparation).

Zhang, X. Y., Gong, S. L., Shen, Z. X., Mei, F. M., Xi, X. X., Liu, L. C., Zhou, Z. J., Wang, D., Wang, Y. Q., and Cheng, Y.: Characterization of soil dust aerosol in China and its transport and distribution during 2001 ACE-Asia: 1. Network observations, J. Geophys. Res.-Atmos., 108, 4261, 2003.

Zhao, C., Hu, Z., Qian, Y., Leung, L. R., Huang, J., Huang, M., Jin, J., Flanner, M. G., Zhang, R., Wang, H., Yan, H., Lu, Z., and Streets, D. G.: Simulating black carbon and dust and their radiative forcing in seasonal snow: a case study over North China with field campaign measurements, Atmos. Chem. Phys., 14, 11475-11491, 2014.

Acosta, J. A., Faz, A., Kalbitz, K., Jansen, B., and Martinez-Martinez, S.: Heavy metal concentrations in particle size fractions from street dust of Murcia (Spain) as the basis for risk assessment, J. Environ. Monitor., 13, 3087-3096, 10.1039/c1em10364d, 2011.

Aleksandropoulou, V., Torseth, K., and Lazaridis, M.: Atmospheric Emission Inventory for Natural and Anthropogenic Sources and Spatial Emission Mapping for the Greater Athens Area, Water Air Soil Pollut., 219, 507-526, 10.1007/s11270-010-0724-2, 2011.

Arhami, M., Kuhn, T., Fine, P. M., Delfino, R. J., and Sioutas, C.: Effects of sampling artifacts and operating parameters on the performance of a semicontinuous particulate elemental carbon/organic carbon monitor, Environ. Sci. Technol., 40, 945-954, 10.1021/es0510313, 2006.

Ax, W., Malchow, H., Koren, H., and Fischer, H.: Studies on immunological reactions in vitro, Sbornik vedeckych praci Lekarske fakulty Karlovy university v Hradci Kralove, 13, 287-292, 1970.

Bergstrom, R. W., Russell, P. B., and Hignett, P.: Wavelength dependence of the absorption of black carbon particles: Predictions and results from the TARFOX experiment and implications for the aerosol single scattering albedo, J. Atmos. Sci., 59, 567-577, Doi 10.1175/1520-0469(2002)059<0567:Wdotao>2.0.Co;2, 2002.

Bi, J. R., Huang, J. P., Hu, Z. Y., Holben, B. N., and Guo, Z. Q.: Investigating the aerosol optical and radiative characteristics of heavy haze episodes in Beijing during January of 2013, J. Geophys. Res.-Atmos., 119, 9884-9900, 10.1002/2014JD021757, 2014.

Bond, T. C., Bussemer, M., Wehner, B., Keller, S., Charlson, R. J., and Heintzenberg, J.: Light absorption by primary particle emissions from a lignite burning plant, Environ. Sci. Technol., 33, 3887-3891, Doi 10.1021/Es9810538, 1999.

Bond, T. C., and Bergstrom, R. W.: Light absorption by carbonaceous particles: An investigative review, Aerosol Sci. Tech., 40, 27-67, 10.1080/02786820500421521, 2006.

Bond, T. C., Doherty, S. J., Fahey, D. W., Forster, P. M., Berntsen, T., DeAngelo, B. J., Flanner, M. G., Ghan, S., Karcher, B., Koch, D., Kinne, S., Kondo, Y., Quinn, P. K., Sarofim, M. C., Schultz, M. G., Schulz, M., Venkataraman, C., Zhang, H., Zhang, S., Bellouin, N., Guttikunda, S. K., Hopke, P. K., Jacobson, M. Z., Kaiser, J. W., Klimont, Z., Lohmann, U., Schwarz, J. P., Shindell, D., Storelvmo, T., Warren, S. G., and Zender, C. S.: Bounding the role of black carbon in the climate system: A scientific assessment, J. Geophys. Res.-Atmos., 118, 5380-5552, 10.1002/jgrd.50171, 2013.

Brandt, R. E., Warren, S. G., and Clarke, A. D.: A controlled snowmaking experiment testing the relation between black carbon content and reduction of snow albedo, J. Geophys. Res.-Atmos., 116, Artn D08109, 10.1029/2010jd015330, 2011.

Cachier, H., Liousse, C., Buatmenard, P., and Gaudichet, A.: Particulate Content of Savanna Fire Emissions, J. Atmos. Chem., 22, 123-148, Doi 10.1007/Bf00708185, 1995.

Cao, J. J., Lee, S. C., Chow, J. C., Watson, J. G., Ho, K. F., Zhang, R. J., Jin, Z. D., Shen, Z. X., Chen, G. C., Kang, Y. M., Zou, S. C., Zhang, L. Z., Qi, S. H., Dai, M. H., Cheng, Y., and Hu, K.: Spatial and seasonal distributions of carbonaceous aerosols over China, J. Geophys. Res.-Atmos., 112, Artn D22s11, 10.1029/2006jd008205, 2007.

Carmagnola, C. M., Domine, F., Dumont, M., Wright, P., Strellis, B., Bergin, M., Dibb, J., Picard, G., Libois, Q., Arnaud, L., and Morin, S.: Snow spectral albedo at Summit, Greenland: measurements and numerical simulations based on physical and chemical properties of the snowpack, Cryosphere, 7, 1139-1160, 10.5194/tc-7-1139-2013, 2013.

Che, H., Zhang, X. Y., Xia, X., Goloub, P., Holben, B., Zhao, H., Wang, Y., Zhang, X. C., Wang, H., Blarel, L., Damiri, B., Zhang, R., Deng, X., Ma, Y., Wang, T., Geng, F., Qi, B., Zhu, J., Yu, J., Chen, Q., and Shi, G.: Ground-based aerosol climatology of China: aerosol optical depths from the China Aerosol Remote Sensing Network (CARSNET) 2002-2013, Atmos. Chem. Phys., 15, 7619-7652, 10.5194/acp-15-7619-2015, 2015a.

Che, H. Z., Yang, Z. F., Zhang, X. Y., Zhu, C. Z., Ma, Q. L., Zhou, H. G., and Wang, P.: Study on the aerosol optical properties and their relationship with aerosol

chemical compositions over three regional background stations in China, Atmos. Environ., 43, 1093-1099, 10.1016/j.atmosenv.2008.11.010, 2009.

Che, H. Z., Wang, Y. Q., and Sun, J. Y.: Aerosol optical properties at Mt. Waliguan Observatory, China, Atmos. Environ., 45, 6004-6009, 10.1016/j.atmosenv.2011.07.050, 2011.

Che, H. Z., Wang, Y. Q., Sun, J. Y., Zhang, X. C., Zhang, X. Y., and Guo, J. P.: Variation of Aerosol Optical Properties over the Taklimakan Desert in China, Aerosol Air Qual. Res., 13, 777-785, 10.4209/aaqr.2012.07.0200, 2013.

Che, H. Z., Zhao, H. J., Wu, Y. F., Xia, X. G., Zhu, J., Wang, H., Wang, Y. Q., Sun, J. Y., Yu, J., Zhang, X. Y., and Shi, G. Y.: Analyses of aerosol optical properties and direct radiative forcing over urban and industrial regions in Northeast China, Meteorol. Atmos. Phys., 127, 345-354, 10.1007/s00703-015-0367-3, 2015b.

Chen, S. Y., Huang, J. P., Zhao, C., Qian, Y., Leung, L. R., and Yang, B.: Modeling the transport and radiative forcing of Taklimakan dust over the Tibetan Plateau: A case study in the summer of 2006, J. Geophys. Res.-Atmos., 118, 797-812, 10.1002/jgrd.50122, 2013.

Chu, D. A., Kaufman, Y. J., Ichoku, C., Remer, L. A., Tanre, D., and Holben, B. N.: Validation of MODIS aerosol optical depth retrieval over land, Geophys. Res. Lett., 29, Artn 1617, 10.1029/2001gl013205, 2002.

Cong, Z., Kang, S., Kawamura, K., Liu, B., Wan, X., Wang, Z., Gao, S., and Fu, P.: Carbonaceous aerosols on the south edge of the Tibetan Plateau: concentrations, seasonality and sources, Atmos. Chem. Phys., 15, 1573-1584, 10.5194/acp-15-1573-2015, 2015.

Coz, E., Casuccio, G., Lersch, T. L., Moreno, T., and Artinano, B.: Anthropogenic Influenced Mineral Dust Ambient Fine Particles At An Urban Site In Barcelona (Spain), Chem. Eng. Trans., 22, 101-106, 10.3303/Cet1022016, 2010.

Dang, C., and Hegg, D. A.: Quantifying light absorption by organic carbon in Western North American snow by serial chemical extractions, J. Geophys. Res.-Atmos., 119, 10.1002/2014JD022156, 2014.

de Mourgues, G., Fischer, L., and Felman, D.: Salter's" innominate osteotomy" of the pelvis for inequality of inferior limbs in a child, after complex injuries of the pelvis and one femur, Lyon chirurgical, 66, 62, 1970.

Doherty, S. J., Warren, S. G., Grenfell, T. C., Clarke, A. D., and Brandt, R. E.: Light-absorbing impurities in Arctic snow, Atmos. Chem. Phys., 10, 11647-11680, 10.5194/acp-10-11647-2010, 2010.

Doherty, S. J., Grenfell, T. C., Forsstrom, S., Hegg, D. L., Brandt, R. E., and Warren, S. G.: Observed vertical redistribution of black carbon and other insoluble light-absorbing particles in melting snow, J. Geophys. Res.-Atmos., 118, 5553-5569, 10.1002/jgrd.50235, 2013.

Doherty, S. J., Dang, C., Hegg, D. A., Zhang, R. D., and Warren, S. G.: Black carbon and other light-absorbing particles in snow of central North America, J. Geophys. Res.-Atmos., 119, 12807-12831, 10.1002/2014JD022350, 2014.

Flanner, M. G., Zender, C. S., Randerson, J. T., and Rasch, P. J.: Present-day climate forcing and response from black carbon in snow, J. Geophys. Res.-Atmos., 112, Artn D11202, 10.1029/2006jd008003, 2007.

Flanner, M. G., Zender, C. S., Hess, P. G., Mahowald, N. M., Painter, T. H., Ramanathan, V., and Rasch, P. J.: Springtime warming and reduced snow cover from carbonaceous particles, Atmos. Chem. Phys., 9, 2481-2497, 2009.

Flanner, M. G.: Arctic climate sensitivity to local black carbon, J. Geophys. Res.-Atmos., 118, 1840-1851, 10.1002/jgrd.50176, 2013.

Friedl, M. A., Sulla-Menashe, D., Tan, B., Schneider, A., Ramankutty, N., Sibley, A., and Huang, X. M.: MODIS Collection 5 global land cover: Algorithm refinements and characterization of new datasets, Remote Sens. Environ., 114, 168-182, 10.1016/j.rse.2009.08.016, 2010.

Ginoux, P., Garbuzov, D., and Hsu, N. C.: Identification of anthropogenic and natural dust sources using Moderate Resolution Imaging Spectroradiometer (MODIS) Deep Blue level 2 data, J. Geophys. Res.-Atmos., 115, Artn D05204, 10.1029/2009jd012398, 2010.

Givati, A., and Rosenfeld, D.: Quantifying precipitation suppression due to air pollution, J. Appl. Meteorol., 43, 1038-1056, Doi 10.1175/1520-0450(2004)043<1038:Qpsdta>2.0.Co;2, 2004.

Goudie, A. S., and Middleton, N. J.: Saharan dust storms: nature and consequences, Earth Sci. Rev., 56, 179-204, Doi 10.1016/S0012-8252(01)00067-8, 2001.

Grenfell, T. C., Doherty, S. J., Clarke, A. D., and Warren, S. G.: Light absorption from particulate impurities in snow and ice determined by spectrophotometric analysis of filters, Appl. Opt., 50, 2037-2048, 10.1364/Ao.50.002037, 2011.

Guan, X., Huang, J., Guo, R., Yu, H., Lin, P., and Zhang, Y.: Role of radiatively forced temperature changes in enhanced semi-arid warming in the cold season over east Asia, Atmos. Chem. Phys., 15, 13777-13786, 10.5194/acp-15-13777-2015, 2015.

Hadley, O. L., and Kirchstetter, T. W.: Black-carbon reduction of snow albedo, Nat. Clim. Change, 2, 437-440, 10.1038/Nclimate1433, 2012.

Hansen, J., and Nazarenko, L.: Soot climate forcing via snow and ice albedos, Proc. Nat. Acad. Sci. U.S.A., PNAS 101, 423-428, 10.1073/pnas.2237157100, 2004.

Hansen, J., Sato, M., Ruedy, R., Nazarenko, L., Lacis, A., Schmidt, G. A., Russell, G., Aleinov, I., Bauer, M., Bauer, S., Bell, N., Cairns, B., Canuto, V., Chandler, M., Cheng, Y., Del Genio, A., Faluvegi, G., Fleming, E., Friend, A., Hall, T., Jackman, C., Kelley, M., Kiang, N., Koch, D., Lean, J., Lerner, J., Lo, K., Menon, S., Miller, R., Minnis, P., Novakov, T., Oinas, V., Perlwitz, J., Perlwitz, J., Rind, D., Romanou, A., Shindell, D., Stone, P., Sun, S., Tausnev, N., Thresher, D., Wielicki, B., Wong, T., Yao, M., and Zhang, S.: Efficacy of climate forcings, J. Geophys. Res.-Atmos., 110, Artn D18104, 10.1029/2005jd005776, 2005.

Hegg, D. A., Warren, S. G., Grenfell, T. C., Doherty, S. J., Larson, T. V., and Clarke, A. D.: Source Attribution of Black Carbon in Arctic Snow, Environ. Sci. Technol., 43, 4016-4021, 10.1021/es803623f, 2009.

Hegg, D. A., Warren, S. G., Grenfell, T. C., Doherty, S. J., and Clarke, A. D.: Sources of light-absorbing aerosol in arctic snow and their seasonal variation, Atmos. Chem. Phys., 10, 10923-10938, 10.5194/acp-10-10923-2010, 2010.

Holben, B. N., Eck, T. F., and Fraser, R. S.: Temporal and Spatial Variability of Aerosol Optical Depth in the Sahel Region in Relation to Vegetation Remote Sensing, Int. J. Remote Sens., 12, 1147-1163, 1991.

Holben, B. N., Tanre, D., Smirnov, A., Eck, T. F., Slutsker, I., Abuhassan, N., Newcomb, W. W., Schafer, J. S., Chatenet, B., Lavenu, F., Kaufman, Y. J., Castle, J. V., Setzer, A., Markham, B., Clark, D., Frouin, R., Halthore, R., Karneli, A., O'Neill, N. T., Pietras, C., Pinker, R. T., Voss, K., and Zibordi, G.: An emerging ground-based aerosol climatology: Aerosol optical depth from AERONET, J. Geophys. Res.-Atmos., 106, 12067-12097, Doi 10.1029/2001jd900014, 2001.

Holben, B. N., Eck, T. F., Slutsker, I., Smirnov, A., Sinyuk, A., Schafer, J., Giles, D., and Dubovik, O.: AERONET's Version 2.0 quality assurance criteria - art. no.

64080Q, Remote Sensing of the Atmosphere and Clouds, 6408, Q4080-Q4080, Artn 64080q, 10.1117/12.706524, 2006.

Hsu, S. C., Liu, S. C., Huang, Y. T., Chou, C. C. K., Lung, S. C. C., Liu, T. H., Tu, J. Y., and Tsai, F. J.: Long-range southeastward transport of Asian biosmoke pollution: Signature detected by aerosol potassium in Northern Taiwan, J. Geophys. Res.-Atmos., 114, Artn D14301, 10.1029/2009jd011725, 2009.

Huang, J. P., Fu, Q. A., Zhang, W., Wang, X., Zhang, R. D., Ye, H., and Warren, S. G.: Dust and Black Carbon in Seasonal Snow across Northern China, Bull. Amer. Meteor. Soc., 92, 175-181, 10.1175/2010BAMS3064.1, 2011.

Huang, J. P., Wang, T. H., Wang, W. C., Li, Z. Q., and Yan, H. R.: Climate effects of dust aerosols over East Asian arid and semiarid regions, J. Geophys. Res.-Atmos., 119, 11398-11416, 10.1002/2014JD021796, 2014.

Huang, J. P., Liu, J. J., Chen, B., and Nasiri, S. L.: Detection of anthropogenic dust using CALIPSO lidar measurements, Atmos. Chem. Phys., 15, 11653-11665, 10.5194/acp-15-11653-2015, 2015a.

Huang, Z. W., Huang, J. P., Hayasaka, T., Wang, S. S., Zhou, T., and Jin, H. C.: Short-cut transport path for Asian dust directly to the Arctic: a case study, Environ. Res. Lett., 10, Artn 114018, 10.1088/1748-9326/10/11/114018, 2015b.

Ianniello, A., Spataro, F., Esposito, G., Allegrini, I., Hu, M., and Zhu, T.: Chemical characteristics of inorganic ammonium salts in PM2.5 in the atmosphere of Beijing (China), Atmos. Chem. Phys., 11, 10803-10822, 10.5194/acp-11-10803-2011, 2011.

Ichoku, C., Chu, D. A., Mattoo, S., Kaufman, Y. J., Remer, L. A., Tanre, D., Slutsker, I., and Holben, B. N.: A spatio-temporal approach for global validation and analysis of MODIS aerosol products, Geophys. Res. Lett., 29, Artn 1616, 10.1029/2001gl013206, 2002a.

Ichoku, C., Levy, R., Kaufman, Y. J., Remer, L. A., Li, R. R., Martins, V. J., Holben, B. N., Abuhassan, N., Slutsker, I., Eck, T. F., and Pietras, C.: Analysis of the performance characteristics of the five-channel Microtops II Sun photometer for measuring aerosol optical thickness and precipitable water vapor, J. Geophys. Res.-Atmos., 107, Artn 4179, 10.1029/2001jd001302, 2002b.

IPCC: Climate Change 2013: The Physical Science Basis. Contribution of Working Group I to the Fifth Assessment Report of the Intergovernmental Panel on Climate Change, Stocker, T. F., Qin, D., Plattner, G. K., Tignor, M., Allen, S. K., Boschung, J., Nauels, A., Xia, Y., Bex, V., and Midgley, P. M., Cambridge Univ. Press, Cambridge, United Kingdom and New York, NY, USA, 2013.

Jacobson, M. Z.: Climate response of fossil fuel and biofuel soot, accounting for soot's feedback to snow and sea ice albedo and emissivity, J. Geophys. Res.-Atmos., 109, Artn D21201, 10.1029/2004jd004945, 2004.

Jaffe, D., Anderson, T., Covert, D., Kotchenruther, R., Trost, B., Danielson, J., Simpson, W., Berntsen, T., Karlsdottir, S., Blake, D., Harris, J., Carmichael, G., and Uno, I.: Transport of Asian air pollution to North America, Geophys. Res. Lett., 26, 711-714, Doi 10.1029/1999gl900100, 1999.

Kamani, H., Ashrafi, S. D., Isazadeh, S., Jaafari, J., Hoseini, M., Mostafapour, F. K., Bazrafshan, E., Nazmara, S., and Mahvi, A. H.: Heavy Metal Contamination in Street Dusts with Various Land Uses in Zahedan, Iran, B. Environ. Contam. Tox., 94, 382-386, 10.1007/s00128-014-1453-9, 2015.

Kang, L. T., Huang, J. P., Chen, S. Y., and Wang, X.: Long-term trends of dust events over Tibetan Plateau during 1961-2010, Atmos. Environ., 125, 188-198, 10.1016/j.atmosenv.2015.10.085, 2016.

Kaufman, Y. J., Tanre, D., Gordon, H. R., Nakajima, T., Lenoble, J., Frouin, R., Grassl, H., Herman, B. M., King, M. D., and Teillet, P. M.: Passive remote sensing of tropospheric aerosol and atmospheric correction for the aerosol effect, J. Geophys. Res. Atmos., 102, 16815-16830, Doi 10.1029/97jd01496, 1997.

Kim, W., Doh, S. J., and Yu, Y.: Anthropogenic contribution of magnetic particulates in urban roadside dust, Atmos. Environ., 43, 3137-3144, 10.1016/j.atmosenv.2009.02.056, 2009.

Koch, D., Menon, S., Del Genio, A., Ruedy, R., Alienov, I., and Schmidt, G. A.: Distinguishing Aerosol Impacts on Climate over the Past Century, J. Climate, 22, 2659-2677, 10.1175/2008JCLI2573.1, 2009.

Kokhanovsky, A. A., and Zege, E. P.: Scattering optics of snow, Appl. Opt., 43, 1589-1602, Doi 10.1364/Ao.43.001589, 2004.

Kotthaus, S., Smith, T. E. L., Wooster, M. J., and Grimmond, C. S. B.: Derivation of an urban materials spectral library through emittance and reflectance spectroscopy, Isprs J. Photogramm., 94, 194-212, 10.1016/j.isprsjprs.2014.05.005, 2014.

Lafon, S., Sokolik, I. N., Rajot, J. L., Caquineau, S., and Gaudichet, A.: Characterization of iron oxides in mineral dust aerosols: Implications for light absorption, J. Geophys. Res.-Atmos., 111, Artn D21207. 10.1029/2005jd007016, 2006.

Li, G. J., Chen, J., Ji, J. F., Yang, J. D., and Conway, T. M.: Natural and anthropogenic sources of East Asian dust, Geology, 37, 727-730, 10.1130/G30031a.1, 2009.

Li, S. Y., Lei, J. Q., Xu, X. W., Wang, H. F., and Gu, F.: Dust Source of Sandstorm in the Tarim Basin, Northwest China, Adv. Environ. Sci. Eng., 518-523, 4592-4598, 10.4028/www.scientific.net/AMR.518-523.4592, 2012.

Li, X. Y., Liu, L. J., Wang, Y. G., Luo, G. P., Chen, X., Yang, X. L., Hall, M. H. P., Guo, R. C., Wang, H. J., Cui, J. H., and He, X. Y.: Heavy metal contamination of urban soil in an old industrial city (Shenyang) in Northeast China, Geoderma, 192, 50-58, 10.1016/j.geoderma.2012.08.011, 2013.

Light, B., Eicken, H., Maykut, G. A., and Grenfell, T. C.: The effect of included particulates on the spectral albedo of sea ice, J. Geophys. Res.-Oceans, 103, 27739-27752, Doi 10.1029/98jc02587, 1998.

Lorenz, K., Preston, C. M., and Kandeler, E.: Soil organic matter in urban soils: Estimation of elemental carbon by thermal oxidation and characterization of organic matter by solid-state C-13 nuclear magnetic resonance (NMR) spectroscopy, Geoderma, 130, 312-323, 10.1016/j.geoderma.2005.02.004, 2006.

Loveland, T. R., and Belward, A. S.: The IGBP-DIS global 1 km land cover data set, DISCover: first results, Int. J. Remote Sens., 18, 3291-3295, 1997.

Mahowald, N. M., and Luo, C.: A less dusty future?, Geophys. Res. Lett., 30, Artn 1903, 10.1029/2003gl017880, 2003.

Mahowald, N. M., Baker, A. R., Bergametti, G., Brooks, N., Duce, R. A., Jickells, T. D., Kubilay, N., Prospero, J. M., and Tegen, I.: Atmospheric global dust cycle and iron inputs to the ocean, Global Biogeochem. CY., 19, Artn Gb4025, 10.1029/2004gb002402, 2005.

Ming, J., Xiao, C. D., Sun, J. Y., Kang, S. C., and Bonasoni, P.: Carbonaceous particles in the atmosphere and precipitation of the Nam Co region, central Tibet, J. Environ. Sci., 22, 1748-1756, 10.1016/S1001-0742(09)60315-6, 2010.

Morys, M., Mims, F. M., Hagerup, S., Anderson, S. E., Baker, A., Kia, J., and Walkup, T.: Design, calibration, and performance of MICROTOPS II handheld

ozone monitor and Sun photometer, J. Geophys. Res.-Atmos., 106, 14573-14582, Doi 10.1029/2001jd900103, 2001.

Motoyoshi, H., Aoki, T., Hori, M., Abe, O., and Mochizuki, S.: Possible effect of anthropogenic aerosol deposition on snow albedo reduction at Shinjo, Japan, J. Meteorol. Soc. Jpn., 83A, 137-148, Doi 10.2151/Jmsj.83a.137, 2005.

Novakov, T., Menon, S., Kirchstetter, T. W., Koch, D., and Hansen, J. E.: Aerosol organic carbon to black carbon ratios: Analysis of published data and implications for climate forcing, J. Geophys. Res.-Atmos., 110, Artn D21205, 10.1029/2005jd005977, 2005.

Painter, T. H., Barrett, A. P., Landry, C. C., Neff, J. C., Cassidy, M. P., Lawrence, C. R., McBride, K. E., and Farmer, G. L.: Impact of disturbed desert soils on duration of mountain snow cover, Geophys. Res. Lett., 34, Artn L12502, 10.1029/2007gl030284, 2007.

Painter, T. H., Deems, J. S., Belnap, J., Hamlet, A. F., Landry, C. C., and Udall, B.: Response of Colorado River runoff to dust radiative forcing in snow, Proc. Nat. Acad. Sci. U.S.A., PNAS 107, 17125-17130, 10.1073/pnas.0913139107, 2010.

Painter, T. H., Bryant, A. C., and Skiles, S. M.: Radiative forcing by light absorbing impurities in snow from MODIS surface reflectance data, Geophys. Res. Lett., 39, Artn L17502, 10.1029/2012gl052457, 2012.

Painter, T. H., Seidel, F. C., Bryant, A. C., Skiles, S. M., and Rittger, K.: Imaging spectroscopy of albedo and radiative forcing by light-absorbing impurities in mountain snow, J. Geophys. Res.-Atmos., 118, 9511-9523, 10.1002/jgrd.50520, 2013.

Park, S. U., and Park, M. S.: Aerosol size distributions observed at Naiman in the Asian dust source region of Inner Mongolia, Atmos. Environ., 82, 17-23, 10.1016/j.atmosenv.2013.09.054, 2014.

Pedersen, C. A., Gallet, J. C., Strom, J., Gerland, S., Hudson, S. R., Forsstrom, S., Isaksson, E., and Berntsen, T. K.: In situ observations of black carbon in snow and the corresponding spectral surface albedo reduction, J. Geophys. Res.-Atmos., 120, 1476-1489, 10.1002/2014JD022407, 2015.

Pio, C. A., Legrand, M., Oliveira, T., Afonso, J., Santos, C., Caseiro, A., Fialho, P., Barata, F., Puxbaum, H., Sanchez-Ochoa, A., Kasper-Giebl, A., Gelencser, A., Preunkert, S., and Schock, M.: Climatology of aerosol composition (organic versus inorganic) at nonurban sites on a west-east transect across Europe, J. Geophys. Res.-Atmos., 112, Artn D23s02, 10.1029/2006jd008038, 2007.

Porter, J. N., Miller, M., Pietras, C., and Motell, C.: Ship-based sun photometer measurements using Microtops sun photometers, J. Atmos. Oceanic Technol., 18, 765-774, Doi 10.1175/1520-0426(2001)018<0765:Sbspmu>2.0.Co;2, 2001.

Pu, W., Wang, X., Zhang, X. Y., Ren, Y., Shi, J. S., Bi, J. R., and Zhang, B. D.: Size Distribution and Optical Properties of Particulate Matter (PM10) and Black Carbon (BC) during Dust Storms and Local Air Pollution Events across a Loess Plateau Site, Aerosol Air Qual. Res., 15, 2212-2224, 10.4209/aaqr.2015.02.0109, 2015.

Qian, Y., Wang, H. L., Zhang, R. D., Flanner, M. G., and Rasch, P. J.: A sensitivity study on modeling black carbon in snow and its radiative forcing over the Arctic and Northern China, Environ. Res. Lett., 9, Artn 064001, 10.1088/1748-9326/9/6/064001, 2014.

Qian, Y., Yasunari, T. J., Doherty, S. J., Flanner, M. G., Lau, W. K. M., Ming, J., Wang, H. L., Wang, M., Warren, S. G., and Zhang, R. D.: Light-absorbing Particles in Snow and Ice: Measurement and Modeling of Climatic and

Hydrological impact, Adv. Atmos. Sci., 32, 64-91, 10.1007/s00376-014-0010-0, 2015.

Qiao, Q. Q., Huang, B. C., Zhang, C. X., Piper, J. D. A., Pan, Y. P., and Sun, Y.: Assessment of heavy metal contamination of dustfall in northern China from integrated chemical and magnetic investigation, Atmos. Environ., 74, 182-193, 10.1016/j.atmosenv.2013.03.039, 2013.

Remer, L. A., Tanre, D., Kaufman, Y. J., Ichoku, C., Mattoo, S., Levy, R., Chu, D. A., Holben, B., Dubovik, O., Smirnov, A., Martins, J. V., Li, R. R., and Ahmad, Z.: Validation of MODIS aerosol retrieval over ocean, Geophys. Res. Lett., 29, Artn 1618, 10.1029/2001gl013204, 2002.

Rosenfeld, D., Rudich, Y., and Lahav, R.: Desert dust suppressing precipitation: A possible desertification feedback loop, Proc. Nat. Acad. Sci. U.S.A.,PNAS 98, 5975-5980, DOI 10.1073/pnas.101122798, 2001.

Routray, A., Mohanty, U. C., Osuri, K. K., and Prasad, S. K.: Improvement of Monsoon Depressions Forecast with Assimilation of Indian DWR Data Using WRF-3DVAR Analysis System, Pure Appl. Geophys., 170, 2329-2350, 10.1007/s00024-013-0648-z, 2013.

Rozenberg, G.: Optical characteristics of thick weakly absorbing scattering layers, Dokl. Akad. Nauk SSSR, 145, 775-777,1962.

Smith, T. M., Gao, J. D., Calhoun, K. M., Stensrud, D. J., Manross, K. L., Ortega, K. L., Fu, C. H., Kingfield, D. M., Elmore, K. L., Lakshmanan, V., and Riedel, C.: Examination of a Real-Time 3DVAR Analysis System in the Hazardous Weather Testbed, Weather Forecast., 29, 63-77, 10.1175/Waf-D-13-00044.1, 2014.

Srivastava, K., and Bhardwaj, R.: Analysis and very short range forecast of cyclone "AILA" with radar data assimilation with rapid intermittent cycle using ARPS 3DVAR and cloud analysis techniques, Meteorol. Atmos. Phys., 124, 97-111, 10.1007/s00703-014-0307-7, 2014.

Tegen, I., and Fung, I.: Contribution to the Atmospheric Mineral Aerosol Load from Land-Surface Modification, J. Geophys. Res.-Atmos., 100, 18707-18726, Doi 10.1029/95jd02051, 1995.

Tegen, I., Harrison, S. P., Kohfeld, K. E., Engelstaedter, S., and Werner, M.: Emission of soil dust aerosol: Anthropogenic contribution and future changes, Geochimica Et Cosmochimica Acta, 66, A766-A766, 2002.

Tegen, I., Werner, M., Harrison, S. P., and Kohfeld, K. E.: Relative importance of climate and land use in determining present and future global soil dust emission, Geophys. Res. Lett., 31, Artn L05105, 10.1029/2003gl019216, 2004.

Thompson, L. G., Davis, M. E., Mosleythompson, E., and Liu, K. B.: Pre-Incan Agricultural Activity Recorded in Dust Layers in 2 Tropical Ice Cores, Nature, 336, 763-765, Doi 10.1038/336763a0, 1988.

Toon, O. B., Mckay, C. P., Ackerman, T. P., and Santhanam, K.: Rapid Calculation of Radiative Heating Rates and Photodissociation Rates in Inhomogeneous Multiple Scattering Atmospheres, J. Geophys. Res.-Atmos., 94, 16287-16301, Doi 10.1029/Jd094id13p16287, 1989.

Wallach, D. F. H., and Fischer, H.: Membrane aspects of the immune response. Report of a workshop held in Titisee, Schwarzwald, Germany, October 13–15, 1969, FEBS Lett. , 9, 129-135, 1970.

Wang, M., Xu, B. Q., Zhao, H. B., Cao, J. J., Joswiak, D., Wu, G. J., and Lin, S. B.: The Influence of Dust on Quantitative Measurements of Black Carbon in Ice and

Snow when Using a Thermal Optical Method, Aerosol Sci. Tech., 46, 60-69, 10.1080/02786826.2011.605815, 2012.

Wang, P., Che, H. Z., Zhang, X. C., Song, Q. L., Wang, Y. Q., Zhang, Z. H., Dai, X., and Yu, D. J.: Aerosol optical properties of regional background atmosphere in Northeast China, Atmos. Environ., 44, 4404-4412, 10.1016/j.atmosenv.2010.07.043, 2010a.

Wang, X., Huang, J. P., Ji, M. X., and Higuchi, K.: Variability of East Asia dust events and their long-term trend, Atmos. Environ., 42, 3156-3165, 10.1016/j.atmosenv.2007.07.046, 2008.

Wang, X., Huang, J. P., Zhang, R. D., Chen, B., and Bi, J. R.: Surface measurements of aerosol properties over northwest China during ARM China 2008 deployment, J. Geophys. Res.-Atmos., 115, Artn D00k27, 10.1029/2009jd013467, 2010b.

Wang, X., Doherty, S. J., and Huang, J. P.: Black carbon and other light-absorbing impurities in snow across Northern China, J. Geophys. Res.-Atmos., 118, 1471-1492, 10.1029/2012JD018291, 2013a.

Wang, X., Pu, W., Zhang, X. Y., Ren, Y., and Huang, J. P.: Water-soluble ions and trace elements in surface snow and their potential source regions across northeastern China, Atmos. Environ., 114, 57-65, 10.1016/j.atmosenv.2015.05.012, 2015.

Wang, X. G., Parrish, D., Kleist, D., and Whitaker, J.: GSI 3DVar-Based Ensemble-Variational Hybrid Data Assimilation for NCEP Global Forecast System: Single-Resolution Experiments, Mon. Weather. Rev., 141, 4098-4117, 10.1175/Mwr-D-12-00141.1, 2013b.

Wang, Z. W., Gallet, J. C., Pedersen, C. A., Zhang, X. S., Strom, J., and Ci, Z. J.: Elemental carbon in snow at Changbai Mountain, northeastern China: concentrations, scavenging ratios, and dry deposition velocities, Atmos. Chem. Phys., 14, 629-640, 10.5194/acp-14-629-2014, 2014.

Wang, X., Xu, B. Q., and Ming, J.: An Overview of the Studies on Black Carbon and Mineral Dust Deposition in Snow and Ice Cores in East Asia, J Meteorol Res-Prc, 28, 354-370, 2014.

Warren, S. G., and Wiscombe, W. J.: A Model for the Spectral Albedo of Snow .2. Snow Containing Atmospheric Aerosols, J. Atmos. Sci., 37, 2734-2745, Doi 10.1175/1520-0469(1980)037<2734:Amftsa>2.0.Co;2, 1980.

Warren, S. G. and Wiscombe, W. J.: Dirty Snow after Nuclear-War, Nature, 313, 467-470, 1985.

Warren, S. G.: Optical Properties of Snow, Rev. Geophys., 20, 67-89, Doi 10.1029/Rg020i001p00067, 1982.

Wedepohl, K. H.: The Composition of the Continental Crust, Geochimica Et Cosmochimica Acta, 59, 1217-1232, 1995.

Wright, P., Bergin, M., Dibb, J., Lefer, B., Domine, F., Carman, T., Carmagnola, C., Dumont, M., Courville, Z., Schaaf, C., and Wang, Z. S.: Comparing MODIS daily snow albedo to spectral albedo field measurements in Central Greenland, Remote Sens. Environ., 140, 118-129, 10.1016/j.rse.2013.08.044, 2014.

Wuttke, S., Seckmeyer, G., Bernhard, G., Ehramjian, J., McKenzie, R., Johnston, P., and O'Neill, M.: New spectroradiometers complying with the NDSC standards, J. Atmos. Oceanic Technol., 23, 241-251, 2006a.

Wuttke, S., Seckmeyer, G., and Konig-Lang, G.: Measurements of spectral snow albedo at Neumayer, Antarctica, Ann. Geophys., 24, 7-21, 2006b.

Xia, X. A., Chen, H. B., Wang, P. C., Zong, X. M., Qiu, J. H., and Gouloub, P.: Aerosol properties and their spatial and temporal variations over North China in spring 2001, Tellus B., 57, 28-39, 2005.

Xia, X. G., Li, Z. Q., Holben, B., Wang, P., Eck, T., Chen, H. B., Cribb, M., and Zhao, Y. X.: Aerosol optical properties and radiative effects in the Yangtze Delta region of China, J. Geophys. Res.-Atmos., 112, Artn D22s12, 10.1029/2007jd008859, 2007.

Xu, B. Q., Cao, J. J., Hansen, J., Yao, T. D., Joswia, D. R., Wang, N. L., Wu, G. J., Wang, M., Zhao, H. B., Yang, W., Liu, X. Q., and He, J. Q.: Black soot and the survival of Tibetan glaciers, Proc. Nat. Acad. Sci. U.S.A., 106, 22114-22118, 10.1073/pnas.0910444106, 2009.

Xu, B. Q., Cao, J. J., Joswiak, D. R., Liu, X. Q., Zhao, H. B., and He, J. Q.: Post-depositional enrichment of black soot in snow-pack and accelerated melting of Tibetan glaciers, Environ. Res. Lett. , 7, 10.1088/1748-9326/7/1/014022, 2012.

Yasunari, T. J., Bonasoni, P., Laj, P., Fujita, K., Vuillermoz, E., Marinoni, A., Cristofanelli, P., Duchi, R., Tartari, G., and Lau, K. M.: Estimated impact of black carbon deposition during pre-monsoon season from Nepal Climate Observatory - Pyramid data and snow albedo changes over Himalayan glaciers, Atmos. Chem. Phys., 10, 6603-6615, 10.5194/acp-10-6603-2010, 2010.

Yasunari, T. J., Koster, R. D., Lau, W. K. M., and Kim, K. M.: Impact of snow darkening via dust, black carbon, and organic carbon on boreal spring climate in the Earth system, J. Geophys. Res.-Atmos., 120, 5485-5503, 10.1002/2014jd022977, 2015.

Ye, H., Zhang, R. D., Shi, J. S., Huang, J. P., Warren, S. G., and Fu, Q.: Black carbon in seasonal snow across northern Xinjiang in northwestern China, Environ. Res. Lett., 7, Artn 044002, 10.1088/1748-9326/7/4/044002, 2012.

Yesubabu, V., Srinivas, C. V., Hariprasad, K. B. R. R., and Baskaran, R.: A Study on the Impact of Observation Assimilation on the Numerical Simulation of Tropical Cyclones JAL and THANE Using 3DVAR, Pure Appl. Geophys., 171, 2023-2042, 10.1007/s00024-013-0741-3, 2014.

Zawadzka, O., Makuch, P., Markowicz, K. M., Zielinski, T., Petelski, T., Ulevicius, V., Strzalkowska, A., Rozwadowska, A., and Gutowska, D.: Studies of aerosol optical depth with the use of Microtops II sun photometers and MODIS detectors in coastal areas of the Baltic Sea, Acta Geophysica, 62, 400-422, 10.2478/s11600-013-0182-5, 2014.

Zege, Ė. P., Ivanov, A. P., and Katsev, I. L.: Image transfer through a scattering medium, Springer Verlag, 1991.

Zhang, R., Hegg, D. A., Huang, J., and Fu, Q.: Source attribution of insoluble light-absorbing particles in seasonal snow across northern China, Atmos. Chem. Phys., 13, 6091-6099, 10.5194/acp-13-6091-2013, 2013.

Zhang, R., Jing, J., Tao, J., Hsu, S. C., Wang, G., Cao, J., Lee, C. S. L., Zhu, L., Chen, Z., Zhao, Y., and Shen, Z.: Chemical characterization and source apportionment of PM2.5 in Beijing: seasonal perspective, Atmos. Chem. Phys. , 13, 7053-7074, 10.5194/acp-13-7053-2013, 2013.

Zhang, R. J., Arimoto, R., An, J. L., Yabuki, S., and Sun, J. H.: Ground observations of a strong dust storm in Beijing in March 2002, J. Geophys. Res.-Atmos., 110, 10.1029/2004jd004589, 2005.

Zhang, X. L., Wu, G. J., Kokhanovsky, A., Yao, T. D., and Tong D.: Spectral albedo parameterization for dirty snow with considering mirco-physicochemical

properties of impurities – Part I: Theory and preliminary evaluation, 2016 (preparation).

Zhang, X. Y., Gong, S. L., Shen, Z. X., Mei, F. M., Xi, X. X., Liu, L. C., Zhou, Z. J., Wang, D., Wang, Y. Q., and Cheng, Y.: Characterization of soil dust aerosol in China and its transport and distribution during 2001 ACE-Asia: 1. Network observations, J. Geophys. Res.-Atmos., 108, Artn 4261, 10.1029/2002jd002632, 2003.

Zhao, C., Hu, Z., Qian, Y., Leung, L. R., Huang, J., Huang, M., Jin, J., Flanner, M. G., Zhang, R., Wang, H., Yan, H., Lu, Z., and Streets, D. G.: Simulating black carbon and dust and their radiative forcing in seasonal snow: a case study over North China with field campaign measurements, Atmos. Chem. Phys., 14, 11475-11491, 10.5194/acp-14-11475-2014, 2014.

Ofosu, F. G., Hopke, P. K., Aboh, I. J. K., and Bamford, S. A.: Characterization of fine particulate sources at Ashaiman in Greater Accra, Ghana, Atmos Pollut Res, 3, 301-310, 2012.